

DISSERTATION

# Chiral Symmetry Breaking in Strong Magnetic Fields

## A field theoretical and a holographic perspective

ausgeführt zum Zwecke der Erlangung des akademischen Grades eines Doktors der Naturwissenschaften unter der Leitung von

Univ.-Prof. DI Dr. Anton Rebhan  
Privatdoz. Dr. Andreas Schmitt  
Institut für theoretische Physik (E136) der Technischen Universität Wien

eingereicht an der  
Fakultät für Physik der Technischen Universität Wien  
von

**Dipl.-Ing. Florian Preis**  
Matrikelnummer 0026546  
Anton-Sattler-Gasse 100/35, 1220 Wien

Diese Dissertation haben begutachtet:

---

(Univ.-Prof. DI Dr. Anton Rebhan)

---

(Priv.-Doz. Dr. Johanna Erdmenger)

Wien, 02.01.2014

---

(Dipl.-Ing. Florian Preis)



# Deutsche Kurzfassung der Dissertation

Das Hauptaugenmerk dieser Arbeit liegt auf der Analyse der spontanen Brechung der chiralen Symmetrie der starken Wechselwirkungen unter dem Einfluss eines Magnetfeldes. Nach einem kurzen historischen Abriss, welcher der Einführung der Isospin- und axialen Symmetrie in den starken Wechselwirkungen dient, wird die spontane Symmetriebrechung am Beispiel des Nambu–Jona-Lasino (NJL) Modells im Detail dargestellt. Nach einem weiteren historischen Überblick der Ereignisse die zur Formulierung der Quanten Chromodynamik führten, wird der Einfluss von Temperatur und chemischen Potential auf die spontane Brechung der chiralen Symmetrie anhand des NJL Modells besprochen. Eine weitere Methode, die sich für die Untersuchung der chiralen Symmetrie anbietet, bedient sich des sogenannten holographischen Prinzips. Hierbei bildet man eine stark wechselwirkende Quantenfeldtheorie auf eine supersymmetrische Gravitationstheorie ab. In dieser Arbeit wird das Sakai–Sugimoto Modell zum Zwecke einer holographischen Analyse der zuvor genannten Mechanismen herangezogen.

Der Hauptteil dieser Dissertation widmet sich der Untersuchung der chiralen Symmetriebrechung in starken Magnetfeldern anhand des NJL Modells sowie des Sakai–Sugimoto Modells und basiert auf den Veröffentlichungen [145, 146, 147]. Entgegen der Erwartung, dass ein Magnetfeld die Brechung der chiralen Symmetrie verstärkt – dieser Effekt wird magnetische Katalyse genannt, zeigt sich, dass bei endlichem chemischen Potential ein umgekehrter Effekt – hier als inverse magnetische Katalyse bezeichnet – auftritt. Beide Modelle zeigen beeindruckende qualitative Übereinstimmung. Da das Sakai–Sugimoto Modell die Einführung von Baryonen erlaubt, wird der Einfluss jener auf die inverse magnetische Katalyse ebenfalls studiert. Es zeigt sich, dass Baryonen inverse magnetische Katalyse verstärken. Um auch diese Ergebnisse einem Vergleich mit einem feldtheoretischen Zugang zu unterziehen wird abschließend im Walecka Modell der Phasenübergang zu dichter Kernmaterie unter dem Einfluss eines Magnetfeldes untersucht. Die fehlende Übereinstimmung in diesem Fall wird einerseits der fehlenden Einbeziehung der chiralen Symmetrie im

Walecka Modell und andererseits dem großen Rang der Farb-Symmetriegruppe im Sakai–Sugimoto Modell zugeschrieben.

# Abstract

This thesis aims at discussing the spontaneous breaking of a chiral symmetry of strong interactions in a background magnetic field. After brief historical introduction to isospin and axial symmetry we turn to a more detailed analysis of the spontaneous breaking of chiral symmetry utilizing the Nambu–Jona-Lasino (NJL) model. In another historical outline the events that led to the formulation of quantum chromodynamics are presented, followed by studying the influence of finite temperature and chemical potential on chiral symmetry breaking in the NJL model. Another approach to the analysis of chiral symmetry breaking utilizes the so-called holographic principle, which allows for encoding a quantum field theory in a higher dimensional gravitational theory. Here we will employ the Sakai–Sugimoto model.

The discussion of chiral symmetry breaking in a strong magnetic field and comparing the results obtained in the NJL model and the Sakai–Sugimoto model comprises the main part of this thesis and is based on the publications [145, 146, 147]. In contrast to the expectation that a magnetic field enhances chiral symmetry breaking, which is known as magnetic catalysis, we will observe the opposite effect at finite chemical potential, which we will call inverse magnetic catalysis. Since the Sakai–Sugimoto model allows for incorporating baryons, we will also study their influence on the phase diagram for chiral symmetry breaking. It turns out that with baryons inverse magnetic catalysis is even more pronounced. In order to compare these results also with a field theoretical approach, we discuss the influence of a magnetic field on the transition to nuclear matter in the Walecka model. The disagreement between the results in this case is attributed on the one hand to the insufficient incorporation of chiral symmetry breaking in the Walecka model and on the other hand to the necessarily large number of colors in the Sakai–Sugimoto model.



*Für Julia und Marilu*





# Contents

<b>0</b>	<b>Overview</b>	<b>1</b>
<b>1</b>	<b>A hidden symmetry</b>	<b>7</b>
<b>2</b>	<b>Chiral symmetry breaking</b>	<b>17</b>
2.1	The NJL model . . . . .	22
<b>3</b>	<b>Thermodynamics of chiral symmetry breaking</b>	<b>31</b>
3.1	Towards quarks and gluons . . . . .	31
3.2	The thermodynamics of the NJL model . . . . .	36
<b>4</b>	<b>A geometric picture of chiral symmetry breaking</b>	<b>43</b>
4.1	The gauge–gravity duality . . . . .	43
4.2	The Witten model . . . . .	44
4.3	The Sakai–Sugimoto model . . . . .	46
4.4	Large $N_c$ baryons . . . . .	48
4.5	NJL limit . . . . .	51
<b>5</b>	<b>Chiral symmetry breaking in a magnetic field in the NJL model</b>	<b>53</b>
5.1	Fermions in a magnetic field . . . . .	54
5.2	NJL model in an external magnetic field . . . . .	56
5.3	Magnetic catalysis . . . . .	57
5.4	Inverse magnetic catalysis . . . . .	59
<b>6</b>	<b>Chiral symmetry breaking in a magnetic field in holography</b>	<b>65</b>
6.1	Set up . . . . .	66
6.2	Equations of motion, conserved currents and force balancing . . . . .	69
6.3	Semianalytic solution to the equations of motion . . . . .	74
6.4	Broken chiral symmetry without baryons . . . . .	76
6.5	Broken chiral symmetry with baryons . . . . .	79
6.6	Symmetric phase . . . . .	85

---

6.7	Chiral phase transition without baryons . . . . .	87
6.8	Chiral symmetry breaking with baryons . . . . .	92
<b>7</b>	<b>Walecka model with magnetic field</b>	<b>97</b>
7.1	Lagrangian . . . . .	98
7.2	Charged baryons . . . . .	100
7.3	Neutral baryons . . . . .	104
7.4	Binding energy . . . . .	105
7.5	Large $N_c$ . . . . .	108
<b>8</b>	<b>Conclusion</b>	<b>111</b>
<b>A</b>	<b>Appendix</b>	<b>117</b>
A.1	Chiral Symmetry of the NJL Lagrangian . . . . .	117
A.2	Noether's theorem . . . . .	118
A.3	Imaginary time formalism and thermal field theory . . . . .	119
A.4	Chern–Simons 5-form . . . . .	126
A.5	Approximations close to the baryon onset . . . . .	126
	<b>Bibliography</b>	<b>131</b>

# Overview

Considering only quarks with masses small compared to the characteristic scale of Quantum Chromodynamics (QCD),  $\Lambda_{\text{QCD}} \approx 200 \text{ MeV}$ , the QCD Lagrangian exhibits an approximate chiral symmetry. Exploiting the mechanism of spontaneous symmetry breaking has led to important progress in understanding QCD, in particular in the low energy regime. For instance, the pions can be identified with the (pseudo-) Goldstone bosons of QCD with two flavors - one for each broken generator of the axial transformations. This thesis will focus on the spontaneous breaking of chiral symmetry under the influence of strong magnetic fields.

Strong magnetic fields relevant for QCD are realized in two important instances: non-central relativistic heavy ion collisions performed at the Relativistic Heavy Ion Collider (RHIC) in Brookhaven as well as at the Large Hadron Collider (LHC) near Geneva, and magnetars, a special type of compact astrophysical objects. In the former the magnetic field in the interaction region produced by the two colliding nuclei reaches up to  $10^{18} \text{ G}$  [164]. In the reaction region the temperature is expected to be above the deconfinement temperature while the chemical potential is small, hence a so-called quark gluon plasma (QGP) is formed. Compact stars probe another region of the QCD phase diagram in the in the plane of chemical potential and temperature, namely that of small temperatures and (quark) chemical potentials of the order of the QCD scale. From observations of gamma ray bursts coming from magnetars

combined with the measured spin down of magnetars the value of the magnetic field on the surface of the star is estimated to be about  $10^{15}$  G [57]. Using the virial theorem one can infer that the field in the core may reach up to  $10^{18} - 10^{19}$  G [118].

After converting Gaußian units to natural Heaviside–Lorentz units one finds that  $10^{18}$  G  $\sim (140 \text{ MeV})^2$ , i.e. the strength of the afore mentioned magnetic fields is comparable to the QCD scale and might therefore have observable consequences in the physics of the experiments at heavy ion colliders and on the observations of magnetars. For example an observed charge separation in the quark gluon plasma formed in non-central relativistic heavy ion collisions might be due to the so-called chiral magnetic effect [112, 73, 113]. In the case of compact stars the internal structure is under much debate in particular the question whether quark matter is present in the core of these stars or entire quark stars might exist. Furthermore we ask if that matter is chirally symmetric or possibly in a superfluid state.

From a theoretical perspective a description of both of these QCD "laboratories" is very challenging. Since QCD is an asymptotically free theory, the coupling only becomes small at asymptotically high temperature or chemical potential, hence the application of perturbative methods for the description of heavy ion collisions and magnetars is rather limited. However perturbative methods serve as starting points for extrapolations to the relevant intermediate energy regimes. For example, at asymptotically high temperatures it is well known that QCD is in the quark gluon plasma phase. The quark gluon plasma produced in heavy ion collider experiments turned out to be rather strongly coupled (sQGP) and may be described by hydrodynamics. The ratio of viscosity over entropy density extracted from the measurements of the elliptical flow in peripheral collisions is lower than that of any other known substance. So far only the application of holographic methods succeeded in predicting such a small value [143]. Note that the  $\mathcal{N} = 4$  super Yang–Mills theory translated via the so-called AdS/CFT correspondence to a super gravity theory is even infinitely strongly coupled [123]. The only first principle calculations available at the moment are offered by lattice QCD. However, calculating transport properties is extremely difficult in lattice QCD. Furthermore the applicability of lattice QCD (lQCD) is limited to the region  $\mu/T \ll 1$  in the QCD phase diagram due to the so-called sign problem.

At asymptotically large chemical potentials and small temperatures, where perturbative QCD (pQCD) is applicable, 3-flavor QCD matter is in the so-called color-flavor-locked (CFL) phase [5, 6]. A diquark condensate breaks the local color symmetry

as well as the global chiral symmetry down to the diagonal subgroup  $SU(3)_{c+L+R}$ . Also the transition temperature to quark matter (QM) at asymptotic chemical potential can be computed from first principles [38, 39, 160] and turns out to be second order. Taking corrections due to gluons at finite but still very large chemical potential into account the transition becomes first order [83, 124].

If upon increasing the chemical potential the hadronic phase is superseded by normal quark matter, by CFL or some other color superconducting phase is a matter of debate. For the time being the description of this part of the QCD phase diagram where all compact stars reside has to rely on model calculations.

At low energies an effective theory called chiral perturbation ( $\chi$ PT) theory is available [176]. It is found by formulating the most general Lagrangian that shares the same symmetries with QCD and obeys other quantum field theory principles such as unitarity. Its fundamental excitations describe the Nambu–Goldstone bosons of chiral symmetry.

The various energy regimes discussed above and the tools that are used to describe the physics there are summarized in the QCD phase diagram in the  $T - \mu$ -plane Fig. 0.1.

The study of the spontaneous breaking of chiral symmetry in the parameter space of temperature, chemical potential and magnetic field in two very prominent models will constitute the core of this thesis. The first - somehow more conservative approach - will utilize the Nambu–Jona-Lasino (NJL) model [131, 132, 174, 102], which is a field theoretical model sharing the same symmetries with QCD. However, since the interaction of quarks via gluon exchange is replaced by a four fermion interaction, the model can only be expected to share qualitative features with QCD. Most notably, the quarks are not confined. Moreover, the model is nonrenormalizable. Therefore quantitative results will depend on the regularization scheme and the value of the cutoff parameter. The second is the Sakai–Sugimoto model [156, 157], which employs a non-supersymmetric, non-conformal version of the gauge–gravity duality, which exhibits a confinement deconfinement transition. In a certain limit of the model parameters the Sakai–Sugimoto model is conjectured to be dual to a nonlocal NJL model [11]. This thesis aims at calculating the critical surface for chiral symmetry breaking in the parameter space of temperature, chemical potential and magnetic field in both models and compare the respective phase diagrams. The main idea is to gain insight and reliability by extracting common properties and dif-

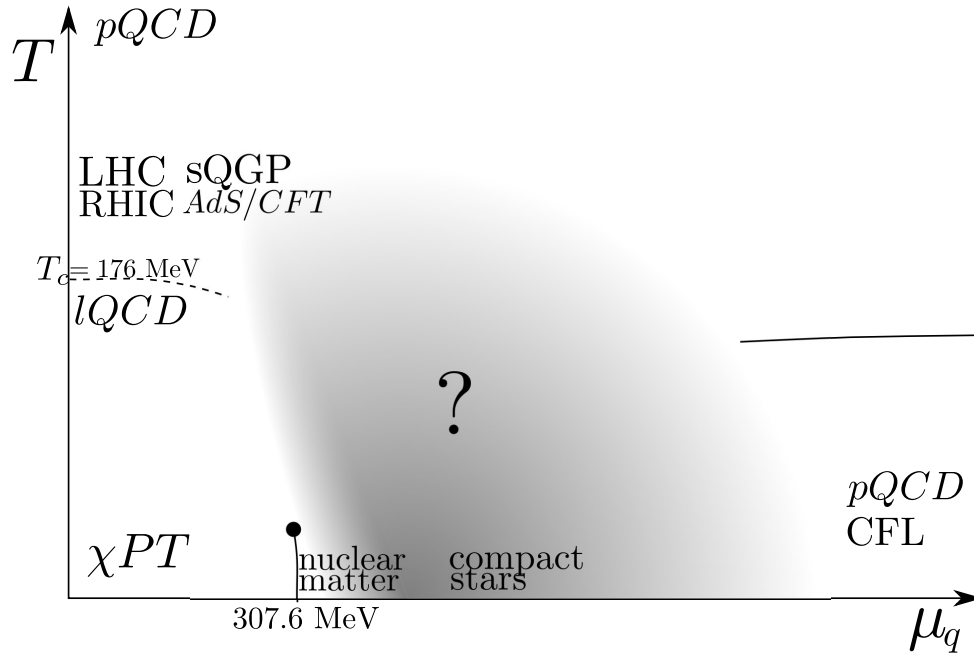


Figure 0.1: The QCD phase diagram. The solid line starting at  $T = 0$ ,  $\mu_q = 307.6$  MeV shows the well-studied first order liquid-gas transition to nuclear matter. The short solid line in the lower right corner denotes the first order transition temperature to the QM phase. The question mark subsumes all the open issues regarding the QCD phase diagram. Some of these are given in the following list: Is the deconfinement crossover known from lQCD and denoted by the dashed line turning into a first order transition at finite  $\mu$ ? Does chiral symmetry restore for some  $\mu$  at  $T = 0$ ? What is a compact star made of/which phases are found between the well-known CFL phase and the nuclear matter phase?

ferences of the results of both approaches.

Chapter 1 serves as an historical introduction to chiral symmetry in the pre-QCD era. We will proceed with discussing the spontaneous breaking of chiral symmetry in chapter 2 utilizing the NJL model of nucleons as an example. We will basically follow the original work by Nambu and Jona-Lasino but utilizing the 1PI effective action. This has the advantage that on the one hand everything is derived from one single generating functional and on the other hand renders the transition to finite temperature and density, which will be needed later on, smooth. After a brief overview over the developments of the 60's and 70's of the last century that led to the formulation QCD we analyse the thermodynamics of the NJL model, which we then

reinterpret as a model of quarks in chapter 3. In chapter 4 we introduce a geometric, i.e. holographic realization of chiral symmetry breaking – the Sakai–Sugimoto model. Chapters 5 and 6 constitute the core of this thesis and are based on the publications [145, 146, 147] by the author together with his supervisors Anton Rebhan and Andreas Schmitt. By solving the Dirac equation in a background magnetic field the Landau level quantization is demonstrated and immediate consequences of it are discussed. First we will analyse the phase diagram for chiral symmetry breaking in the NJL model and then compare this to the corresponding one in the Sakai–Sugimoto model. We will show that both models exhibit the so-called magnetic catalysis at vanishing chemical potential and finite temperature: the magnetic field enhances chiral symmetry breaking. Surprisingly at finite chemical potential and relatively small temperatures an external magnetic field has exactly the opposite effect: It can restore chiral symmetry in the system. In [145] this behavior was termed inverse magnetic catalysis. We will thoroughly discuss the physics behind inverse magnetic catalysis. Furthermore, since the Sakai–Sugimoto model allows for incorporating baryons, we will investigate how baryons affect the chiral phase transition at finite magnetic field and chemical potential but zero temperature. In order to compare our results with a field theoretical model describing baryons we will employ the Walecka model at finite magnetic field, see chapter 7, before we close with a concluding discussion and final remarks in chapter 8.





# A hidden symmetry

Symmetry has been one of the most important guiding principles for studying elementary particle physics. In particular the development of the theory of strong interaction called Quantum Chromodynamics (QCD), which together with the theory of electro-weak interactions constitutes the standard model of elementary particle physics, benefited tremendously from exploiting global as well as local (gauge) symmetries.

Shortly after the discovery of the neutron Werner Heisenberg introduced the concept of isospin<sup>1</sup> in 1932 [103]. The neutron and proton are nearly degenerate with respect to their masses

$$m_N \approx 939 \text{ MeV}/c^2, \quad m_P \approx 938 \text{ MeV}/c^2. \quad (1.1)$$

Neglecting electromagnetic and weak interactions one could regard proton and neutron as states of a single entity – the nucleon (a two component wavefunction). The simplest and nontrivial guess suggests that the nucleon is a doublet in the funda-

---

<sup>1</sup>The term isospin was coined by Eugene Wigner in his 1937 paper [178].

mental representation of  $SU(2)$ :

$$\psi_N = \begin{pmatrix} \psi_p \\ \psi_n \end{pmatrix}, \quad \psi_{\bar{N}} = \begin{pmatrix} -\psi_{\bar{n}} \\ \psi_{\bar{p}} \end{pmatrix}, \quad (1.2)$$

$$I = \frac{1}{2}, \quad I_i = \frac{1}{2}\sigma^i, \quad (1.3)$$

$$Q = I_3 + \frac{1}{2}B, \quad (1.4)$$

where the wave function of the nucleon  $\psi_N$  is written as doublet in isospin space, the wave functions of the proton  $\psi_p$  and of the neutron  $\psi_n$  are Dirac spinors, and a bar denotes the respective anti-particle.  $I$  denotes the total isospin and  $I_i$  the generators of  $SU(2)$  represented by the Pauli matrices  $\sigma^i$  with  $i = 1, 2, 3$ . In the last line we relate the charge with the third component of the isospin and baryon number  $B$ , which is a conserved quantity. Note that the factor  $1/2$  is needed in order to yield the center of charge of the nucleon doublet.

In Heisenberg's treatment of the nuclear interactions the isospin formulation has merely the purpose of bringing formulae into concise form. No physical implications were drawn from it, in particular the interactions are not isospin symmetric. However, Heisenberg was thinking of a spinless electron obeying Bose statistics that exchanges charge between the proton and the neutron. After Fermi explained  $\beta$ -decay by emission of an electron and an anti-neutrino from the neutron [64], Tamm and Iwanenko independently explained the interactions of neutrons and protons via simultaneous emission and absorption of an electron and an anti-neutrino in 1934 [169, 107]. These pictures did not succeed in explaining experimental data, in particular the range and magnitude of the interaction. In the same year Yukawa remedied these deficiencies by introducing massive charged field quanta that are exchanged between proton and neutron[187] - meson exchange theory was born. Yukawa predicted the existence of a particle with one unit of elementary charge and a mass 200 times that of an electron and its anti-particle, which were later called the charged pions  $\pi^\pm$ . Originally the pion was thought of as the scalar potential component of a four vector potential in analogy with electrodynamics. However, after their discovery experiments revealed the pseudoscalar nature of the pions. In isospin formulation, which Yukawa also adopted, the pions act as ladder operators on the nucleon wave function increasing or decreasing the third component of isospin by one unit and thereby increasing or decreasing the charge.

In the following year proton–proton scattering experiments [172] and their analysis [35] revealed that nucleon–nucleon interactions are charge independent. In [35] it was shown that after correcting the data of [172] on proton–proton scattering for Coulomb repulsion, the parameters were the same as for the comparable proton–neutron scattering in the  $^1S$  channel. Assuming that the same is true for neutron–neutron scattering one concludes that the theory describing the interaction of these particles must be symmetric under the action of  $SU(2)$  that continuously turns protons into neutrons and vice versa. A first attempt towards such a theory of nuclear structure was published in the same volume of Physical Review [46].

The discovery of the muon [133] with a mass 207 times that of the electron in 1937 immediately drew attention to Yukawa's meson exchange theory. However, it turned out that the muon does not interact strongly with the nucleons – the charged pions were discovered several years later in 1947 [137, 119]. Nevertheless, the misinterpretation of the muon's nature gave an important impetus to the theoretical development of the theory of strong interactions. Kemmer combined the meson exchange theory with isospin symmetry [111] – at that time known as charge independence hypothesis – and showed that in order to satisfy isospin symmetry a neutral meson – the neutral pion  $\pi^0$  – has to exist. The neutral pion predicted by Kemmer was after the proton the second particle to be decisively discovered in an accelerator experiment in 1949 [30] (only preliminary evidence for its existence was found in cosmic ray observations). Note, that the masses of the pions are  $m_{\pi^\pm} \approx 140 \text{ MeV}/c^2$  and  $m_{\pi^0} \approx 135 \text{ MeV}/c^2$ , hence they are light compared to the masses of the nucleon states. This is the first historical instance that proved the predictive power of the concept of isospin symmetry.

In 1954 by Chinowsky and Steinberger [49] demonstrated that pions are pseudoscalar particles. Therefore, the Lagrangian describing the interaction of nucleons with pions can be written as as

$$\mathcal{L}_{\text{int}} = ig_{\pi NN} \pi^i \bar{\psi}_N \gamma_5 \sigma^i \psi_N, \quad (1.5)$$

$$\pi^\pm = \frac{1}{\sqrt{2}} (\pi^1 \mp i\pi^2), \quad \pi^0 = \pi^3, \quad (1.6)$$

with  $g_{\pi NN}^2/4\pi = 15$  as a commonly accepted value [155].

In the same year as the charged pions also other particles, later called kaons and hyperons, were discovered, which behaved somewhat strangely [153]: they were

frequently produced nucleon scattering events but had a rather long life time. In [75] Gell-Mann and independently Nishijima in [128] explained this behavior. One of the most important corner stones of his work was to retain isospin conservation in strong interactions. Gell-Mann supposed that the strange fermions have integral isospin, while strange bosons have half-integral isospin. This concept is called "displaced isospin multiplets". For example the  $K^+$  and the  $K^0$  constitute a isospin doublet. In order to complete the picture Gell-Mann postulated the existence of  $K^-$  and  $\bar{K}^0$ <sup>2</sup>. The  $\Lambda^0$  is an isospin singlet, while the two hyperons  $\Sigma^+$  and  $\Sigma^-$  are part of an isospin triplet, hence Gell-Mann and Pais postulated a  $\Sigma^0$  particle [82]. Furthermore  $\Xi^-$  should be part of a isospin doublet, hence a  $\Xi^0$  should exist. All these particles were indeed found later on, proving again the power of isospin symmetry.

A further important hypothesis is "associated production", i.e. the strange particles are always produced in even numbers if the primary particles are non-strange. After the collision the strange particles are moving away from each other, rendering the inverse reaction impossible. Provided that the coupling is minimal, electromagnetism cannot change isospin. The last resort for the decay of strange particles are thus some hypothetical weak interactions ("possibly similar in nature to *beta*-decay"), explaining the long lifetime of strange particles. Furthermore, Gell-Mann postulated that  $|\Delta I_3| = 1/2$  in weak decays in order to explain certain decay processes. Each particle is labeled by three quantum numbers, each of which is conserved in strong interactions,  $I$ ,  $I_3$  and  $Q$ , in contrast to the previous picture of charge independence, where  $Q$  and  $I_3$  were not independent, see equation (1.4). In [76] this is summarized in a new formula for the charge of hadrons

$$Q = I_3 + \frac{1}{2}(B + S), \quad (1.7)$$

called Gell-Mann–Nishijima formula<sup>3</sup> where  $1/2(B + S)$  now accounts for the center of charge of the displaced isospin multiplets and  $S$  quantifies the displacement of the multiplets. Consequently strangeness  $S$  must necessarily be conserved in strong

<sup>2</sup>In the original papers there are two groups of four strange mesons degenerate in mass but distinct in parity, which accounts for the experimental fact that the  $K^+$  decays into three as well as two pions. This is due to the by then unresolved  $\theta$ - $\tau$  puzzle.

<sup>3</sup>Actually [135] is the reference where formula (1.7) was published first. Strangeness is called  $V$ -charge there, since strange particles were usually called  $V$ -particles at that time. Nishijima's findings were very nicely summarized in [136].

interactions and the  $|\Delta I_3| = 1/2$  rule in weak decay translates to  $|\Delta S| = 1$ . The sum  $B + S$  is called hypercharge  $Y$ .

After the conjecture by Lee and Yang [120] that parity might be violated in weak interactions, had been confirmed by the experiments performed by Wu [186], theorists were prompted to assume that anti-neutrinos participating in nuclear  $\beta$  decay are right handed only. Starting with an current–current interaction describing the beta decay of the neutron, one is led to the consequence that the emitted electrons are left handed and that they are fully left polarized as their velocity approaches the speed of light in full accordance with Wu's experiments. Equivalently one might replace the electron  $\psi_e$  in the interaction Lagrangian by  $P_L\psi_e$ , where  $P_{L/R}$  denotes the projection operator to left- and right-handed particles respectively

$$P_{L/R} = \frac{1}{2}(1 \mp \gamma_5). \quad (1.8)$$

Feynman and Gell-Mann [66] went further by proposing that all fermions appearing in the interaction Lagrangian are restricted by  $P_L$ . Hence,  $\beta$ -decay would be described by

$$\sum_i C_i (\overline{P_L\psi_n}\mathcal{O}_iP_L\psi_p) (\overline{P_L\psi_\nu}\mathcal{O}_iP_L\psi_e), \quad (1.9)$$

where  $C_i$  are coupling constants and  $\mathcal{O}_i$  denote all possible elements of the Dirac algebra. However, as a direct consequence of this assumption only vector and axial-vector couplings remain after applying Dirac algebra rules, leading to a single coupling constant  $G$

$$\frac{1}{\sqrt{2}}G (\overline{\psi_n}\gamma^\rho P_L\psi_p) (\overline{\psi_\nu}\gamma_\rho P_L\psi_e). \quad (1.10)$$

Furthermore a universal coupling for all weak interactions was proposed, for example also the interaction Lagrangian for muon decay reads

$$\frac{1}{\sqrt{2}}G (\overline{\psi_\mu}\gamma^\rho P_L\psi_{\nu'}) (\overline{\psi_\nu}\gamma_\rho P_L\psi_e). \quad (1.11)$$

Of course the effective coupling constants measured in experiments might differ due to renormalization effects, for example due to the strong interactions involved. One can fix  $G$  by requiring that it equals the measured coupling constant of the vector part of nuclear  $\beta$ -decay, the Fermi coupling constant  $G_F$ , which can be obtained from  $^{14}\text{O}$  decay. From the lifetime of the muon one can also extract the effective

coupling  $G_\mu$  and it turns out that its value is remarkably close to the value of  $G_F$ . In pure leptonic decays there are no large terms known that are capable of renormalizing the coupling. However, in the case where nucleons are involved one expects renormalization due to virtual pions that nucleons can emit but obviously this is not the case. There exists an analogous situation in electromagnetic interaction of protons: the cloud of virtual pions does not disturb the coupling  $e$  of photons to protons. Of course the charge distribution measured by electron scattering is changed as the electron's energy increases but the *total charge* measured at low energies is not. More precisely, the Ward–Takahashi identity guarantees that the field strength renormalization and the vertex renormalization cancel and hence the electromagnetic form factor is not renormalized. This is related to gauge invariance which guarantees the conservation of the electric current to which *all charged particles* contribute. More formally, while the second term and thus the whole expression of

$$J_\mu^{\text{el}} = \bar{\psi}_N \gamma_\mu \left( \frac{1}{2} + I_3 \right) \psi_N \quad (1.12)$$

is not conserved, the expression

$$J_\mu^{\text{el}} = \bar{\psi}_N \gamma_\mu \frac{1}{2} \psi_N + \bar{\psi}_N \gamma_\mu I_3 \psi_N + i \left[ \pi^\dagger I_3^{(\text{adj})} \nabla_\mu \pi - (\nabla_\mu \pi)^\dagger I_3^{(\text{adj})} \pi \right] \quad (1.13)$$

is. Likewise, in order to explain the agreement of  $G_F$  and  $G_\mu$ , Feynman and Gell-Mann proposed that the nuclear part of the isospin changing vector current, assumes the form

$$J_\mu^{V,\pm} = \bar{\psi}_N \gamma_\mu I_\pm \psi_N + i \left[ \pi^\dagger I_\pm^{(\text{adj})} \nabla_\mu \pi - (\nabla_\mu \pi)^\dagger I_\pm^{(\text{adj})} \pi \right], \quad (1.14)$$

is conserved and replaces the corresponding term in (1.10). In absence of electromagnetic interactions this simply reflects the invariance under global  $U(1) \times SU(2)$  transformation of strong interactions, i.e. baryon number conservation and isospin symmetry. The conserved currents corresponding to these symmetries are on the one hand the isospin singlet term in (1.13) and on the other hand the isotriplet formed by the second and third term in (1.13) together with (1.14). The addition of the pion terms immediately yields further possible reactions, e.g. the pion  $\beta$ -decay  $\pi^\pm \rightarrow \pi^0 + e^\pm + \bar{\nu}_e$  with a predicted branching ratio of about  $10^{-8}$ , which was observed 1962 at CERN [54]. Note, this again was a consequence of imposing isospin symmetry.

One now might wonder whether the vector current conservation hypothesis can also be extended to the axial current. Experiments indicated a ratio of the Fermi and the Gamow-Teller constant squared of about 1.3. However, due to experimental uncertainties  $G_F^2/G_A^2 = 1$  was not excluded, in which case also the axial current would be conserved by the same arguments as before. If this turns out not to be the case, the deviation from unity is probably due to renormalization effects, nevertheless the smallness of these effects calls for an explanation. Feynman and Gell-Mann suggested to investigate the possibility of a conserved axial current and the involved symmetry groups further.

The possibility of a divergenceless axial current was immediately ruled out in [170, 84]: The  $V - A$  theory also predicts the pure leptonic decay  $\pi^\pm \rightarrow \mu^\pm + \bar{\nu}_\mu$  as well as  $\pi^\pm \rightarrow e^\pm + \bar{\nu}_e$  with a branching ratio  $1.233 \times 10^{-4}$ , which can be understood as resulting from the virtual process in which the pion dissociates into a nucleon loop, which then decays into muon and anti-neutrino. In [170] Taylor demonstrated, that neither process can take place in case of  $\partial_\mu J_A^\mu = 0$ . Since the pions form an isotriplett pseudoscalar, they can be created by an axial isospin current. This matrix element can be parametrized by

$$\langle 0 | J_\mu^{A,i}(x) | \pi^j(p) \rangle = -i p_\mu f_\pi(p^2) \delta^{ij} e^{-ip \cdot x}, \quad (1.15)$$

where  $f_\pi(p^2 \equiv m_\pi^2) = 93 \text{ MeV}$  denotes the pion decay constant. Taylor argued that in the current-current interaction describing leptonic decay the term in Eq. (1.15) is contracted with the lepton current, thus only the component parallel to  $p_\mu$  can contribute. But because of  $\partial \cdot J^{A,i} = 0$  this amplitude must vanish. Put in simpler terms, taking the divergence on both sides of (1.15), we observe that the  $\partial \cdot J^{A,i}$  can only vanish in the limit of massless pions.

The absence of an electronic decay mode was regarded as a feature of the conserved axial vector proposal, since at that time it appeared to be ruled out experimentally, however the absence of the most probable decay mode into muons would be disastrous for the  $V - A$  theory. The conserved vector current hypothesis responsible for explaining both decay modes would have to be dropped after all, leaving the equality of  $G_\mu$  and  $G_F$  as an unresolved mystery. Fortunately experiments performed at CERN in the end of the same year in which Feynman's and Gell-Mann's paper was published showed a clear signal of the electronic decay events with a branching ratio

close to the theoretical value. This first stringent test of the  $V - A$  theory marks also the first major physical discovery at CERN [63].

Goldberger and Treiman in [84] also objected to the conserved axial current hypothesis. The matrix element for the axial part of nuclear beta decay reads

$$\mathcal{M}_A = \overline{\psi}_e \gamma^\mu P_L \psi_\nu \langle N | J_\mu^{A,+} | N \rangle. \quad (1.16)$$

The nucleon part demanding Lorentz invariance can be parametrized in terms of form factors by

$$\langle N | J_\mu^{A,+}(q) | N \rangle = \overline{\psi}_p(p) \left[ \gamma_\mu \gamma^5 F_1^5(q^2) + \frac{i\sigma_{\mu\nu} q^\nu}{2m_N} \gamma^5 F_2^5(q^2) + q_\mu \gamma^5 F_3^5(q^2) \right] \psi_n(n), \quad (1.17)$$

where  $q = p - n$  is the momentum transfer and  $G_A = F_1^5(q^2 = 0)$  is the Gamov–Teller coupling constant. The induced tensor term is irrelevant for the following discussion and is excluded experimentally. Imposing the conservation hypothesis and using the Dirac equation  $\gamma \cdot k_N \psi_N = m_N \psi_N$  we find

$$0 = \overline{\psi}_p(p) \left[ 2m_N F_1^5(q^2) + q^2 F_3^5(q^2) \right] \gamma^5 \psi_n(n) \Rightarrow F_3^5(q^2) = -\frac{2m_N F_1^5(q^2)}{q^2} \quad (1.18)$$

The computation of the matrix element for the discussed process yields a ratio of the induced pseudoscalar coupling and the effective axial vector coupling, which is excluded experimentally and would be far too large in particular at very small momentum transfer.

Nevertheless, one can draw valuable conclusions from this calculation. Let us rewrite the axial vector current inserting the result (1.18)

$$\langle N | J_\mu^{A,+}(q) | N \rangle = \overline{\psi}_p(p) \left[ \gamma_\mu \gamma^5 F_1^5(q^2) - \frac{2m_N q_\mu}{q^2} \gamma^5 F_1^5(q^2) \right] \psi_n(n). \quad (1.19)$$

The last term in brackets attracted Yoichiro Nambu's curiosity [129], because if it existed, it would indicate an intermediate massless charged pseudoscalar particle. No such particle had been found, but there exists the relatively light pion, which possesses exactly these quantum numbers. If we, despite of Taylor's arguments, equate this term with a process that describes the coupling of pions to nucleons as in (1.5) and the subsequent decay described by (1.15) we find

$$\begin{aligned} -\overline{\psi}_p(p) \frac{2m_N q^\mu}{q^2} \gamma^5 F_1^5(q^2) \psi_n(n) &= \sqrt{2} g_{\pi NN} \overline{\psi}_p(p) \gamma^5 \psi_n(n) \frac{i}{q^2} i \sqrt{2} q^\mu f_\pi \\ &\Rightarrow m_N G_A = g_{\pi NN} f_\pi, \\ g_{\pi NN} f_\pi &= 1276.83. \end{aligned} \quad (1.20)$$



The identity (1.20) is the Goldberger–Treiman relation, which was obtained in [85, 86] using a completely different method, namely dispersion relations, in order to compute the pion decay. The Goldberger–Treiman relation is in rather good agreement with experiment. Using the currently accepted value  $G_A = 1.27$  and an averaged nucleon mass  $m_N = 938.92$  [24], the left hand side yields  $m_N G_A = 1192.42$ . The original approach as well as the calculation presented here rest on very crude and partially contradicting assumptions. For example, for an exactly conserved axial current  $G_A = 1$  and the agreement with experiment would get worse. Nambu proposed instead of using the exactly conserved axial current a *partially* conserved axial current in order to accommodate his derivation of the Goldberger–Treiman relation and the objections of Taylor, Goldberger and Treiman against a conserved axial current. Instead of (1.19) the form

$$\langle N | J_\mu^{A,+}(q) | N \rangle = \bar{\psi}_p(p) \left[ \gamma_\mu \gamma^5 F_1^5(q^2) + \frac{2m_N q_\mu}{q^2 - m_\pi^2} \gamma^5 \tilde{F}_3^5(q^2) \right] \psi_n(n), \quad (1.21)$$

for the axial current together with the conditions

$$F_1^5(0) = G_A \approx \tilde{F}_3^5(0), \quad (1.22)$$

$$F_1^5(q^2) \sim \tilde{F}_3^5(q^2) \quad \text{for } q^2 \ll m_\pi^2, \quad (1.23)$$

should be used.

Gell-Mann and coworkers [80, 26, 25] arrived at similar conclusions from analysing the so-called  $\sigma$ -model. However, Nambu's conclusions drawn from these observation were more far reaching. The most important insight was uncovering the role the pions played in the *partially conserved axial current* (PCAC) hypothesis, which was mainly guided by the experience gained while working in the field of superconductivity and BCS–Bogoliubov theory. We will follow Nambu's reasoning in the next chapter.



## Chiral symmetry breaking

Let us first discuss the heuristic picture of superconductivity or superfluidity. Given the thermodynamic potential of a fermionic many body system at  $T = 0$

$$\Omega = E - \mu N,$$

one observes that there exists an instability of the Fermi surface. Assuming for the moment that the particles are free, one can place two fermions above the Fermi surface without any energy penalty: while  $E$  is raised by  $2\mu$ , the second term compensates this increase because  $N \rightarrow N + 2$ . Provided that there exists a net attractive interaction between the fermions, one could lower  $\Omega$  via the binding energy of these so-called Cooper pairs [52]. The Cooper pairs, having bosonic quantum numbers, can form a Bose-Einstein condensate and are responsible for the emergence of an energy gap of the quasi-particles (the "dressed" fermions) [16], see also Eqs. (2.1)–(2.3). These quasi-particles are a coherent mixture of particles and holes described by a so-called Bogoliubov transformation, which was introduced in [31] in order to diagonalize the Hamiltonian of the problem. Here lies the crux of the BCS–Bogoliubov theory: The quasiparticles are not eigenstates of charge in case of a superconductor or fermion number in the case of a superfluid, although one started from a symmetric Hamiltonian. For example, upon accelerating a quasiparticle it becomes increasingly electron like. It can deposit or pick up charge in the

particle bath constituted by the Cooper pairs, which are themselves charged under the respective local or global symmetry group. In consequence the expression of the energy gap is gauge dependent and so is the derivation of the Meissner effect, which in turn is often viewed as defining a superconductor as a perfect diamagnet. This led several theorists to doubt the correctness of the BCS–Bogoliubov theory. In the early attempts to circumvent this obstacle, e.g. [9, 8], it was soon realized that when treating the Meissner effect in a gauge invariant fashion one encounters collective excitations of bound quasi-particle pairs that behave phonon like, i.e. gapless bosonic modes. However, in the case of a superconductor, after taking the Coulomb interaction of electrons into account, these gapless modes are absorbed in the usual plasma mode<sup>1</sup>. In a superfluid with no long range forces this does not happen. Nambu refined the gauge invariant discussion of the Meissner effect [130] by introducing techniques from elementary particle physics, i.e. a Dyson–Schwinger formulation of the problem and discussing Ward–Takahashi identities. The following conclusions are of relevance for our discussion here: due to the condensation of Cooper pairs, regarding the states of the system the symmetry of the underlying theory is spontaneously broken. Also there is no manifestly conserved charge. This can be seen from the equations of motion of the quasi-particles

$$E\Psi = \epsilon_p \sigma^3 \Psi + \phi \sigma^1 \Psi, \quad (2.1)$$

$$\Psi = \begin{pmatrix} \psi_{p,\uparrow} \\ \psi_{-p,\downarrow}^* \end{pmatrix}, \quad (2.2)$$

$$\Rightarrow E_p = \pm \sqrt{\epsilon_p^2 + \phi^2} \quad (2.3)$$

where  $\epsilon_p$  is the kinetic energy measured from the Fermi surface and  $\phi$  is the energy gap. The first component  $\psi_{p,\uparrow}$  of the spinor  $\Psi$  correspond to a quasi-electron with momentum  $p$  and spin up while  $\psi_{-p,\downarrow}^*$  corresponds to a quasi-electron hole with momentum  $p$  and spin up. The two component spinor  $\Psi$  is an element of the so-called Nambu–Gorkov space, a notation which is particularly convenient when treating su-

<sup>1</sup>This ensures that the full particle spectrum in a superconductor is indeed gapped. Note that this is also the first historical instance where the Anderson–Kibble–Higgs mechanism was described. The plasma frequency can be read as a photon mass. Furthermore, there are also static screening masses. The longitudinally polarized photons acquire the so-called Debye mass. The Meissner effect can also be understood by giving the photon an effective (Meissner) mass. In a pioneering work by Anderson [10] these ideas were transferred to elementary particle physics in order to reconcile gauge symmetry with a massive Yang–Mills field.

perconductivity in a gauge invariant manner. Observe that the off-diagonal energy gap term couples quasi-particle with quasi-particle holes. Moreover, it takes an energy  $E \geq 2\phi$  to excite a quasi-particle leaving a quasi-particle hole with opposite momentum charge and spin.

The gapless modes mentioned above necessarily emerge, in order to restore the symmetry in the sense that they ensure the conservation of the Noether current corresponding to the symmetry of the Lagrangian. "In general, they are excited when a quasi-particle is accelerated in the medium, and play the role of a back-flow around the particle, compensating the change of charge localized on the quasi-particle wave packet" [131].

Let us now make a connection to the case discussed at the end of the preceding section. The conservation of an axial current triplet should be related to a symmetry of a fundamental strong interaction Lagrangian, i.e. invariance with respect to axial transformations given by

$$\psi_N \rightarrow \exp(i\alpha^j \gamma^j \gamma^5) \psi_N.$$

Together with the well known isospin symmetry  $SU(2)_V$ , this is equivalent to saying that left- and right-handed components of the nucleon transform independently under  $SU(2)$ . Therefore it is called the chiral symmetry group  $SU(2)_L \times SU(2)_R$ . However, even in a free theory describing nucleons such a hypothetical symmetry is explicitly broken by a finite nucleon mass, simply because it couples left- and right-handed components, which can be seen from the equations of motion for free fermions

$$E\psi_{(M)} = \alpha^j \frac{1}{i} \nabla^j \psi_{(M)} + \gamma^0 M \psi_{(M)},$$

in a chiral representation of the Dirac matrices

$$\gamma^0 = \begin{pmatrix} 0 & 1 \\ 1 & 0 \end{pmatrix}, \quad \alpha^j = \gamma^0 \gamma^j = \begin{pmatrix} -\sigma^j & 0 \\ 0 & \sigma^j \end{pmatrix}, \quad \gamma^5 = \begin{pmatrix} -1 & 0 \\ 0 & 1 \end{pmatrix}.$$

We will now discuss the relation of massive Dirac spinors  $\psi_{(M)}$  to massless fermions  $\psi_{(0)}$ . Using translational invariance in  $x$  and anticipating the positive and negative frequency solutions we start with an ansatz

$$u_{(M)}^s(\vec{k}) e^{-ikx}, \quad v_{(M)}^s(\vec{k}) e^{ikx}, \quad k^0 > 0$$

where  $u_{(M)}^s(\vec{k})$  and  $v_{(M)}^s(\vec{k})$  only depend on the 3-momentum  $\vec{k}$  and contain two component spinors  $\xi^s$  labeled by  $s = \pm$  and obeying  $\xi^{s,\dagger} \xi^{s'} = \delta_{s,s'}$ . With the ansatz above

the Dirac equation becomes

$$(\not{k} - M)u = 0, \quad -(\not{k} + M)v = 0.$$

Hence a complete set of normalized solutions is given by<sup>2</sup>

$$\begin{aligned} u_{(M)}^s(\vec{k}) &= \frac{1}{4V\sqrt{k_0(k_0 + M)}} (\not{k} + M) \phi^s, \\ v_{(M)}^s(\vec{k}) &= \frac{1}{4V\sqrt{k_0(k_0 + M)}} (\not{k} - m) \eta^s, \\ &\Rightarrow k_0 = \sqrt{k^2 + M^2}, \\ \phi^s &= \begin{pmatrix} \xi^s \\ \xi^s \end{pmatrix}, \quad \eta^s = \varphi_s \gamma^5 \phi^{-s}, \end{aligned}$$

with  $\varphi^s$  a phase factor not be specified for now. These states are orthogonal in the sense

$$\begin{aligned} \int d^3x u_{(M)}^{s\dagger}(\vec{k}) u_{(M)}^{s'}(\vec{k}') e^{-i(k'-k)x} &= \delta_{s,s'} \delta_{\vec{k},\vec{k}'}, \\ \int d^3x v_{(M)}^{s\dagger}(\vec{k}) v_{(M)}^{s'}(\vec{k}') e^{i(k'-k)x} &= \delta_{s,s'} \delta_{\vec{k},\vec{k}'}, \\ \int d^3x v_{(M)}^{s\dagger}(\vec{k}) u_{(M)}^{s'}(\vec{k}') e^{-i(k'+k)x} &= 0, \end{aligned}$$

The relative sign of left- and right-handed components in the spinor  $\eta^s$  is chosen in order to yield a well defined limit  $\vec{k} \rightarrow 0$ . The reason for inverting the two component spinor index is chosen in hindsight on the quantization of the Dirac field, which amounts to expanding the spinor fields with respect to these eigenspinors augmented with annihilation ( $a, b$ ) and creation operators ( $a^\dagger, b^\dagger$ ) as follows

$$\psi_{(M)}(x) = \sum_{\vec{k}, s} \left( u_{(M)}^s(\vec{k}) a_{(M)}(\vec{k}, s) + v_{(M)}^s(\vec{k}) b_{(M)}^\dagger(\vec{k}, s) \right).$$

Both,  $a_{(M)}^\dagger(\vec{k}, s)$  and  $b_{(M)}^\dagger(\vec{k}, s)$  create particles with energy  $k_0 \geq 0$ , momentum  $\vec{k}$  containing two component spinors  $\xi^s$ , i.e.  $b_{(M)}^\dagger(\vec{k}, s)$  creates particles with the opposite properties of the accompanying spinor  $v_{(M)}^s(\vec{k}) \exp(ikx)$ . Restricting the choice of the spinors  $\xi^s$  further by demanding

$$\hat{k} \vec{\sigma} \xi^s = s \xi^s,$$

<sup>2</sup>We use the abbreviations  $k := \sqrt{\vec{k}^2}$  and  $\hat{k} := \vec{k}/k$ .

both,  $a_{(M)}^\dagger(\vec{k}, s)$  and  $b_{(M)}^\dagger(\vec{k}, s)$  create particles with helicity  $s$ . The quantization condition for fermions then leads to the only non-trivial anticommutation relations for the creation and annihilation operators

$$\{a_{(M)}(\vec{k}, s), a_{(M)}^\dagger(\vec{k}', s')\} = \delta_{k,k'}\delta_{s,s'}, \quad \{b_{(M)}(\vec{k}, s), b_{(M)}^\dagger(\vec{k}', s')\} = \delta_{k,k'}\delta_{s,s'},$$

where the label  $s$  denotes helicity. In the massless case, one can easily show that the helicity eigenstates also become eigenstates of  $\gamma^5$  with chirality  $\chi = s$ .

Let us assume that at time  $t = 0$  we prepare the spinors such that  $\psi_{(M)} = \psi_{(0)}$ . Thus there exists a canonical transformation that relates the creation and annihilation operators for the massless and massive sectors which can be found by projecting the mode expansion of  $\psi_{(0)}$  onto  $\int d^3x u_{(M)}^\dagger(\vec{k})e^{ikx}$  and  $\psi_{(0)}^\dagger$  onto  $\int d^3x v_{(M)}^s(\vec{k})e^{ikx}$

$$\begin{aligned} a_{(M)}(\vec{k}, s) &= f(k)a_{(0)}(\vec{k}, s) + s\varphi_{-s}g(k)b_{(0)}^\dagger(-\vec{k}, s), \\ b_{(M)}(\vec{k}, s) &= f(k)b_{(0)}(\vec{k}, s) - s\varphi_s g(k)a_{(0)}^\dagger(-\vec{k}, s), \\ f(k) &= \sqrt{\frac{k_0 + k}{2k_0}}, \quad g(k) = \sqrt{\frac{k_0 - k}{2k_0}}. \end{aligned}$$

By choosing  $\varphi_s = \varphi_{-s}$  and since  $f^2 + g^2 = 1$  the transformation is a Bogoliubov transformation from the massless creation and annihilation operators to those that diagonalize the Hamiltonian with a mass-gap. In the following we set  $\varphi_s \equiv 1$ .

The vacuum  $|0\rangle_{(M)}$  which is annihilated by  $a_{(M)}(\vec{k}, s)$  and  $b_{(M)}(\vec{k}, s)$  can be written in terms of  $a_{(0)}(\vec{k}, s)$  and  $b_{(0)}(\vec{k}, s)$  as

$$|0\rangle_{(M)} = \prod_{\vec{k}, s} \left( \sqrt{\frac{k_0 + M}{2k_0}} - s\sqrt{\frac{k_0 - M}{2k_0}} a_{(0)}^\dagger(\vec{k}, s) b_{(0)}^\dagger(-\vec{k}, s) \right) |0\rangle_{(0)},$$

thus it might be viewed as being composed of fermion–anti-fermion pairs with zero total momentum and spin but chirality  $\pm 2$ . These pairs should be thought of as the analogue of Cooper pairs with chirality playing the role of charge. Note that in the same way as the charge quasi-electron in a superconductor approaches  $-e$  with increasing momentum, i.e. it becomes more electron like, and thereby exchanging charge with the particle bath provided by the Cooper pairs, the massive fermion with positive helicity becomes "increasingly right handed" since  $u \rightarrow 1$  and  $v \rightarrow 0$  as  $k \gg M$ .

Also, a glance at equations (2.1)– (2.3) suggests that the mass term, which is off-diagonal, corresponds to the energy gap. As is well known, it takes  $E \geq 2M$  to produce a fermion anti-fermion pair. The Weyl representation of the Dirac spinor is like the Nambu–Gorkov space representation. Now in order to reconcile the breaking of chiral symmetry due to  $M$  with the Noether theorem, i.e. with the conservation of the axial current we were led to an expression for the axial current like (1.19) and observe that the second term can be interpreted as a massless particle. We have related this mode to the pions, which are the lightest particles relevant for the strong interactions and may conclude that they correspond to the gapless mode in a BCS–superfluid. Nambu suggested that due to a finite but small bare mass of the nucleons the axial symmetry is explicitly broken and therefore pions receive a finite mass.

Although this picture is very intriguing we are still lacking of a dynamical mechanism that explains such spontaneous creation of mass for nucleons. In 1961 Nambu together with Giovanni Jona-Lasinio proposed a model that made this correspondence with BCS–Bogoliubov theory precise.

## 2.1 The NJL model

After Nambu and Jona–Lasinio discussed the general scheme of spontaneous chiral symmetry breaking  $U(1)_V \times U(1)_A \rightarrow U(1)$  in the chiral limit in their first paper [131], they included isospin in [132]. They used the model Lagrangian

$$\mathcal{L} = \bar{\psi} (i\gamma^\mu \partial_\mu - m) \psi + G \left[ (\bar{\psi}\psi)^2 + (\bar{\psi}i\gamma^5\vec{t}\psi)^2 \right], \quad (2.4)$$

with an isospin doublet spinor  $\psi$  with bare mass  $m$ . Since the mass dimension of  $[\psi] = 3/2$  and consequently the coupling constant has mass dimension  $[G] = -2$  the model is non-renormalizable. Therefore we will have to specify an ultraviolet cut-off  $\Lambda$  in UV-divergent integrals. The four fermion interaction is chosen in order to study the general features of spontaneous chiral symmetry breaking, i.e. we are agnostic about what the fundamental interaction of the fermions really is but we cannot trust quantitative predictions. Nevertheless, it turned out that also the quantitative results describe the masses of pions, the pion nucleon coupling and the ratio of Fermi to Gamow–Teller coupling quite accurately. An analogous four fermion interaction term is also obtained in BCS theory in the limit of a large phonon mass.



The Lagrangian (2.4) in the chiral limit  $m \rightarrow 0$  is invariant under the global symmetry group  $SU(2)_L \times SU(2)_R \times U(1)_V$  (the explicit proof can be found in appendix A.1)

$$\begin{aligned}\psi &\rightarrow e^{-i\alpha}\psi, \\ \psi &\rightarrow e^{-i\alpha^j \hat{t}^j}\psi, \\ \psi &\rightarrow e^{-i\gamma^5 \alpha^j \hat{t}^j}\psi.\end{aligned}$$

A possible  $U(1)_A$  is excluded because no iso- and pseudoscalar meson with a relatively small mass is known. We will revisit the axial  $U(1)$  problem in the next chapter. The conserved Noether currents are found via a total variation of the action as discussed in appendix A.2. For the infinitesimal transformations we have

$$\begin{aligned}\delta^{0,V}\psi &= -\alpha i\psi, \\ \delta^{j,V}\psi &= -\alpha^j i\hat{t}^j\psi, \\ \delta^{j,A}\psi &= -\alpha^j i\gamma^5 \hat{t}^j\psi.\end{aligned}$$

which yields the conserved currents and the associated charges

$$\begin{aligned}J_\mu^{0,V} &= \bar{\psi}\gamma_\mu\psi \quad \rightarrow Q = \int_\Sigma d^3x\psi^\dagger\psi, \\ J_\mu^{j,V} &= \bar{\psi}\gamma_\mu\hat{t}^j\psi \quad \rightarrow Q^j = \int_\Sigma d^3x\psi^\dagger\hat{t}^j\psi, \\ J_\mu^{j,A} &= \bar{\psi}\gamma_\mu\gamma^5\hat{t}^j\psi \quad \rightarrow Q_5^j = \int_\Sigma d^3x\psi^\dagger\gamma^5\hat{t}^j\psi,\end{aligned}$$

where  $\Sigma$  denotes a spatial hypersurface. Employing the quantization condition for fermions  $\{\psi(x), \psi^\dagger(y)\} = \delta(x-y)$  we find the following current algebra

$$\begin{aligned}[Q^i, Q^j] &= i\varepsilon^{ijk}Q^k, \\ [Q^i, Q_5^j] &= i\varepsilon^{ijk}Q_5^k, \\ [Q_5^i, Q_5^j] &= i\varepsilon^{ijk}Q^k,\end{aligned}\tag{2.5}$$

where the  $\varepsilon^{ijk}$  are the structure constants of  $SU(2)$ . The first line shows that the vector isospin charges form a subalgebra, while the second line shows that the axial charges transform in the adjoint representation of  $SU(2)_V$ . The last line will be of importance later on.

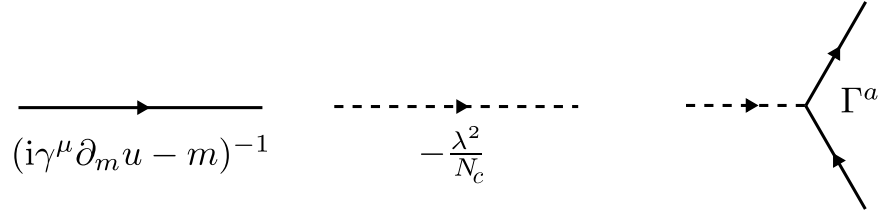


Figure 2.1: The Feynman diagrams of the bosonized NJL model.

Before we move on to discuss spontaneous symmetry breaking we make an intermediate step and bosonize the Lagrangian 2.4 using a so-called Hubbard–Stratonovich transformation [166, 105]. The new Lagrangian, which reads

$$\mathcal{L} = \bar{\psi} (i\gamma^\mu \partial_\mu - m) \psi + \sigma \bar{\psi} \psi + \pi^i \bar{\psi} i\gamma^5 2l^i \psi - \frac{1}{4G} (\sigma^2 + \pi^2), \quad (2.6)$$

is equivalent to the original upon using the equations of motion for  $\sigma$  and  $\pi^i$

$$\begin{aligned} \sigma &= 2G \bar{\psi} \psi, \\ \pi^i &= 2G \bar{\psi} i\gamma^5 2l^i \psi. \end{aligned} \quad (2.7)$$

As a further step we introduce an artificial degree of freedom of the fermions: let us assume, that the fermions are in the fundamental representation of some additional global symmetry group  $SU(N_c)$ , with  $N_c$  - the rank - being large,  $N_c \gg 1$ . Accordingly, we replace the coupling  $G$  by  $\lambda^2 = 2GN_c$  referred to as the 't Hooft coupling, with  $\lambda$  held fixed as  $N_c \rightarrow \infty$ . This has the effect of keeping the norm of the color singlet Dirac bilinears  $\sigma$  and  $\pi^i$  fixed. Furthermore, we introduce the vector  $\phi^a = (\sigma, \pi^i)$  with  $a \in [0, \dots, 3]$ , as well as the matrices  $\Gamma^a = (1, i\gamma^5 2l^i)$ . Hence the Lagrangian assumes the compact form

$$\mathcal{L} = \bar{\psi} (i\gamma^\mu \partial_\mu - m + \phi^a \Gamma^a) \psi - \frac{N_c}{2\lambda^2} \phi^2. \quad (2.8)$$

The Feynman graphs corresponding to this Lagrangian are depicted in figure 2.1.

Let us now explore the spontaneous breaking of chiral symmetry in more detail. In addition we will introduce a thermal field theory approach for later convenience. Details are discussed in appendix A.3. In the following  $\tau$  - it denotes Euclidean time. Following the steps developed in [108] we arrive at the 1PI effective action in imaginary time formalism, which is a functional of the vacuum expectation (VEV)

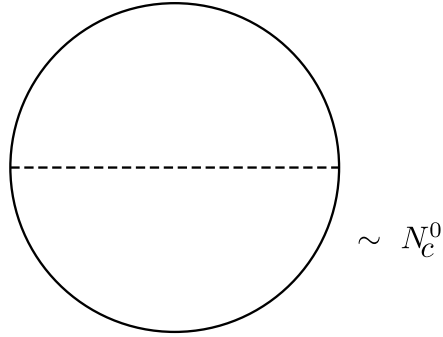


Figure 2.2: The lowest loop order correction to the 1PI effective action.

values  $\phi_c^a(x)$ ,  $\bar{\psi}_c(x)$  and  $\psi_c(x)$

$$\Gamma[\phi_c, \psi_c, \bar{\psi}_c] = \int d\tau d^3x \bar{\psi}_c \left( i\gamma^\mu \partial_\mu^x - m + \phi_c^a(x) \Gamma^a + \mu \gamma^0 \right) \psi_c - \frac{N_c}{2\lambda^2} \phi_c^2 + N_c \text{Tr} \ln S^{-1} + V_{1\text{PI}}^{n \geq 2 \text{ loop}} + \text{const}. \quad (2.9)$$

The tree level action in (2.9) is of order  $N_c$  explicitly in the second term and implicitly in the fermionic part where we sum over the (suppressed) color index of the fermions. Since the tree level inverse propagator is a unit matrix in color space

$$1_{N_c \times N_c} S^{-1} = 1_{N_c \times N_c} (i\gamma^\mu \partial_\mu - m + \phi_c^a \Gamma^a + \mu \gamma^0), \quad (2.10)$$

we also find a factor  $N_c$  in front of the trace log term. The lowest order contribution to  $V_{1\text{PI}}^{n \geq 2 \text{ loop}}$  is depicted in figure 2.2 and is of order  $N_c^0$ , since for the fermion loop we get a factor of  $N_c$  which cancels against the factor  $N_c$  coming from the bosonic tree level propagator. The reader can easily convince herself that any higher order 1PI loop diagram is of order  $N_c^0$  or smaller. For each new boson line the order in  $N_c$  is diminished and each new fermion loop comes automatically with a new boson line. Thus in the large  $N_c$  limit the 1 loop approximation (also referred to as Hartree- or mean field approximation) of the 1PI action becomes exact.

The gap equation, determining the vacuum expectation values of the fields is

$$\frac{\delta \Gamma}{\delta \eta_c^A} = 0,$$

where  $\eta_c^A$  represents any of the fields appearing in the action. We will assume in the following that only the bosons have a non-vanishing VEV; in particular for the bosons we assume  $\phi_c^a = (\Sigma, 0) = \text{const}$ . Note that in the inverse fermion propagator

$\Sigma$  represents a mass term, hence we denote by

$$M = m - \Sigma$$

the dressed fermion mass.

In this case the only nontrivial gapequation reads

$$-\frac{N_c}{\lambda^2} \phi^a(x) + N_c \text{tr}(S(x, x) \Gamma^a) = \quad (2.11)$$

$$-\frac{N_c}{\lambda^2} \Sigma + N_c \text{tr}(S(x, x)) = 0, \quad (2.12)$$

where the trace sums over Dirac and isospin space only. As usual  $S(y, x)$  denotes the propagator, which is inverse to the operator  $S_x^{-1}$  in the sense that

$$S^{-1} S(y, x) = \delta(x - y).$$

Upon using the momentum space representation of the fermion propagator the gap equation becomes

$$\frac{N_c}{\lambda^2} \frac{M - m}{M} = 4N_l N_c \sum_n \int d^3k \frac{T}{(\omega_n + i\mu)^2 + \varepsilon_k^2}, \quad (2.13)$$

where  $N_l = 2$  is the rank of the isospin group, and the sum is over the index  $n$  which labels the Fermionic Matsubara frequencies  $\omega_n = (2n + 1)\pi T$ .

Note that the effective action is invariant under chiral transformations in the chiral limit  $m \rightarrow 0$ , thus

$$\delta_\alpha \Gamma = \int d^4x \frac{\delta \Gamma}{\delta \eta_c^A(x)} \delta_\alpha \eta_c^A(x) = 0, \quad (2.14)$$

The equation above is a Ward–Takahashi identity for one point functions. Furthermore, from (2.14) we can derive a chain of Ward–Takahashi identities for higher n-point functions by successive functional differentiation, e.g.

$$\int d^4x \frac{\delta^2 \Gamma}{\delta \eta_c^B \delta \eta_c^A(x)} \delta_\alpha \eta_c^A(x) + \frac{\delta \Gamma}{\delta \eta_c^A(x)} \frac{\delta \delta_\alpha \eta_c^A(x)}{\delta \eta_c^B} = 0. \quad (2.15)$$

The second factor vanishes on the solutions of the gap equation for variations of the fields  $\eta_c$  that are linear in the fields. We conclude that a non-vanishing  $\delta_\alpha \eta_c^A(x)$  is an eigenvector of the inverse propagator

$$D_{AB}^{-1}(y, x) = \frac{\delta^2 \Gamma}{\delta \eta_c^B(y) \delta \eta_c^A(x)}$$

with vanishing eigenvalue.

In our case the only non-vanishing contribution is  $\delta_\alpha \eta_c^A = \delta_\alpha \pi_c^i = \alpha^i \Sigma = \text{const.}$  then equation (2.15) reads

$$\Sigma \int d^4x \frac{\delta^2 \Gamma}{\delta \pi_c^i(0) \delta \pi_c^j(x)} = \lim_{\rho \rightarrow 0} \Sigma \int d^4x e^{i\rho x} \frac{\delta^2 \Gamma}{\delta \pi_c^i(0) \delta \pi_c^j(x)} \quad (2.16)$$

$$= \Sigma D_{ij}^{-1}(\rho^2 = 0) = 0. \quad (2.17)$$

Since the solution for  $\rho^2$  to the pole condition

$$D^{-1}(\rho^2) = 0 \quad (2.18)$$

gives the mass of the particle, we conclude from (2.17) that the pions are massless if  $\Sigma \neq 0$ , in accordance with Nambu's expectations from BCS theory. Here we proved this more generally via the Ward–Takahashi identity of the 1PI effective action. The general statement, that if a (global) symmetry is spontaneously broken, there must exist massless modes is called the Goldstone theorem [87, 88]. Accordingly, the gapless modes are called Nambu–Goldstone bosons. Typical examples of these can be found in condensed matter systems:

- phonons in a lattice of ions due to broken translation and rotation invariance
- magnons in a ferromagnet due to broken rotation invariance
- phonons in Helium-4 due to broken particle number conservation

We will show explicitly that the pions are massless in the mean field approximation employed here: The inverse propagator for the bosons is

$$\begin{aligned} \frac{\delta^2 \Gamma}{\delta \phi_c^b(y) \delta \phi_c^a(x)} &= -\frac{N_c}{\lambda^2} \delta_{ab} \delta(x, y) - N_c \text{tr} \left( S(x, y) \Gamma^b S(y, x) \Gamma^a \right), \\ \Rightarrow D_{ab}^{-1}(\rho^2) &= -\frac{N_c}{\lambda^2} \delta_{ab} + N_c T \sum_n \int d^3k \text{tr} \left( \frac{1}{\not{k} - M} \Gamma^a \frac{1}{\not{k} + \not{p} - M} \Gamma^b \right). \end{aligned}$$

In the limit of vanishing momentum for the pions this becomes

$$D_{ij}^{-1}(\rho^2 = 0) = -\frac{N_c}{\lambda^2} \delta_{ij} + 4\delta_{ij} N_l N_c \sum_n \int d^3k \frac{T}{(\omega_n + i\mu)^2 + \varepsilon_k^2},$$

which vanishes by virtue of the gap equation (2.13), provided that  $m \rightarrow 0$ . In a similar calculation for the  $\sigma$  boson propagator we set  $\vec{p} = 0$  and observe that for

$p^0 = 2M$  the momentum integral becomes the same as in the gap equation and cancels the first term provided we take the chiral limit. In summary we found three massless pions and one scalar meson with  $m_\sigma = 2M$ . Since both are constituted by two fermions with mass  $M$  we conclude that the pions have binding energy  $2M$  while the sigma meson is marginally bound.

With respect to the discussion at the end of the previous section we might be interested in showing explicitly in the NJL model that the axial current is conserved in the chiral limit in spite of the finite dressed fermion mass  $M$ . In order to do that we couple an external axial vector field  $A_\mu^i$  to the axial current by adding

$$\bar{\psi} A^i \gamma^5 \psi$$

to the Lagrangian. The global axial symmetry can now be promoted to a local symmetry with the infinitesimal transformation parameter  $\alpha(x)$  provided that  $A_\mu^i \rightarrow A_\mu^i - \partial_\mu \alpha^i(x)$ . The Ward–Takahashi identity for 3-point functions is

$$\int d^4x \frac{\delta^3 \Gamma}{\delta \eta_c^C \delta \eta_c^B \delta \eta_c^A(x)} \delta_\alpha \eta_c^A(x) + \frac{\delta^2 \Gamma}{\delta \eta_c^B \delta \eta_c^A(x)} \frac{\delta \delta_\alpha \eta_c^A(x)}{\delta \eta_c^C} + \frac{\delta^2 \Gamma}{\delta \eta_c^C \delta \eta_c^A(x)} \frac{\delta \delta_\alpha \eta_c^A(x)}{\delta \eta_c^B} = 0. \quad (2.19)$$

Now only  $\delta_\alpha A_\mu^i = -\partial_\mu \alpha^i(x)$  and  $\delta_\alpha \pi_c^i = \alpha^i \Sigma$  are non-vanishing and we choose  $\eta_c^B = \bar{\psi}_c$  as well as  $\eta_c^C = \psi_c$ , which yields

$$\int d^4x \partial_\mu^x \frac{\delta^3 \Gamma}{\delta \psi_c(z) \delta \bar{\psi}_c(y) \delta A_\mu^i(x)} \alpha^i(x) + \frac{\delta^3 \Gamma}{\delta \psi_c(z) \delta \bar{\psi}_c(y) \delta \pi_c^i(x)} \alpha^i(x) \Sigma - \frac{\delta^2 \Gamma}{\delta \psi_c(x) \delta \bar{\psi}_c(y)} i \vec{\alpha} \vec{\gamma}^5 \delta(x, z) - i \delta(x, y) \vec{\alpha} \vec{\gamma}^5 \frac{\delta^2 \Gamma}{\delta \psi_c(z) \delta \bar{\psi}_c(x)} = 0, \quad (2.20)$$

where the first term has been integrated by parts and the surface integral has been omitted and due care has to be taken with the order of the fermionic derivatives. In accordance with our previous observation, in case the chiral symmetry is spontaneously broken the vertex of the fermions with an external axial current has to be accompanied by an emission of a pion, which then decays – the second term in (2.20). Since we absorbed the fermion-pion coupling constant into the definition of the pion fields we can read off  $-\Sigma/g_{\pi\psi\psi} = M/g_{\pi\psi\psi} = f_\pi$ , which is the Goldberger–Treiman relation, which in this context measures the strength of the spontaneous symmetry breaking – the condensate  $\Sigma$ .

To make the picture complete we rederive the pion decay constant from the coupling to the external axial current

$$\begin{aligned} \frac{\delta^2 \Gamma}{\delta \pi_c^j(y) \delta A_\mu^i(x)} &= -N_c \text{tr} \left( S(x, y) i \gamma^5 \frac{j^i}{2} S(y, x) \gamma^\mu \gamma^5 i^j \right) \\ \Rightarrow -2i N_l N_c M \delta^{ij} p^\mu \sum_n \int d^3 k &\frac{T}{\left[ (\omega_n + i\mu)^2 + \varepsilon_{\vec{k}}^2 \right] \left[ (\omega_n + p^0 + i\mu)^2 + \varepsilon_{\vec{k}+\vec{p}}^2 \right]} \\ &= -i p^\mu \delta^{ij} \frac{f_\pi}{g_{\pi\psi\psi}}. \end{aligned} \quad (2.21)$$

In all the involved integrals the sum over the fermionic Matsubara frequencies can be performed, but the 3-momentum integral is UV divergent. Since the NJL model is non-renormalizable, all results, e.g., the magnitude of the gap and the order of phase transitions, will depend on the regulator as well as on the regularization scheme. We use the proper time regularization scheme [162]. In this procedure, the integrand of divergent expressions is recast into so-called proper time integrals,

$$(k^2 + b^2)^{-a} = \frac{1}{\Gamma(a)} \int_0^\infty d\tau \tau^{a-1} e^{-\tau(k^2+b^2)}, \quad (2.22)$$

and one then performs the momentum integral before the proper time integral. The UV divergence of the momentum integral reappears at the lower bound of the proper time integral, which therefore has to be regularized. We set the lower bound to  $1/\Lambda^2$ . In the chiral limit we have to fit the two parameters of the model - the coupling constant and the cut-off - to two out of the three related quantities  $f_\pi$ ,  $g_{\pi\psi\psi}$  and  $M$ .





# Thermodynamics of chiral symmetry breaking

## 3.1 Towards quarks and gluons

In the 1960's chiral symmetry was one of the major inputs for finding the fundamental theory governing the strong interactions. In [77, 78, 134] Gell-Mann and Yuval Ne'eman independently developed a scheme, known as the "eightfold way" that embedded the isospin multiplets of hadrons displaced by strangeness into representations of the larger symmetry group  $SU(3)_V$ .

In [79] Gell-Mann proposed the existence of so-called quarks (at that time merely a mathematical concept) that constitute hadrons. These fermions - in the following denoted by  $\psi$  - live in the fundamental representation of  $SU(3)_V$  and are called up  $u$ , down  $d$  and strange  $s$  with charge  $2/3$ ,  $-1/3$  and  $-1/3$  respectively. Each species is carrying baryon number  $1/3$ . Mesons are made of  $\bar{\psi}\psi$ , while baryons are made of  $\psi\psi\psi$ . The lowest meson configurations are then in the singlet and adjoint representations of  $SU(3)_V$  while the lowest lying baryon configurations are in the singlet, adjoint and decuplet representation. Of course it is natural to imagine that there are now also accompanying axial transformations, i.e. whatever the fundamental theory

might be, the  $SU(3)$  analogue of the current algebra in Eq. (2.5) should hold. This idea was developed further by Gell-Mann in Ref. [81].

The current algebra approach soon proved successful when so-called sum rules (integral relations for physical observables) were obtained that were in principle testable by experiment. Most notably the Adler-Weissberger sum rule [177, 1, 2] allowed for calculating the axial vector coupling constant from the neutrino reaction cross section. In its original formulation it used the PCAC assumption in the sense that the divergence of the axial current is proportional to the pion field, first stated in [80] to relate the renormalization of the axial vector coupling constant to the total proton–pion cross section.

Despite the intense search for fractionally charged particles none could be found in collider experiments as well as in cosmic radiation. However, high energy proton–proton collisions at a center of mass energy above 10 GeV revealed that hadrons might indeed have an internal structure [142]. It seemed that hadrons are made of a cloud of loosely bound objects since a lot of hadrons are produced in such a scattering but only a tiny fraction has significant transversal momentum. In the late 1960's this picture was tested by the SLAC-MIT deep inelastic scattering experiments. 20 GeV electrons were scattered from a fixed hydrogen target. While the momentum distribution of the scattered electrons was in accordance with a target of charged point particles, hardly ever a scattered proton was detected. What was seen was a large number of hadrons. The picture one had in mind is a proton shattered by the high energy electron and thereby absorbing kinetic energy, which in turn is released by hadron jets, hence the term *deep inelastic* scattering. Inspired by ideas of Feynman, Bjorken [29] developed a parton model that predicted scaling, i.e. the inelastic electron–proton cross section depends only on the ratio

$$x := \frac{-q^2}{2M\nu},$$

where  $q$  measures the momentum exchange,  $M$  is the nucleon mass and  $\nu = E - E'$  is the energy transfer in the nucleon rest frame [92]. Essentially Bjorken scaling means that the structure of a proton "looks the same for an electromagnetic probe no matter how hard the proton is struck" [142]. The  $x$  can be identified with the fraction of the longitudinal momentum of the proton the struck parton is carrying, and by assumption one neglects interactions with other partons. For some so far not explained reason the parton itself is not observed but a jet of hadrons is released.

It seems that at these high energies the partons are governed by a free quantum field theory, but at the same time they are strongly bound into hadrons. There were two other outstanding problems at that time. The first, already observed in 1964, is that for example one of the states in the  $SU(3)_V$  decuplet is  $\Delta^{++}$  with charge +2, spin 3/2 and which is an  $uuu$  state. If quarks are fermions with spin 1/2 this means that  $\Delta^{++}$  is totally symmetric in spin and flavor, in conflict with the spin-statistics theorem. In [99] Han and Nambu resolved the issue by the ad hoc assumption of an additional quantum number that triples each quark flavor. This quantum number was later called color. By assumption physical low energy states have to be a color singlet, this property was later called color confinement. Let us again assume that quarks lie in the fundamental representation of a (for now global) special unitary group - the simplest guess is  $SU(3)_c$ . The tensor representations of  $SU(N_c)$  always provide one with two invariant objects: one is  $\delta_j^i$ , which amounts to contraction of an object in the fundamental representation of  $SU(N_c)$  and one in the dual representation. The second is the totally antisymmetric  $\varepsilon_{i_1 \dots i_{N_c}}$ , which allows to form a singlet made of  $N_c$  objects in the fundamental representation. Thus singlets of  $SU(3)_c$  are

$$\bar{\psi}_a \psi^a, \quad \varepsilon_{abc} \psi^a \psi^b \psi^c, \quad \varepsilon^{abc} \bar{\psi}_a \bar{\psi}_b \bar{\psi}_c,$$

representing mesons and (anti-) baryons. Such a tripling of quarks would also resolve another problem found a few years later in which chiral symmetry again played an important role: the (QED) axial anomaly [3, 20] (for an introduction to anomalies in quantum field theory see [27]), which explains the decay  $\pi^0 \rightarrow 2\gamma$ , from first principles, in particular the electromagnetic coupling is minimal. Before, this decay mode could only be accounted for with a phenomenological term, see eg. [76]. In the context of a quark model where quarks carry fractional charges the decay amplitude is wrong by a factor of 1/3 compared to experiment – also here three additional color degrees of freedom would account for the missing factor, as was shown in 1972 by Bardeen, Fritzsche and Gell-Mann [18]<sup>1</sup>. In the same year, Fritzsche and Gell-Mann in essence already formulated a Lagrangian containing an  $SU(3)_c$  gauge field called gluon and a minimally coupled 3-flavor quark term [70].

In 1973 David Gross together with Frank Wilczek and David Politzer independently showed that non-abelian gauge theories exhibit asymptotic freedom [93, 144], i.e.

<sup>1</sup>This seems also to be the reference in which the term color was coined.

at large momentum (relevant for deep inelastic scattering) the running coupling constant becomes small. The running of the coupling constant at one-loop order for an  $SU(3)_c$  gauge theory coupled to  $N_f$  light quarks may be written as [142]

$$\alpha_s(Q) = \frac{2\pi}{\left(11 - \frac{2}{3}N_f\right) \ln\left(\frac{Q}{\Lambda_{\text{QCD}}}\right)},$$

where  $\Lambda_{\text{QCD}}$  is a mass scale defined such that at  $Q^2 \approx \Lambda_{\text{QCD}}^2$  the coupling becomes strong as  $Q^2$  is decreased. Experimental measurements show that  $\Lambda_{\text{QCD}} \approx 200$  MeV. This behavior of the coupling explains the hadron jets in deep inelastic scattering experiments: instead of a free parton we observe the hadrons produced by Schwinger particle creation. Furthermore, soon the corrections to Bjorken scaling due to the running coupling were verified experimentally. The second ingredient that forbids detecting isolated colored objects - confinement - was shown for discretized Euclidean (pure glue) QCD at strong coupling by Kenneth Wilson in [179]. An analytic proof that full QCD is confining is still missing. However lattice QCD shows overwhelming evidence that this is indeed the case, see eg. [13, 12] for results with physical quark masses.

We summarize these developments in the QCD Lagrangian

$$\mathcal{L} = -\frac{1}{4} \text{tr} F^{\mu\nu,a} F_{\mu\nu}^a + \sum_{i=1}^{N_f} \bar{\psi}^i (i\not{D} - m_i) \psi^i,$$

where  $D_\mu = \partial_\mu - igA_\mu^a t^a$ , is the covariant derivative with respect to the color gauge group, and the  $t^a$  denote the eight generators of  $SU(3)_c$  in the fundamental representation normalized by

$$\text{tr} t^a t^b = \frac{1}{2} \delta^{ab},$$

and  $g$  denotes the coupling<sup>2</sup>.

Note that the masses of the nowadays six known quark flavors are widely spread over many orders of magnitude. For instance the masses of the three lightest flavors

<sup>2</sup>The relation to  $\alpha_s(Q)$  given above is such that for some arbitrary renormalization point  $Q = M$ ,  $\alpha_s(M) = g^2/4\pi$ . In turn one usually removes the dependence on the arbitrary point by trading it for the mass scale  $\Lambda_{\text{QCD}}$  defined by the equation (at one-loop order)

$$1 = \frac{g^2}{8\pi^2} \left(11 - \frac{2}{3}N_f\right) \ln\left(\frac{M}{\Lambda_{\text{QCD}}}\right) \quad (3.1)$$

are given by  $m_u = 2.3_{-0.5}^{+0.7}$  MeV,  $m_d = 4.8_{-0.3}^{+0.5}$  MeV, and  $m_s = 95 \pm 5$  MeV [24]. Even in case of  $N_f = 2$  QCD the fundamental Lagrangian is not isospin/ flavor symmetric. The crucial point is that QCD comes with an inherent mass scale<sup>3</sup>  $\Lambda_{\text{QCD}}$  as mentioned above. With respect to this scale the masses of up and down quarks (and to some extent that of the strange quark) might be viewed as a small perturbation and thus chiral symmetry is approximately intact.

Now the crucial question arises, why is then  $U(1)_A$  not spontaneously broken, or put differently, where is the Nambu–Goldstone mode associated with  $U(1)_A$ ? It turned out that there exists a pseudo-scalar particle denoted by  $\eta'$  that is a flavor singlet, however it is very massive -  $m_{\eta'} = 957.78 \pm 0.06$  MeV - and is actually the heaviest meson in the  $U(3)_V$  pseudoscalar meson nonet. The non-abelian analogue of the chiral anomaly responsible for the neutral pion decaying into two photons comes to the rescue. If fermions couple to gauge fields, the chiral symmetry is explicitly broken by radiative corrections even in the chiral limit. This is called an anomaly, because a classical symmetry is broken on the quantum level. While the QED anomaly affecting the third isospin component of the axial vector current, which annihilates a  $\pi^0$ , can be viewed as a small perturbation leaving the chiral symmetry intact, this is no longer true for the non-abelian analogue, which affects precisely the isospin singlet axial current

$$\partial_\mu J^{0,A} = -\frac{g^2 N_f}{32\pi^2} \epsilon^{\mu\nu\rho\tau} F_{\mu\nu}^a F_{\rho\tau}^a. \quad (3.2)$$

There exist semi-classical solutions to the equations of motion of Euclidean Yang–Mills theory with finite energy interpreted as pseudo particles called instantons [168]. They have finite width in Euclidean time and space and correspond to a tunneling process between different vacua. Furthermore the gauge field configuration is such that (3.2) is non-vanishing. The integral over

$$-\frac{g^2}{32\pi^2} \epsilon^{\mu\nu\rho\tau} F_{\mu\nu}^a F_{\rho\tau}^a$$

gives an integer number called the winding or instanton number distinguishing the different vacua of the Yang–Mills theory.

In full QCD it is difficult to calculate the magnitude of the consequences of the anomalous violation of chiral symmetry, however in the limit of a large number of

<sup>3</sup>Note that the classical theory is conformally invariant. In the quantum theory this symmetry is broken by the conformal anomaly at one-loop level.

colors [167], which we already encountered in chapter 2, this was done by Witten and Veneziano in Refs. [181, 173]. We replace  $g$  by  $\lambda/\sqrt{N_c}$ , where again  $\lambda$  denotes the 't Hooft coupling, which is kept fixed in the limit  $N_c \rightarrow \infty$ . Then the anomaly becomes

$$-\frac{\lambda^2}{32\pi^2 N_c} \epsilon^{\mu\nu\rho\tau} F_{\mu\nu}^a F_{\rho\tau}^a,$$

and thus is suppressed for  $N_c \rightarrow \infty$  and therefore  $\eta'$  becomes a Nambu–Goldstone boson in large  $N_c$  QCD with  $m_{\eta'} \sim 1/\sqrt{N_c}$ . This is an important result in the context of this thesis, since when calculating the chiral phase transition surface in the Sakai–Sugimoto model which claims to be a holographic dual of large  $N_c$  QCD we will restrict ourselves to  $N_f = 1$  for simplicity, therefore the chiral symmetry group is  $U(1)_V \times U(1)_A$ . The Witten–Veneziano result allows us to study spontaneous breaking of chiral symmetry using that restriction. Sakai and Sugimoto in [156] showed explicitly that the Veneziano–Witten mass formula for the  $\eta'$  is satisfied in their model.

In the next section we will reinterpret the NJL model introduced before accordingly as a model in which chiral symmetry is broken spontaneously by the condensation of quark–anti-quark pairs [174, 102, 114]. For a modern introduction to the quark NJL model see [40]. Of course the interaction via gluons is replaced with the four point fermion interaction and therefore the NJL model lacks the two most important ingredients of QCD: asymptotic freedom and confinement. We will nevertheless press on and discuss now chiral symmetry breaking in the NJL model at finite temperature and chemical potential.

## 3.2 The thermodynamics of the NJL model

We can compute the thermodynamic potential and the gap equation, by inserting momentum representation of  $S^{-1}$  into Eq. (2.9) and performing the thermodynamic limit

$$\Omega = \frac{N_c(M - m)^2}{2\lambda^2} - 2N_f N_c \sum_{e=\pm} \int \frac{d^3k}{(2\pi)^3} \left[ \frac{\epsilon_k}{2} + T \ln \left( 1 + e^{-\frac{\epsilon_k - e\mu}{T}} \right) \right], \quad (3.3)$$

$$\frac{M - m}{2\lambda^2 N_f M} = \int \frac{d^3k}{(2\pi)^3} \frac{1}{\epsilon_k} [1 - f(\epsilon_k - \mu) - f(\epsilon_k + \mu)], \quad (3.4)$$

where  $f(x) \equiv 1/(e^{x/T} + 1)$  is the Fermi-Dirac distribution function. As mentioned before, the (vacuum parts of the) momentum integrals are UV divergent and have to be regularized. Furthermore it is convenient to redefine the coupling again for the numerical analysis by

$$g := \frac{\lambda^2 N_f \Lambda^2}{4\pi^2},$$

which is dimensionless and where  $\Lambda$  denotes the cut-off in the proper-time regularization scheme.

This yields the thermodynamic potential at zero temperature

$$\begin{aligned} \frac{16\pi^2}{N_f N_c} \Omega_{T=0} &= \frac{2\Lambda^2(M-m)^2}{g} + \Lambda^2 \left( \Lambda^2 - M^2 \right) e^{-M^2/\Lambda^2} + M^4 \Gamma \left( 0, \frac{M^2}{\Lambda^2} \right) \\ &\quad - 2\theta(\mu - M) \left[ \frac{\mu k_F}{3} (2\mu^2 - 5M^2) + M^4 \ln \frac{\mu + k_F}{M} \right], \end{aligned} \quad (3.5)$$

where  $\Gamma(a, x)$  is the incomplete gamma function, and the gap equation

$$\begin{aligned} \frac{M-m}{Mg} &= \left[ e^{-M^2/\Lambda^2} - \frac{M^2}{\Lambda^2} \Gamma \left( 0, \frac{M^2}{\Lambda^2} \right) \right] \\ &\quad - 2\theta(\mu - M) \left( \frac{\mu k_F}{\Lambda^2} - \frac{M^2}{\Lambda^2} \ln \frac{\mu + k_F}{M} \right), \end{aligned} \quad (3.6)$$

where we have defined the the Fermi momentum  $k_F = \sqrt{\mu^2 - M^2}$ .

For simplicity we shall discuss the chiral limit  $m = 0$  in the rest of this discussion. In this case,  $M = 0$  is always a solution to the gap equation. Otherwise the solution to the gap equation is always non-trivial. As a consequence each second order phase transition discussed below would become a crossover and of course the numerical value where a first order transition occurs would be shifted.

For  $\mu = 0$ , the gap equation further simplifies since the term  $\propto \theta(\mu - M)$  does not contribute. The right-hand side of equation (3.6) is always smaller than 1. Therefore, a nontrivial solution for  $M$  only exists if the dimensionless coupling constant  $g$  is larger than 1. When it exists, this solution is preferred over the trivial solution, as one can verify with the help of the thermodynamic potential (3.5).

In Fig. 3.1 we show the numerical solution for the gap equation as a function of  $\mu$  for three different coupling constants larger than 1 (i.e., they all admit a nontrivial solution for  $\mu = 0$ ). For all couplings  $g > 1$ , there is a certain critical  $\mu$  where  $M$  goes

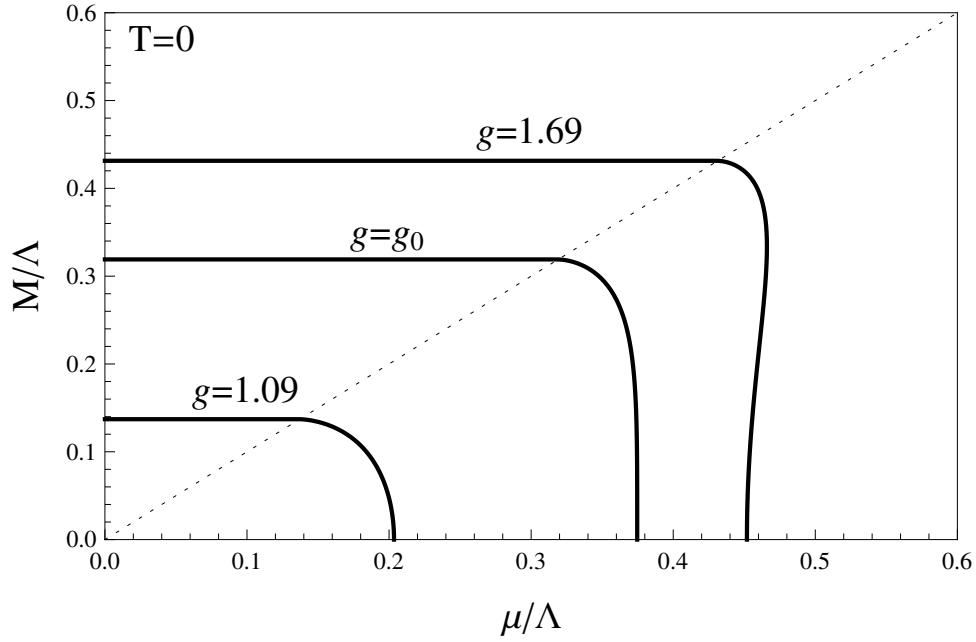


Figure 3.1: The zero-temperature solution to the gap equation for three different values of the coupling  $g$ . The thin dotted line is the line  $\mu = M$ . The solution becomes multi-valued in the region  $\mu > M$  for all couplings larger than  $g_0$  with  $g_0$  given in Eq. (3.8).

to zero. By setting  $m = 0$  and then performing the limit  $M \rightarrow 0$ , (3.6) becomes an equation for  $\mu$ . It is easy to show that this critical  $\mu$  is given by

$$\frac{\mu_0(g)}{\Lambda} = \frac{1}{\sqrt{2}} \sqrt{1 - \frac{1}{g}}. \quad (3.7)$$

If and only if the solution is single-valued, this is the critical  $\mu$  at which the (then second-order) phase transition to the chirally restored phase occurs.

Above a certain coupling, the solution becomes multi-valued, see for instance the line with  $g = 1.69$  in figure 3.1. The coupling where this qualitative change occurs can be computed as follows. By differentiating the gap equation with respect



to  $\mu$  we find

$$\frac{\partial M}{\partial \mu} = - \frac{2k_F}{M \left[ \Gamma \left( 0, \frac{M^2}{\Lambda^2} \right) - 2 \ln \frac{\mu + k_F}{M} \right]}.$$

In accordance with the numerical plot, this derivative is infinite for  $M = 0$ . For all couplings for which the solution is multi-valued, there is another point where the derivative is infinite, which is given by the second pole of the denominator,

$$\mu = M \cosh \frac{\Gamma(0, M^2/\Lambda^2)}{2}.$$

We can now ask for the value of  $g$  at which this point coincides with  $\mu_0(g)$  for  $M \rightarrow 0$ . The resulting equation then yields the coupling where the multi-valuedness sets in. We find

$$g_0 = \frac{1}{1 - \frac{e^{-\gamma_E}}{2}} \simeq 1.390, \quad (3.8)$$

where  $\gamma_E$  is the Euler-Mascheroni constant. In the regime  $1 < g < g_0$  the chiral phase transition is second order and takes place at  $\mu_0(g)$ .

For couplings larger than  $g_0$  the transition is first order and has to be determined numerically. It turns out that the branch with a positive slope is always energetically disfavored. Therefore, in terms of Fig. 3.1, the preferred solution follows the horizontal line  $M(\mu = 0)$  and, for all multi-valued cases, jumps to zero at a certain chemical potential. Whether (and how far) the preferred solution follows the curve into the region  $\mu > M$  depends on the coupling. We find numerically that for couplings below (above)  $g \simeq 2.106$  it does (doesn't). This is a first example of the nontrivial effect of  $\mu$  on the preferred phase: it is not always the phase with the largest dynamical mass that is favored. In more physical terms, for couplings above  $g \simeq 2.106$  the chirally broken phase with vanishing quark density is directly superseded by the quark matter phase, while for smaller couplings there is a region of finite density between these two phases. Since for  $g > 2.106$  there are no complicated effects of the quark density, we can write down a very simple expression for the free energy difference between the broken phase and the restored phase, evaluated at the solution of the gap equation (and using  $M \ll \Lambda$ ),

$$\Delta\Omega = - \frac{M_0^2 \Lambda^2}{16\pi^2} \left( 1 - \frac{1}{g} \right) + \frac{\mu^4}{12\pi^2}, \quad (3.9)$$

with  $M_0$  being the (non-analytical) solution to the gap equation for  $\mu = 0$ . This result is very intuitive: the first, negative, term is the condensation energy, i.e., the energy

gain from the chiral condensate, while the second, positive, term corresponds to the energy costs for pairing which must be paid because the chemical potential has separated fermions from anti-fermions. When the costs exceed the gain, chiral symmetry is restored. This determines the phase transition line. We summarize our discussion of the chiral phase transition at  $B = T = 0$  in Fig. 3.2.

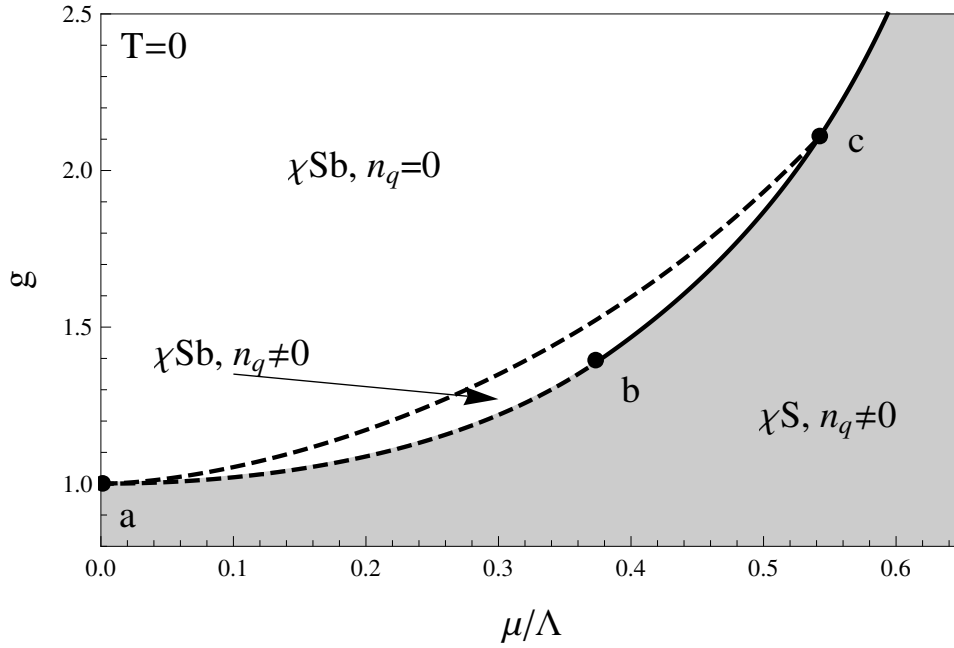


Figure 3.2: The phase diagram at  $T = 0$  in the  $\mu$ - $g$ -plane. Dashed lines indicate second-order, solid lines first-order phase transitions. In the shaded region chiral symmetry is restored ( $\chi S$ ). The points a, b and c correspond to  $(\mu/\Lambda, g) = (0, 1)$ ,  $(e^{-\gamma_E/2}/2, g_0)$ , and  $(0.542, 2.106)$ , respectively, with  $g_0$  given in Eq. (3.8). Between points a and b the transition line is given by  $\mu_0(g)$  from Eq. (3.7). The dashed line between a and c indicates the onset of a finite quark number density  $n_q$  within the chirally broken phase ( $\chi Sb$ ).

For nonzero temperatures, we need to solve the gap equation (3.4) [with the regularization of the vacuum part shown in Eq. (3.6)] numerically. The result for various temperatures and a large coupling (larger than that of point c in Fig. 3.2) is shown in the upper panel of Fig. 3.3. In general, the temperature decreases the gap. Moreover, the temperature can also change the order of the chiral phase transition by removing the multi-valuedness of the solution to the gap equation. The critical

temperature of the chiral phase transition in the  $T$ - $\mu$  phase diagram is shown in the lower panel of Fig. 3.3. The critical point moves towards higher temperatures with increasing coupling. If the phase transition is second order, it is possible to find a closed form for the critical temperature. To this end, one takes Eq. (3.4) (with  $m = 0$ ) and sets  $M = 0$  on the right hand side of the equation. Then, solving for  $T$  yields the critical temperature

$$\frac{T_c(\mu)}{\Lambda} = \sqrt{\frac{3}{2\pi^2}} \sqrt{1 - \frac{1}{g} - 2\frac{\mu^2}{\Lambda^2}}. \quad (3.10)$$

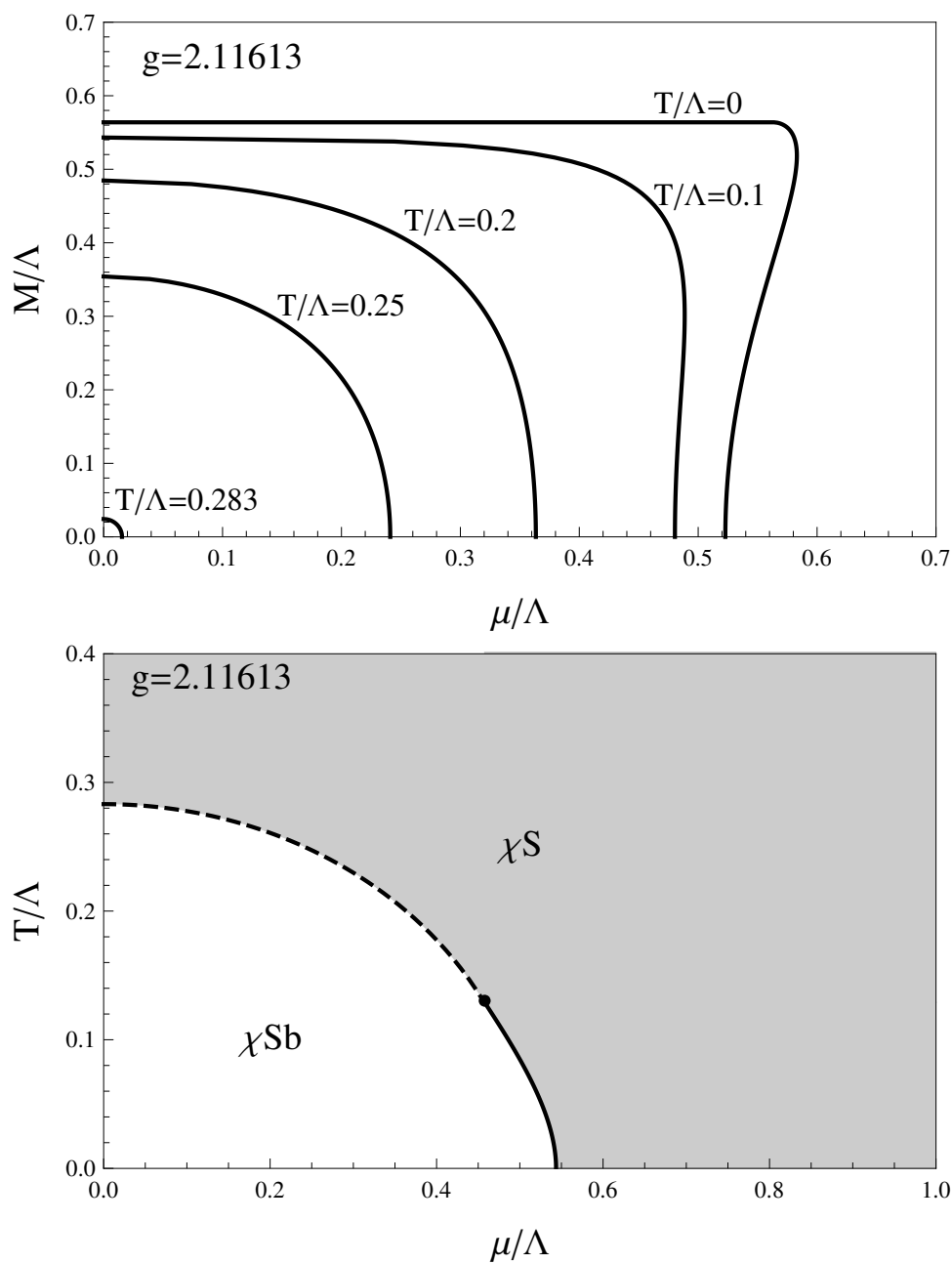


Figure 3.3: Finite-temperature effects on the chiral phase transition in the NJL model. Upper panel: the gap as a function of the chemical potential for a given coupling strength and different values of temperature. Lower panel: the phase diagram in the  $\mu$ - $T$ -plane for the same coupling. The (dashed) second-order phase transition line is given by the analytic expression (3.10).

# A geometric picture of chiral symmetry breaking

## 4.1 The gauge–gravity duality

The model discussed in this section is based on the conjecture that certain strongly coupled quantum gauge theories are equivalent to certain classical gravitational theories in higher dimensions. In the context of string theory, the first realization of this holographic principle known as AdS/CFT correspondence was proposed by Maldacena [123]. In a nutshell, it utilizes two different limits of describing so-called D-branes, which are dynamical objects in string theory that impose Dirichlet boundary conditions on the endpoints of open strings. On the one hand, a stack of  $N_c$  D-branes hosts a maximally supersymmetric  $U(N_c)$  gauge theory coming from the massless excitations of open superstrings; on the other hand, the stack of D-branes is a massive object that curves space-time by coupling to gravitons – coming from the closed strings – with the strength  $\lambda \propto g_s N_c$ , where  $g_s$  denotes the string coupling. Now, let  $N_c \rightarrow \infty$  and keep  $\lambda$  fixed. In the limit  $\lambda \ll 1$ , gravity decouples from the open strings, whose low-energy effective theory is given by the mentioned  $U(N_c)$  super Yang–Mills (SYM) theory. In the case of D3-branes, this gauge theory is four-dimensional. In the opposite limit,  $\lambda \gg 1$ , the stack of D-branes back-reacts

strongly on the background. The metric field that is a solution to the supergravity equations is a so-called black brane solution, which is just a generalization of a black hole to higher dimensions. Gravity far in the asymptotic region also decouples from the system due to the gravitational red shift. Therefore, one can zoom in to the near-horizon region of the space-time, which in the case of D3-branes is given by  $AdS_5 \times S^5$ . The idea behind the AdS/CFT duality is that the classical (super-) gravitational description is fully equivalent to the quantum theory of the large- $N_c$ , large  $\lambda$  limit of the super-Yang-Mills theory. This particular gauge/gravity duality, which has passed many nontrivial tests, has since been greatly generalized and also been used in the form of phenomenological (bottom-up) models.

## 4.2 The Witten model

The Sakai-Sugimoto model [156, 157] is a string-theoretical top-down approach to large- $N_c$  QCD. It is based on a proposal for a holographic dual of a non-supersymmetric large- $N_c$  Yang-Mills theory in four effective dimensions by Witten [184]. In contrast to the original AdS/CFT correspondence, the background is provided by the gravitational field of a stack of D4-branes. The dual field theory now is 4 + 1-dimensional since this is the dimension of the world volume of the D4-branes. The extra dimension is compactified on an  $S^1$  and is used to break supersymmetry on the field theory side: by imposing anti-periodic boundary conditions on the adjoint fermions, they obtain a mass of the order of the inverse radius of the  $S^1$ , called Kaluza–Klein mass  $M_{KK}$ . At one loop level, also the adjoint scalars become massive. Hence, by choosing the radius of the extra dimension small enough and by restricting to low energies, one effectively breaks supersymmetry and effectively reduces the number of dimensions to 3 + 1. However, there is a price to pay for introducing the extra dimension: in order to justify the supergravity approximation for the D4-brane background, the five-dimensional (dimensionful) 't Hooft coupling  $\lambda_5$  has to be large compared to  $M_{KK}^{-1}$ . This corresponds to a large four-dimensional (dimensionless) 't Hooft coupling  $\lambda = \lambda_5 / (2\pi M_{KK}^{-1})$ . In this case, however, the mass gap of the field theory is of the same order as  $M_{KK}$  and thus the Kaluza-Klein modes do not decouple. Only in the opposite limit  $\lambda \ll 1$ , where string corrections are important and which thus is inaccessible, the Kaluza-Klein modes do decouple and the theory becomes dual to large- $N_c$  QCD in 3+1 dimensions (at small energies below

the Kaluza-Klein scale). It has nevertheless turned out that the classical gravity limit of the D4-brane background is a remarkably useful tool for understanding certain nonperturbative properties of (large- $N_c$ ) QCD.

An important property of the Witten model is the existence of a Hawking–Page transition between a soft-wall and a black hole background, which encodes a confinement–deconfinement transition. This feature can be understood either from power counting in  $N_c$  of the corresponding thermodynamic potentials of the gravity backgrounds or by studying the dual to the Wilson line. Confined and deconfined phases correspond to two different geometric backgrounds which are, in coordinates made dimensionless by dividing by the curvature radius  $R$ , given by

$$\frac{ds^2}{R^2} = u^{3/2} \left[ -h_d(u)dt^2 + \delta_{ij}dx^i dx^j + h_c(u)dx_4^2 \right] + \frac{du^2}{f(u)u^{3/2}} + u^{1/2}d\Omega_4^2, \quad (4.1)$$

where

$$f(u) = \begin{cases} 1 - \frac{u_{\text{KK}}^3}{u^3} \\ 1 - \frac{u_T^3}{u^3} \end{cases}, \quad h_d(u) = \begin{cases} 1 \\ 1 - \frac{u_T^3}{u^3} \end{cases}, \quad h_c(u) = \begin{cases} 1 - \frac{u_{\text{KK}}^3}{u^3} & \text{conf.} \\ 1 & \text{deconf.} \end{cases} \quad (4.2)$$

and

$$u_{\text{KK}} = \left( \frac{4\pi}{3} \right)^2 \frac{R^2}{\beta_{x_4}^2} = \frac{4}{9} R^2 M_{\text{KK}}^2, \quad u_T = \left( \frac{4\pi}{3} \right)^2 \frac{R^2}{\beta_\tau^2}. \quad (4.3)$$

Here,  $\beta_{x_4}$  is the period of  $x_4$  – the coordinate of the additional  $S^1$  – necessary to prevent a conical singularity at  $u = u_{\text{KK}}$  in the confined phase. The curvature radius is related to the Yang–Mills coupling  $g_{\text{YM}}$  by

$$R^3 = \pi g_s N_c \ell_s^3 = \frac{g_{\text{YM}}^2 N_c \alpha'}{2M_{\text{KK}}}, \quad (4.4)$$

where  $\ell_s = \sqrt{\alpha'}$  is the string length. In the analytic continuation to Euclidean signature, time is also compactified to a circle with circumference  $\beta_\tau = T^{-1}$ , analogously to finite temperature field theory. Increasing the temperature shrinks the Euclidean time circle. At the point where the circumference of the time circle and the extra dimensional circle match, the Hawking–Page transition takes place. Apart from the metric field the Witten model also contains a nontrivial dilaton and Ramond–Ramond

(RR) flux background given by

$$e^\Phi = u^{3/4} g_s, \quad F_4 = \frac{(2\pi)^3 \ell_s^3 N_c}{\Omega_4} d\Omega_4, \quad (4.5)$$

where  $\Omega_4$  is the volume of the 4-sphere.

### 4.3 The Sakai–Sugimoto model

Sakai and Sugimoto introduced fundamental quarks by placing two stacks of  $N_f$  D8-branes with opposite orientation into the Witten model in the so-called probe limit  $N_f \ll N_c$ , i.e., back-reactions on the geometry are neglected. In the asymptotic region  $u \rightarrow \infty$  the two stacks of D-branes are separated on the Kaluza–Klein circle. In the original model they reside at antipodal points. In the bulk, the D-branes are space filling in the field theory directions,  $x^\mu$ , as well as in the  $S^4$ , and are specified by an embedding function in the  $u$ - $x_4$  subspace. Before going to the gravity description of the D4-branes one can interpret the underlying string picture as follows: strings connecting the D4 with the D8-branes carry one flavor and one color index, hence representing (massless) quarks in the fundamental representation, whereas strings stretching between D8-branes, i.e. the gauge fields living on the D8-branes represent mesons. The local symmetry of the  $U(N_f) \times U(N_f)$  gauge theory supported on the world volume of the stacks of D8-branes translates into a global symmetry via the holographic dictionary, which is interpreted as the chiral symmetry of the field theory. In the confined background, the two stacks of D8-branes are forced to join at  $u_{\text{KK}}$  where the additional  $S^1$  degenerates and therefore form a single stack with gauge symmetry  $U(N_f)$ , see Fig. 4.1. On the field theory side, this reflects the chiral symmetry breaking mechanism. One can use a diagonal subgroup of the full symmetry group to introduce chemical potentials and electromagnetic quantities such as an external, non-dynamical magnetic field. Usually the gauge is chosen such that for example the asymptotic value of the zeroth component of the Abelian gauge field is identified with the quark chemical potential. Due to the probe limit, the deconfinement transition is not affected by a finite chemical potential, trivially leading to a phase diagram in the plane  $T$ - $\mu$  similar to the one discussed for large- $N_c$  QCD in [125]. While loop diagrams with gluons scale as  $N_c^2$  at leading order, loop diagrams with fermions scale with  $N_c$  at leading order. Therefore the fermions cannot affect



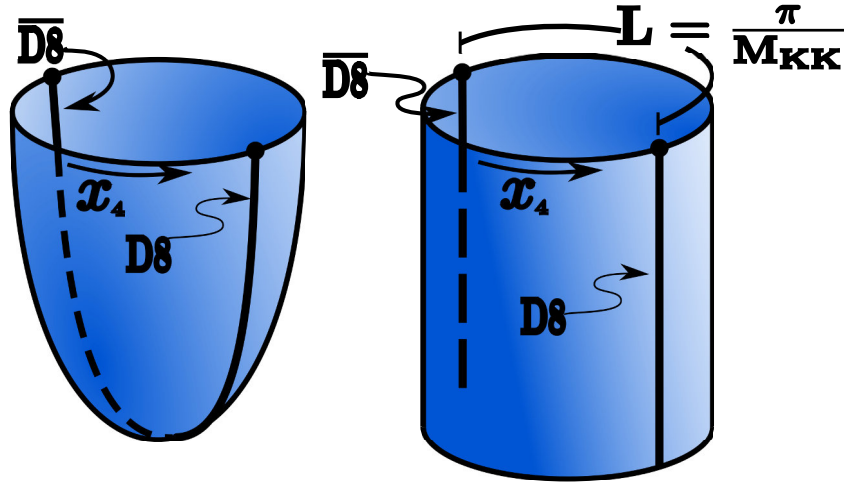


Figure 4.1: The chirally broken (left) and chirally restored phase (right). The blue cylinder and cigar depict the subspace parametrized by  $u$  and  $x_4$  of the gravity background. The tip of the cigar is the location where  $x_4$  degenerates, i.e.  $u = u_{KK}$ , whereas the bottom of the cylinder represents the black hole horizon of the deconfined background geometry  $u = u_T$ .

the phase diagram as long as  $\mu \sim N_c^1$ . Assuming that large  $N_c$  QCD confines the  $\mu - T$  phase diagram looks like the one in Fig. 4.2.

The low-energy effective theory describing the open string fluctuations is a non-abelian Dirac–Born–Infeld (DBI) theory on the probe branes; calculating the fluctuations of the gauge field and the embedding function  $x_4(u)$  corresponds to calculating the meson spectrum. In the so-called  $\mathcal{A}_z = 0$  gauge the  $\mathcal{A}_\mu$  accounts for the massive vector mesons as well as for the massless pions. From the fluctuations of the embedding functions one obtains the massive scalar mesons. The parity of the mesons is determined by the behavior of the fluctuations when switching from the left-handed brane to the right-handed one. The behavior under charge conjugation is found by taking the transpose of the gauge fields, since this amounts to flipping orientation of the strings. Indeed, after fitting the value of the 't Hooft coupling  $\lambda$  and  $M_{KK}$  to the rho meson mass and the pion decay constant, the ratios of the mass spectra roughly match experimental data. The mode expansion used in the calculation of the meson spectrum can also be used to derive an effective action for the mesons which is precisely that of the Skyrme model [165].

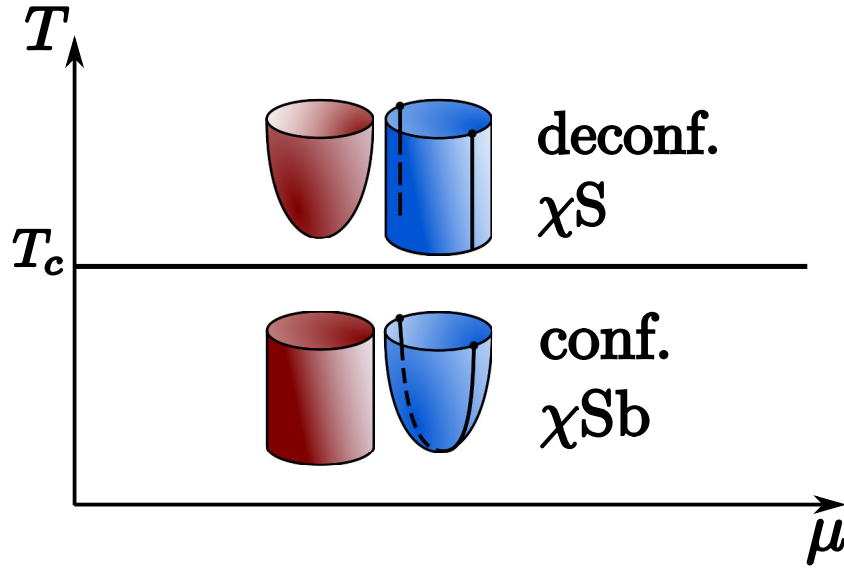


Figure 4.2: The phase diagram for deconfinement in large  $N_c$  QCD. The red cigars and cylinders denote the subspace parametrized by  $u$  and  $\tau$ .

#### 4.4 Large $N_c$ baryons

Apart from the DBI action, the dynamics of D8-branes in a background with nontrivial RR-flux is governed by a Chern–Simons (CS) action, since the D8-brane is magnetically charged under that flux. This contribution allows for introducing baryons in the model. The full action reads

$$\begin{aligned}
 S &= S_{\text{DBI}} + S_{\text{CS}} \\
 &= T_8 \int_{D8} d\tau d^8x e^{-\Phi} \text{Tr} \sqrt{|\det(g_{mn} + 2\pi\alpha' \mathcal{F}_{mn})|} \\
 &\quad + \frac{T_8}{6} \int_{D8} C_3 \text{Tr}(2\pi\alpha' \mathcal{F})^3, \tag{4.6}
 \end{aligned}$$

where  $T_8$  is the D8-brane tension, and  $dC_3 = F_4$ . The last term in (4.6) is describing the coupling of the RR-potential  $C_3$  to the invariant polynomial  $\text{Tr} \mathcal{F}^3$ , where the product of the field strength is understood as a wedge product of the Lie algebra valued 2-forms  $\mathcal{F}$ . This invariant polynomial is a total derivative of the so-called

Chern–Simons 5-form, i.e.  $\text{Tr}\mathcal{F}^3 = d\text{Tr}\mathcal{F}_5^3$ , hence up to boundary terms

$$\begin{aligned} \frac{(2\pi\alpha')^3 T_8}{6} \int_{D8} C_3 dQ_5 &= \frac{(2\pi\alpha')^3 T_8}{6} \int_{D8} F_4 Q_5 = \\ &= \frac{N_c}{6(2\pi)^2} \int_{\mathcal{M}^4 \times \mathbb{R}} Q_5, \end{aligned}$$

where we used  $T_8 = (2\pi)^{-8}(\alpha')^{-9/2}$  and the integral over  $F_4$  defined in (4.5). Since  $U(N_f) \simeq SU(N_f) \times U(1)$  we may split the gauge field into non-abelian and abelian part  $\mathcal{A} = A + 1\hat{A}$  and find up to surface terms for the integral over the Chern–Simons 5-form, see Sec. A.4,

$$\frac{(2\pi\alpha')^3 T_8}{6} \int_{D8} C_3 \text{Tr}\mathcal{F}^3 = \frac{N_c}{6(2\pi)^2} \int_{\mathcal{M}^4 \times \mathbb{R}} \left[ Q_5(A, F) + 3\hat{A}\text{Tr}F^2 + N_f \hat{A} \hat{F}^2 \right]. \quad (4.7)$$

The second term in the integrand couples the  $U(1)$  gauge field to the Pontryagin density, which when integrated over together with the prefactor  $1/8\pi^2$  yields (minus) the winding number  $N_4$  (aka. Pontryagin index, aka. instanton number) of the principal  $SU(N_f)$ -bundle. To be more specific, restricting oneself to  $N_f = 2$ , to the Yang–Mills approximation of the DBI-action as well as to the vicinity of  $u_{KK}$  one finds that the BPST instanton is a solution to the equations of motion [101]. This pseudoparticle has width of order  $\lambda^{-1/2}$ . If we choose the legs of the 4-form  $F^2$  in the directions of  $u$  and  $x^1, x^2$  and  $x^3$ , the instanton density couples to the  $U(1)$  gauge field component  $\hat{A}_0$ , i.e. it acts as a localized source with charge  $N_4 N_c$  for the bulk electric field associated with  $\hat{A}_0$ . As we will see later on, this in turn is related to the quark number density, also given by  $N_4 N_c$ . At the same time the CS action may be regarded as describing the effect of lower dimensional D-branes dissolved in the D8-brane [56], this feature is usually referred to as "branes within branes". In the case at hand the term  $\text{Tr}F^2$  corresponds to a D4-brane.

We will now focus on this perspective on the CS-action: It was shown by Witten in Ref. [185] that the baryon-vertex in  $\mathcal{N} = 4$   $SU(N_c)$ -SYM theory in 4 dimensions is encoded by a D5-brane wrapped on the  $S^5$  in the dual SUGRA description. Sakai and Sugimoto argued in Ref. [156] that in the case of the D4/D8 brane system the baryon vertex corresponds to a D4 brane wrapped on the  $S^4$ . Let us recapitulate the important points in the discussion in Ref. [185]: There the baryon is first constructed as a vertex connecting  $N_c$  external quarks represented as endpoints of fundamental

superstrings at the holographic boundary of spacetime, all oriented in the same direction. The other endpoints of the strings have to end on a D-brane in the bulk – for example a D5-brane wrapped on the internal  $S^5$  from the perspective of the  $AdS_5$  space time would describe such a vertex. Now a D5-brane wrapped on  $S^5$  carries a charge of  $N_c$  due to the CS-coupling. One of the relevant terms of the D5-brane action reads

$$\frac{1}{2\pi} \int_{\mathbb{R} \times S^5} V \wedge F_5, \quad (4.8)$$

where  $V$  denotes the  $U(1)$ -part of the gauge field living on the world volume of the D5 brane and

$$\frac{1}{2\pi} \int_{S^5} F_5 = N_c. \quad (4.9)$$

Since a gauge field on a compact manifold cannot be charged, Witten concludes that the total charge must vanish and the charge-contribution of  $-N_c$  is exactly provided by the endpoints of  $N_c$  elementary superstrings ending on the wrapped D5 brane. In the case of the Sakai–Sugimoto model we will therefore add to the D8-brane action a source term provided by the DBI action describing a D4-brane wrapped on the  $S^4$ . Since we assume that the gauge fields should have no legs in the  $S^4$  directions the source action should be a suitable distribution of

$$S_{D4} = T_4 \int d\Omega_4 d\tau e^{-\Phi} \sqrt{\det g}. \quad (4.10)$$

Since D4-branes are massive, precisely accounted for by the D4-brane action, they feel the gravitational pull of the background space-time [44]. On the other hand the D8-branes in which the D4-branes are dissolved prevent them from falling, hence when calculating the embedding of the D8-branes in the background, one has to take this force balancing into account.

Furthermore, using again the mode expansion of the gauge fields, the CS part of the D8-brane action yields precisely the Wess-Zumino-Witten term of the Skyrme model. Therefore, the large  $N_c$  baryons discussed above correspond to the chiral solitons of the Skyrme model, which describe baryons there. The idea of these solitonic baryons in the Skyrme model originally came from the discussion of baryons in large  $N_c$  QCD in the late 70's and early 80's [180, 183, 182]. Using  $N_c$  counting rules the main conclusions of [180] were that mesons are interacting weakly among

each other  $\sim N_c^0$ , but strongly with baryons  $\sim N_c$ . Furthermore the mass of the baryons is  $\sim N_c$ , i.e. diverging relative to the meson mass  $N_c^0$ . Moreover the size and shape of baryons in the Hartree-Fock approximation is independent of  $N_c$ . The Polyakov–'t Hooft monopoles have similar behavior where now the weak coupling constant is a valid expansion parameter, as is  $1/N_c$  in large  $N_c$  QCD. The monopole mass scales with the inverse of the coupling constant, the equations of motion are independent of the coupling constant, and the electrons scatter non-trivially of the monopoles in the weak coupling limit. In Refs. [183, 182] this analogy was made precise in the context of the Skyrme model. Therefore, one might think of baryons in the Sakai–Sugimoto model bridging the gap between the Skyrme model and the ideas obtained in large  $N_c$  QCD. Further studies concerning baryons and their spectrum in the Sakai–Sugimoto model can be found in [101, 163]. The approximation of point like D4-branes which is utilized in the  $N_f = 1$  case was discussed in [154].

## 4.5 NJL limit

The Sakai–Sugimoto model may also be connected to the NJL model. In the "decompactified" limit where the asymptotic coordinate distance between the D8- and anti-D8-branes is much smaller than the radius of the compactified extra dimension,  $L \ll M_{KK}^{-1}$ , the Sakai–Sugimoto model is dual to a non-local NJL model [11]. As a consequence, in the scenario with broken chiral symmetry, the D8-branes now in general join at  $u_0 > u_{KK}$ . The difference  $u_0 - u_{KK}$  is commonly interpreted as the constituent quark mass within a meson, which is realized as a string with both end points attached to the tip of the joined D8-branes hanging down to the bottom of the geometry. With a sufficiently small asymptotic separation of the flavor branes, it is also possible to find an energetically preferred phase with broken chiral symmetry in the deconfined background [4], see Fig. 4.3. The resulting phase diagram at finite chemical potential was first discussed in [104]. By reducing  $L$  compared to  $M_{KK}^{-1}$ , the temperature range where the system is confined becomes small compared to the temperature range governed by the deconfined and chirally broken phase. Eventually, the resulting phase diagram resembles the NJL result (where no confined phase is present) shown in the right panel of Fig. 3.3. Consequently, the Sakai–Sugimoto model allows for interpolating between a non-local NJL model ( $L \ll M_{KK}^{-1}$ ) and – modulo the caveats mentioned in section 4.2 – large- $N_c$  QCD ( $L = \pi M_{KK}^{-1}$ ). In the former

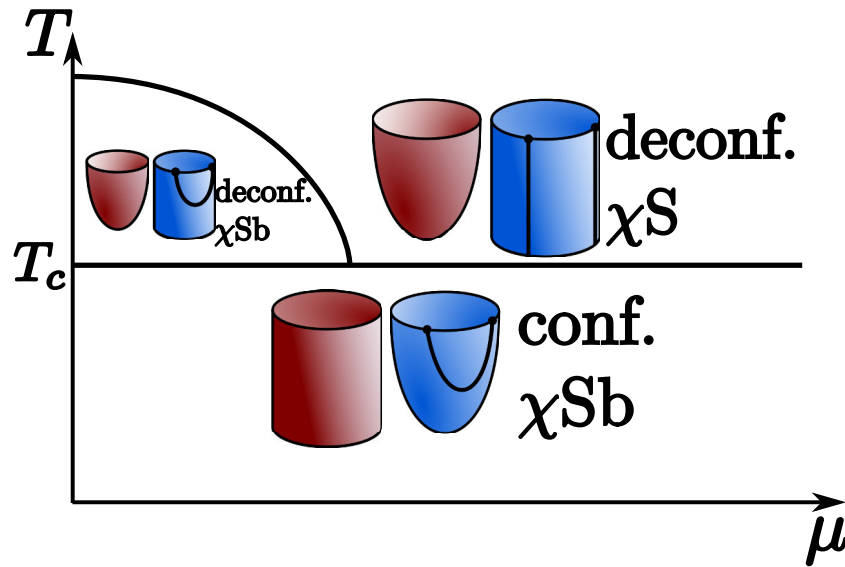


Figure 4.3: The phase diagram for deconfinement and chiral symmetry breaking with small asymptotic D8-brane separation.

limit, the flavor D8-branes do not probe deeply the background geometry produced by the color D4-branes (which corresponds to neglecting gluon dynamics), while in the latter the gluons dominate. In [21] point like D4-branes as baryon sources were introduced in the non-antipodal D8-brane configuration.

## Chiral symmetry breaking in a magnetic field in the NJL model

We will now focus on the effect of a background magnetic field on the chiral phase transition of QCD, or to be more precise in the NJL and the Sakai–Sugimoto model. In order to understand what effects a magnetic field might have on the formation of the chiral condensate, let us recapitulate the general discussion given in [96]. As can be seen from Eq. (2.12), calculating the chiral condensate in field theory amounts to calculating a fermion loop. Let the bare fermion mass be finite for the moment in order to regulate possible IR divergences and regularize the UV divergence via a cut-off in some suitable scheme, e.g., Schwinger's proper time method. In the following section we will show that in the presence of a magnetic field one has to take Landau quantization of the transverse momentum of the charged fermions into account. It turns out that if one performs the chiral limit in the calculation of the fermion loop, an IR singularity appears, which can be shown to originate from the lowest Landau level. As a consequence, a mass gap is dynamically generated in order to avoid this IR singularity for any non-vanishing value of the dimensionless coupling constant  $g$  in contrast to the previous results without magnetic field, where  $g > 1$  was a necessary condition for chiral symmetry breaking. The precise form of the gap is of course dictated by the form of the interactions in the model under consideration.

This effect – termed magnetic catalysis – was first found in the Gross-Neveu model [116, 115] and later on in several NJL model calculations [96, 95, 98, 74] and in QED [97] as well as in holographic approaches [67, 60, 68, 69, 45, 32, 59]. It also plays an important role in the context of graphene [94, 89]. For QCD, it was found in a lattice calculation (however, with unphysical quark masses) that the critical temperature increases with the magnetic field [53], in accordance with magnetic catalysis. However, recently the Budapest-Wuppertal collaboration found (with physical quark masses) that the maximum of the quark susceptibility drops significantly at temperatures about 140 MeV under the influence of a magnetic field [15], i.e., the opposite effect was observed. It remains an open and interesting question what prevents magnetic catalysis to persist for larger temperatures in QCD. For simplicity we restrict the chiral symmetry group to  $U(1)_V \times U(1)_A$ , i.e.  $N_f = 1$  in the following discussions.

## 5.1 Fermions in a magnetic field

Let us consider a homogeneous background magnetic field  $\vec{B} = (0, 0, B)$  by choosing the Landau gauge fixing condition with  $\vec{A} = (-yB, 0, 0)$ . Within this ansatz, the eigenfunctions of the Hamiltonian are proportional to  $\exp[i(\omega_n \tau + k_x x + k_z z)]$ . Using this, we split the Dirac Hamiltonian in a longitudinal and a transverse part with respect to the direction of the magnetic field,  $H_D = H_L + H_T$ , where

$$\begin{aligned} H_L &= \gamma^0 \gamma^3 k_z + \gamma^0 M, \\ H_T &= \text{sgn}(q) \sqrt{2|q|B} \begin{pmatrix} -1 & 0 \\ 0 & 1 \end{pmatrix} \otimes \begin{pmatrix} 0 & a^\dagger \\ a & 0 \end{pmatrix}, \end{aligned} \quad (5.1)$$

with

$$a \equiv \sqrt{\frac{|q|B}{2}} \xi + \text{sgn}(q) i \frac{1}{\sqrt{2|q|B}} (-i\partial_\xi), \quad \xi \equiv y + \frac{k_x}{qB}. \quad (5.2)$$

We see that  $a$  is the annihilation (creation for  $q < 0$ ) operator of the quantum mechanical oscillator, which gives rise to the Landau quantization of the energy spectrum of a charged fermion moving in a background magnetic field. For  $q > 0$ , the



orthogonalized eigenfunctions of the Hamiltonian are given by

$$\begin{aligned} \psi_{k_x, k_z, \ell}^{e, s}(\vec{x}) &= \\ &= \frac{e^{i(k_z z + k_x x)}}{\sqrt{L_x L_z}} \frac{1}{2\sqrt{\kappa_{k_z, \ell} \epsilon_{k_z, \ell}}} \begin{pmatrix} s\sqrt{\kappa_{k_z, \ell} + sk_z} \sqrt{\epsilon_{k_z, \ell} - s\kappa_{k_z, \ell}} \langle \xi | \ell \rangle \\ \sqrt{\kappa_{k_z, \ell} - sk_z} \sqrt{\epsilon_{k_z, \ell} - s\kappa_{k_z, \ell}} \langle \xi | \ell - 1 \rangle \\ es\sqrt{\kappa_{k_z, \ell} + sk_z} \sqrt{\epsilon_{k_z, \ell} + s\kappa_{k_z, \ell}} \langle \xi | \ell \rangle \\ e\sqrt{\kappa_{k_z, \ell} - sk_z} \sqrt{\epsilon_{k_z, \ell} + s\kappa_{k_z, \ell}} \langle \xi | \ell - 1 \rangle \end{pmatrix} \end{aligned} \quad (5.3)$$

where  $\ell = 0, 1, 2, 3, \dots$  denotes the Landau level, where

$$\langle \xi | \ell \rangle = \frac{1}{\sqrt{2^\ell \ell!}} \left( \frac{|q|B}{\pi} \right)^{1/4} e^{-|q|B\xi^2/2} H_\ell(\sqrt{|q|B}\xi), \quad (5.4)$$

$\langle \xi | -1 \rangle \equiv 0$ , and

$$\epsilon_{k_z, \ell} = \sqrt{k_z^2 + M^2 + 2|q|Bl}, \quad \kappa_{k_z, \ell} = \sqrt{k_z^2 + 2|q|Bl}. \quad (5.5)$$

Here,  $H_\ell$  is the  $\ell$ th Hermite polynomial and  $L_i$  is the length of a box with volume  $V$  in the  $i$ th direction. In order to obtain the eigenfunctions for the case  $q < 0$ , one simply replaces  $\langle \xi | \ell \rangle$  with  $\langle \xi | \ell - 1 \rangle$  and vice versa.

From Eq. (5.3) we see that in the lowest Landau level (LLL)  $\ell = 0$  only the  $\text{sgn}(q)s = 1$ -states survive, which are also eigenstates of the helicity operator  $\Sigma_3 = \gamma^0 \gamma^3 \gamma_5$  as well as zero-eigenmodes of  $H_T$ . Therefore, the dynamics of the LLL becomes effectively  $1 + 1$ -dimensional and the fermions are fully polarized. Moreover, in the limit  $M \rightarrow 0$  for  $\text{sgn}(q)e k_z > 0$  ( $< 0$ ) these states are right- (left-) handed only. This is an indication that the magnetic field induces an axial current [127]. Its expectation value is given by

$$\langle j_5^\mu \rangle = -\frac{T}{V} \text{Tr} \frac{\gamma^0 \gamma^\mu \gamma_5}{i\omega_n + \mu - \epsilon}. \quad (5.6)$$

For the diagonal matrix elements of  $\gamma^0 \gamma^3 \gamma_5$  with respect to the eigenspinors above we find

$$(\gamma^0 \gamma^3 \gamma_5)_{e, s, k_z, \ell} = \text{sgn}(q) \frac{sk_z}{\kappa_{k_z, \ell}}. \quad (5.7)$$

Due to the sum over  $s$  in the axial current (5.6), the relation (5.7) shows that only the LLL level contributes. Due to the sum over  $e$  there can only be a finite contribution if

$\mu \neq 0$ . Since we have put the fermions into a box with volume  $V = L_x L_y L_z$ , the range of  $y$  is restricted to  $[-L_y/2, L_y/2]$  and therefore  $k_{x,\max} - k_{x,\min} = L_y |q| B$ , because we have absorbed  $k_x$  into the new coordinate  $\xi$ . Hence, because of  $\Delta k_x = 2\pi/L_x$ , each energy level for given  $e$ ,  $k_z$ ,  $s$  and  $\ell$  has a degeneracy of  $L_x L_y |q| B / (2\pi)$ . In two cases the result for the axial current along the magnetic field can be given in closed form,

$$M = 0, \forall T: \quad \langle j_5^3 \rangle = \frac{qB\mu}{2\pi^2}, \quad (5.8)$$

$$T = 0, \forall M < \mu: \quad \langle j_5^3 \rangle = \frac{qB\sqrt{\mu^2 - M^2}}{2\pi^2}. \quad (5.9)$$

The prefactor  $|q|B/(2\pi)$  found by phase space considerations has a very special role here. It is the difference of the number of zero-eigenmodes of  $H_T$  with  $s = 1$  and  $s = -1$  respectively. This is a topological result since it is given by the index of each  $2 \times 2$  block of  $H_T$ , which in turn is linked to the Euclidean chiral anomaly in two dimensions via the index theorem. Furthermore, the first result is independent of  $T$  which is a special feature of massless  $1 + 1$  dimensional fermions and hence again reflects the effective dimensional reduction.

## 5.2 NJL model in an external magnetic field

Let us return to chiral symmetry breaking, now in the presence of a magnetic field. The thermodynamic potential and the gap equation read

$$\Omega = \frac{N_c M^2}{2\lambda^2} + \frac{N_c |q| B}{2\pi} \sum_{e=\pm} \sum_{\ell=0}^{\infty} \alpha_\ell \int_{-\infty}^{\infty} \frac{dk_z}{2\pi} \left[ \frac{\epsilon_{k_z, \ell}}{2} + T \ln \left( 1 + e^{-\frac{\epsilon_{k_z, \ell} - e\mu}{T}} \right) \right], \quad (5.10)$$

$$\frac{1}{\lambda^2} = \frac{|q| B}{2\pi} \sum_{\ell=0}^{\infty} \alpha_\ell \int_{-\infty}^{\infty} \frac{dk_z}{2\pi} \frac{1}{\epsilon_{k_z, \ell}} [1 - f(\epsilon_{k_z, \ell} - \mu) - f(\epsilon_{k_z, \ell} + \mu)], \quad (5.11)$$

where  $\alpha_\ell \equiv 2 - \delta_{0\ell}$ . Comparing with the corresponding  $B = 0$  expressions in Eqs. (3.3) and (3.4), we see that the effect of the magnetic field is to replace  $\epsilon_k \rightarrow \epsilon_{k_z, \ell}$  and

$$2 \int \frac{d^3 k}{(2\pi)^3} \rightarrow \frac{|q| B}{2\pi} \sum_{\ell=0}^{\infty} \alpha_\ell \int_{-\infty}^{\infty} \frac{dk_z}{2\pi}. \quad (5.12)$$

Using again proper time regularization, the thermodynamic potential at vanishing temperature becomes

$$\begin{aligned} \frac{1}{N_c} \Omega_{T=0} &= \frac{1}{N_c} \Omega_{\mu=T=B=0} \\ &\quad - \frac{(qB)^2}{2\pi^2} \left[ \frac{x^2}{4} (3 - 2 \ln x) + \frac{x}{2} \left( \ln \frac{x}{2\pi} - 1 \right) + \psi^{(-2)}(x) \right] \\ &\quad - \frac{|q|B}{4\pi^2} \theta(\mu - M) \sum_{\ell=0}^{\ell_{\max}} \alpha_{\ell} \left( \mu k_{F,\ell} - M_{\ell}^2 \ln \frac{\mu + k_{F,\ell}}{M_{\ell}} \right). \end{aligned} \quad (5.13)$$

Here,  $\Omega_{\mu=T=B=0}$  is the vacuum part from Eq. (3.5),  $\psi^{(n)}$  the  $n$ -th polygamma function (analytically continued to negative values of  $n$ ), we have abbreviated  $x \equiv M^2/(2|q|B)$ , and

$$M_{\ell} \equiv \sqrt{M^2 + 2|q|B\ell}, \quad k_{F,\ell} \equiv \sqrt{\mu^2 - M_{\ell}^2}, \quad \ell_{\max} \equiv \left\lfloor \frac{\mu^2 - M^2}{2|q|B} \right\rfloor. \quad (5.14)$$

Different regularization schemes – compare for instance with [126], where dimensional regularization is used – only differ in the  $B = 0$  result and in (divergent) terms that depend on  $B$  but are constant in  $M$ , which are omitted. The latter can be viewed as renormalizing the energy content coming solely from the magnetic field.

The corresponding gap equation is

$$\begin{aligned} \frac{1}{g} &= \left[ e^{-M^2/\Lambda^2} - \frac{M^2}{\Lambda^2} \Gamma \left( 0, \frac{M^2}{\Lambda^2} \right) \right] \\ &\quad + 2 \frac{|q|B}{\Lambda^2} \left[ \left( \frac{1}{2} - x \right) \ln x + x + \ln \Gamma(x) - \frac{1}{2} \ln 2\pi \right] \\ &\quad - 2 \frac{|q|B}{\Lambda^2} \sum_{\ell=0}^{\ell_{\max}} \alpha_{\ell} \ln \frac{\mu + k_{F,\ell}}{M_{\ell}} \theta(\mu - M). \end{aligned} \quad (5.15)$$

### 5.3 Magnetic catalysis

Let us first consider the case  $\mu = 0$ , i.e., we can ignore the terms  $\propto \theta(\mu - M)$  in Eqs. (5.13) and (5.15). For small coupling  $g \ll 1$ , the dynamical mass squared will be much smaller than the magnetic field,  $M^2 \ll |q|B$ . Then, with  $M \ll \Lambda$ , the gap

equation becomes

$$\frac{1}{g} \simeq \frac{2|q|B}{\Lambda^2} \ln \sqrt{\frac{|q|B}{\pi M^2}}. \quad (5.16)$$

Now, there is a nontrivial solution for arbitrarily small  $g$ . This is in contrast to the case  $B = 0$  where chiral symmetry can be broken only for  $g > 1$ . The solution is obviously

$$M \simeq \sqrt{\frac{|q|B}{\pi}} e^{-\frac{\pi^2}{|q|B g}}. \quad (5.17)$$

This qualitative effect of the magnetic field on chiral symmetry breaking was termed "magnetic catalysis" in [95] and was since observed in numerous different models. Interestingly, as already mentioned in the introduction, this effect stems mainly from the physics in the LLL. In order to show that, one omits all contributions from  $\ell > 0$  in (5.11) and cuts off the momentum integral at  $\sqrt{|q|B/4\pi}$ , since below that cut-off the LLL dominates. Then, one obtains exactly the result (5.17). Furthermore, the logarithmic IR singularity in (5.16) regulated by the dynamically generated mass is precisely due to the LLL contribution and its  $1 + 1$  dimensional nature. The form of the gap in the weak coupling limit is reminiscent of the BCS gap in a superconductor [17]. In both expressions for the respective gap the relevant density of states appears in the denominator of the exponent. Here it is the density of states of the massless fermions at  $\epsilon_{k_z, \ell=0} = 0$ , whereas in the BCS gap it is the density of states at the Fermi surface. In both cases the dynamics is essentially  $1 + 1$ -dimensional. While in BCS theory this effective dimensional reduction is a consequence of the Fermi surface, here it is provided by the magnetic field. Note that the dimensional reduction is not in conflict with the Mermin–Wagner–Coleman theorem that states that no spontaneous symmetry breaking can occur in  $1 + 1$  dimensions. The reason is that the Nambu–Goldstone modes are neutral, and hence their motion is not restricted by the magnetic field. At extremely large magnetic fields the internal structure of these modes can be resolved which might invalidate this argument [72].

Let us try to understand this effect also less formally using the analogy with BCS super conductivity. As we have discussed briefly in chapter 2, Cooper pairing takes place in a small vicinity of the Fermi surface. An arbitrarily small attractive interaction suffices to induce an instability of the Fermi surface which leads to pairing and the formation of an energy gap. In chiral symmetry breaking at  $\mu = 0$ , the pairing takes place between fermions and anti-fermions at the energy level  $\epsilon = 0$ . However, without a magnetic field, there are actually no constituents available for pairing in

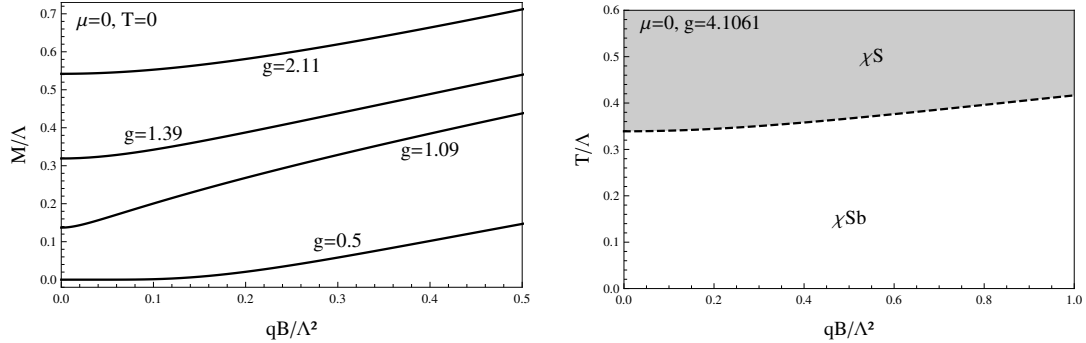


Figure 5.1: Effects of magnetic catalysis on the dynamical mass  $M$  and the critical temperature. Left: the gap at  $T = \mu = 0$  for different couplings. The lowest coupling shown corresponds to a subcritical coupling at  $B = 0$ , i.e., its nonzero value is solely induced by  $B$ . Its behavior at small  $B$  is given by the exponential in Eq. (5.17). Right: the critical temperature for chiral symmetry restoration as a function of  $B$ .

the vicinity of  $\varepsilon = 0$ , since the density of states vanishes there. This is in contrast to the BCS superconductor, where at the Fermi surface plenty of states are available  $\sim \mu^2$ . This we might interpret as the reason for the condition  $g > 1$  for pairing in the NJL model. In terms of the Dirac sea picture we need strong interactions in order to "dig deeper" into the Dirac sea and pair particles with  $\varepsilon \neq 0$ . This is different in a background magnetic field: The density of states at  $\varepsilon = 0$  is  $\sim B$  as explained in the introduction of this chapter, hence even in an infinitesimal vicinity of this "Dirac surface" there are states available for pairing. Given the similarity of the NJL model and a relativistic BCS model where the phonon mediated interaction has been approximated by a point like interaction, it is quite natural that the gaps of both models turn out to share common features.

We show the numerical solution of the gap equation for various values of the coupling for  $T = \mu = 0$  in the left panel of Fig. 5.1. Magnetic catalysis also manifests itself in the critical temperature for chiral symmetry restoration, which, at  $\mu = 0$ , monotonically increases with increasing magnetic field, see right panel of Fig. 5.1.

## 5.4 Inverse magnetic catalysis

We now include the contributions from a non-vanishing chemical potential  $\mu$ . First we discuss the case of weak coupling which corresponds to  $M^2 \ll |q|B$ . Since the

chiral phase transition can be expected to occur at chemical potentials of the order of the mass gap, we may thus also assume  $\mu^2 \ll |q|B$  (we are not interested in the physics far beyond the phase transition). As a consequence, we can employ the lowest Landau level approximation, i.e., drop the contribution of all higher Landau levels. Then, from Eq. (5.13) we conclude that the difference of the thermodynamical potentials of the chirally broken phase and the quark matter phase is

$$\begin{aligned} \Delta\Omega \simeq & \frac{|q|B}{4\pi^2} \left( \mu^2 - \frac{M^2}{2} \right) - \frac{|q|B}{4\pi^2} \mu k_{F,0} \theta(\mu - M) \\ & + \frac{\Lambda^2 M^2}{8\pi^2} \underbrace{\left( \frac{1}{g} - \frac{2|q|B}{\Lambda^2} \ln \sqrt{\frac{|q|B}{\pi M^2}} + \frac{2|q|B}{\Lambda^2} \theta(\mu - M) \ln \frac{\mu + k_{F,0}}{M} \right)}_{=0 \text{ via gap equation}}. \end{aligned} \quad (5.18)$$

Again, we find a very interesting analogy to superconductivity: the resulting expression is exactly the same as for a BCS superconductor with mismatched Fermi momenta – first discussed by Clogston [51] and Chandrasekhar [47] – after  $M$  is replaced by the superconducting gap  $\Delta$ ,  $|q|B$  – the density of states at  $\varepsilon = 0$  – by the average Fermi momentum (squared) of the constituents of a Cooper pair, and  $\mu$  by (half) the difference of the respective Fermi momenta<sup>1</sup>.

To discuss the meaning of  $\Delta\Omega$  for the chiral phase transition, let us first consider the case of a fixed magnetic field  $B$  and start from  $\mu = 0$ , i.e., in the chirally broken phase. Upon increasing  $\mu$ , we will reach the point  $\mu = M/\sqrt{2}$  where  $\Delta\Omega$  changes its sign and thus the phase transition to the chirally restored phase occurs. This point is, in the context of superconductivity, called the Clogston limit. It occurs before the second term has a chance to contribute since still  $\mu < M$ . Now, more importantly for our purpose, let us again start in the chirally broken phase, i.e., from  $\Delta\Omega < 0$ , but now we increase the magnetic field at fixed  $\mu$  (as we have just seen, for the discussion of the phase transition we may assume  $\mu < M$  and thus ignore the term  $\propto \theta(\mu - M)$ ). Since we have started from a negative  $\mu^2 - M^2/2$ , increasing the magnetic field can only make  $\Delta\Omega$  more negative because the dynamical mass

<sup>1</sup>Interestingly, compared to the original work [51, 47] the roles of magnetic field and chemical potential are exactly reversed. There, the splitting of the Fermi surface of the two fermion species (spin up and spin down) was induced by the magnetic field due to Zeemann splitting, while the chemical potential entered via the density of states at the Fermi surface  $\sim k_F^2$ .

increases with  $B$ . Consequently, the magnetic field only brings us "deeper" into the chirally broken phase. This is what we have expected from magnetic catalysis.

However, as we will now explain, for  $g > 1$  and finite chemical potential this expectation is incorrect. We shall rather find that, for intermediate values of the magnetic field, an increasing magnetic field *does* restore chiral symmetry. Let us, to this end, first discuss the numerical solution of the gap equation, see Fig. 5.2. Due to the

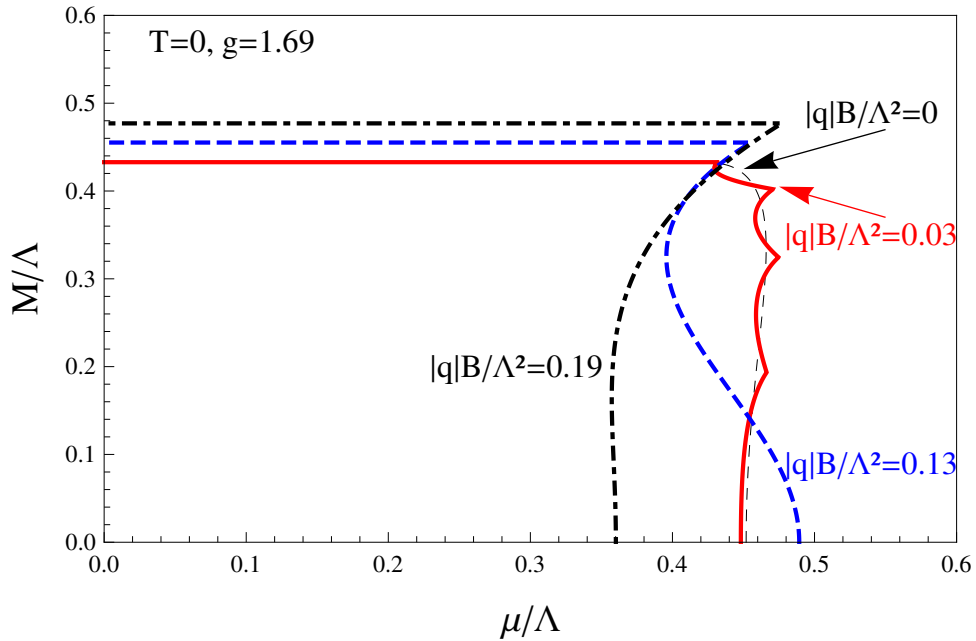


Figure 5.2: The zero-temperature dynamical mass as a function of the chemical potential for different values of the magnetic field. For the lowest nonzero value of  $|q|B$  shown (solid line), Landau level oscillations can be seen. The magnetic field for the two other curves (dashed and dashed-dotted lines) is sufficiently large to suppress all Landau levels except for the lowest.

sum over the Landau levels, the gap exhibits the well-known de Haas–van Alphen oscillations. Similar to the behavior found for  $B = 0$ , only the branches with a negative slope of  $M(\mu)$  can be energetically preferred. Depending on the specific value of  $g$  there might be several phase transitions within the gapped phase into regions with  $\mu > M$ , i.e., with a finite quark number density, before entering the restored phase  $M = 0$ . In general it is also possible that the order of the phase transition into

the restored phase oscillates between first and second order upon varying  $B$ : in the example shown in the plot, at vanishing magnetic field the phase transition is first order, while at  $|q|B/\Lambda^2 = 0.13$  it is second order and at  $|q|B/\Lambda^2 = 0.19$  again first order. We also see that the dashed (blue) curve for the *lower* magnetic field reaches farther in the  $\mu$  direction than the dashed-dotted (black) curve for the *larger* magnetic field. This is a surprise from the point of view of magnetic catalysis: it seems to indicate that the critical chemical potential for chiral symmetry breaking can decrease with increasing magnetic field. We discuss this "inverse magnetic catalysis" in more detail now.

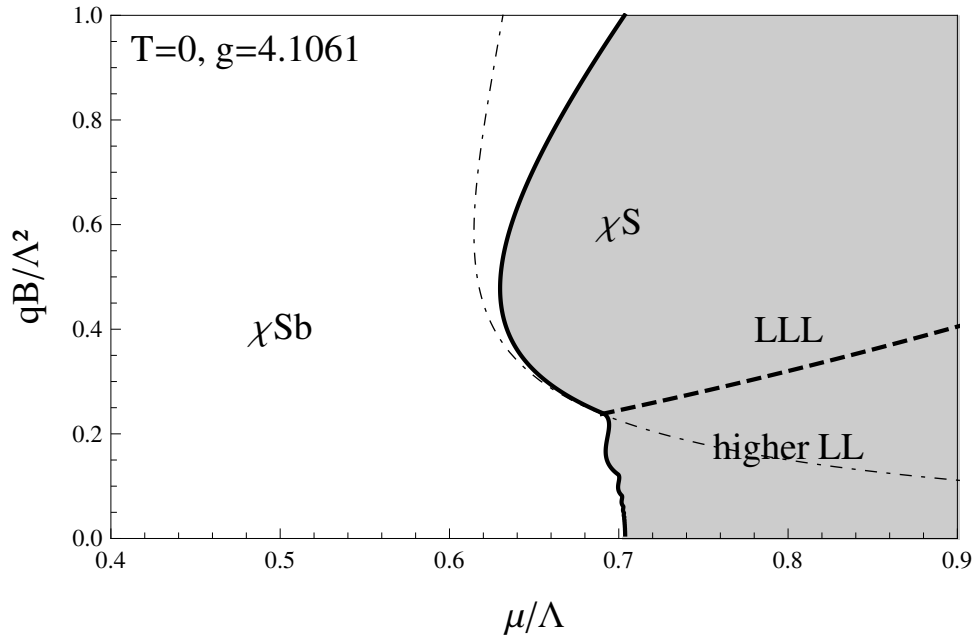


Figure 5.3: Zero-temperature chiral phase transition in the plane of magnetic field and quark chemical potential at a rather large value of the coupling constant such that the phase transition is first order for all magnetic fields. (For smaller values the shape of the transition line is similar, but the order can vary between first and second.) Apart from oscillations at small  $B$  due to higher Landau levels in the chirally restored phase, the critical chemical potential *decreases* up to  $qB/\Lambda^2 \simeq 0.5$ , see explanation in the text. The dashed-dotted line is the approximation to the phase transition line from Eq. (5.20).

To this end, let us consider the "cleaner" case of sufficiently large couplings where symmetry restoration happens in the region  $\mu < M$  for all magnetic fields.



In this case, oscillations of the critical line in the phase diagram originate solely from the restored phase (not from the solution of the gap equation), and the phase transition is always first order. The numerically obtained phase diagram for such a case is shown in Fig. 5.3. From the arguments in the previous section, one might have expected that magnetic catalysis leads to a monotonically increasing critical chemical potential as a function of  $B$  (just like the critical temperature in the right panel of Fig. 5.1). However, this is not the case: there is a region in the phase diagram where, upon increasing  $B$  at fixed  $\mu$ , chiral symmetry is *restored*, in contrast to the weak-coupling case discussed below Eq. (5.18).

In order to understand this phenomenon, let us derive an analytic expression for  $\Delta\Omega$ , analogous to the weak-coupling case. As discussed, for the given large coupling, the solution to the gap equation is simply given by the  $\mu = 0$  solution. For small magnetic fields,  $|q|B \ll M^2$ , we can expand the solution up to second order in the magnetic field,

$$M \simeq M_0 \left[ 1 + \frac{(qB)^2}{6M_0^4 \Gamma(0, M_0^2/\Lambda^2)} \right], \quad (5.19)$$

where  $M_0$  is the solution for  $\mu = B = 0$ . Inserting this solution into Eq. (5.13), we obtain the free energy for the chirally broken phase up to second order in  $B$ . The free energy for the chirally restored phase is, although we can set  $M = 0$ , complicated due to the sum over Landau levels. Let us therefore ignore the higher Landau levels. This seems to contradict our assumption of a small magnetic field which we have made for the chirally broken phase. Nevertheless, we shall see that the phase transition line obtained from this approximation reproduces the full numerical line in a region of intermediate magnetic fields. Since this is exactly the region where the "back bending" of the phase transition line is most pronounced, this serves our purpose to capture the main physics of the inverse magnetic catalysis. With  $M_0 \ll \Lambda$ , the resulting free energy difference is

$$\Delta\Omega \simeq -\frac{M_0^2 \Lambda^2}{16\pi^2} \left( 1 - \frac{1}{g} \right) + \frac{|q|B}{4\pi^2} \mu^2 - \frac{(qB)^2}{24\pi^2} \left[ 1 - 12\zeta'(-1) + \ln \frac{M_0^2}{2|q|B} \right] \quad (5.20)$$

(This is the generalization of Eq. (3.9) to nonzero (but small) magnetic fields.) This expression allows for a qualitatively different phase transition line compared to the weak-coupling limit (5.18) for the following reason. The term linear in  $B$  corresponds

to the cost in free energy to form a fermion–anti-fermion condensate at finite  $\mu$ . Importantly, this cost depends not only on  $\mu$ , but also on the magnetic field. This is also true at weak coupling. However, in that case, the gain from the condensation energy was also linear in  $B$ . This is different here: now, if we start from the chirally broken phase, i.e., from  $\Delta\Omega < 0$ , increasing the magnetic field *can* lead to a change of sign for  $\Delta\Omega$  and thus restore chiral symmetry. This is what we have termed inverse magnetic catalysis in [145]. In this reference, we have also explained that the physical picture can be understood once again in analogy to superconductivity, where, in the presence of a mismatch in Fermi momenta, it is useful to think of a fictitious state where both fermion species are filled up to a common Fermi momentum. Creating such a state costs free energy which may or may not be compensated by condensation. The point of inverse magnetic catalysis is that creating such a fictitious state (where fermions and anti-fermions are not separated by  $\mu$ ) becomes more costly with increasing  $B$ , while  $B$  still enhances the dynamical gap due to magnetic catalysis. The magnetic field thus plays an ambivalent role by counteracting its own catalyzing effect.

This effect was first observed in the NJL model in [58] at  $T = 0$  and in [106] for the full three dimensional  $T$ - $\mu$ - $B$  parameter space, and has been confirmed in various other calculations [62, 34, 48, 14, 7, 61, 65]. Only for sufficiently strong magnetic fields the system enters the regime where magnetic catalysis is dominant. Typical fits of the model-parameters yield a cut-off of the order of a few hundred MeV [40]. Translating this into a scale for the magnetic field shows that the regime of magnetic catalysis is beyond the magnetic field strength expected in compact stars, and thus, if there is any observable effect of the magnetic field for the phase transition between hadronic and quark matter, it is inverse magnetic catalysis.

## Chiral symmetry breaking in a magnetic field in holography

The effect of a homogeneous background magnetic field in the Sakai–Sugimoto model has first been considered in [22]. Shortly thereafter, the effect on the critical temperature for chiral symmetry restoration at vanishing chemical potential has been analyzed with non-antipodal brane separation [110]. Like in the NJL model shown in Fig. 5.1, the critical temperature increases with the magnetic field, which shows that the Sakai–Sugimoto model exhibits magnetic catalysis. Finite chemical potentials have been introduced together with a magnetic field in [171] in the original Sakai–Sugimoto model. The deconfined, chirally symmetric phase was discussed in [121], where a magnetic phase transition within the symmetric phase was found that is reminiscent of a transition to the lowest Landau level. The full phase diagram in the parameter space  $T$ - $\mu$ - $B$  in the deconfined phase was presented in [145]. In particular, the effect of inverse magnetic catalysis effect was found and discussed in this reference.

The Sakai–Sugimoto model can be developed further to include homogeneous baryonic matter, made from point-like approximations to the solitonic baryons mentioned above [21]. Applications in the context of a background magnetic field have been studied in the confined [23] and deconfined [146] backgrounds, the latter study

investigates the effect of baryonic matter on inverse magnetic catalysis and will be presented below.

## 6.1 Set up

For the (dimensionless)  $U(1)$  gauge field we choose the ansatz

$$a = \frac{2\pi\alpha'}{R} \mathcal{A}_\mu dx^\mu = a_0(u)dt + bx^1 dx^2 + a_3(u)dx^3, \quad (6.1)$$

where  $b = 2\pi\alpha'B$  denotes the magnitude of the dimensionless magnetic field strength. Note that the necessity of introducing the third component of the gauge field, which is P-odd, is due to the coupling to  $a_0$  and  $b$  via the (P-odd) CS-action. We denote the asymptotic values of the gauge field and the embedding function  $x_4(u)$  by

$$a_0(\infty) = \mu \equiv \mu_q \frac{2\pi\alpha'}{R}, \quad a_3(\infty) = j, \quad x_4(\infty) = \frac{\ell}{2}, \quad (6.2)$$

where  $\mu_q$  is the dimensionful quark chemical potential<sup>1</sup>, and  $\ell \equiv L/R$  is the dimensionless asymptotic separation of the flavor branes. The boundary value of  $a_3$  can be shown to correspond to a finite expectation value for the pion gradient in the direction of the magnetic field, hence it will only be non vanishing when chiral symmetry is broken. In that case, one has to extremize the on-shell action with respect to  $j$  [171, 23, 151]. From the field theory perspective this means that, if  $j \neq 0$ , the chiral condensate is rotating between a scalar and a pseudoscalar condensate when moving along the  $z$ -direction, i.e., it forms a so-called chiral spiral [161]. Each full turn of the spiral raises the baryon number by one. Therefore, since  $j$  measures the rate of turns per unit length, it is related to the baryon density. Equivalently, one can regard  $j$  as a supercurrent, in analogy to superfluidity, where the phase of the condensate gives the superfluid velocity.

Within our ansatz, the action for each D8-brane describing left- and right-handed fermions respectively becomes

$$S' = \frac{\mathcal{N}V}{2T} \int_{u_i}^{\infty} du \left[ \sqrt{u^5 + b^2 u^2} \sqrt{u^3 f x_4'^2 + \frac{h_d}{f} - a_0'^2 + a_3'^2 h_d} \pm \frac{3b}{2} (a_3 a_0' - a_0 a_3') \right], \quad (6.3)$$

<sup>1</sup>Here we keep the notation of Refs. [145, 146]. Note that in the NJL section  $\mu$  is the dimensionful quark chemical potential.

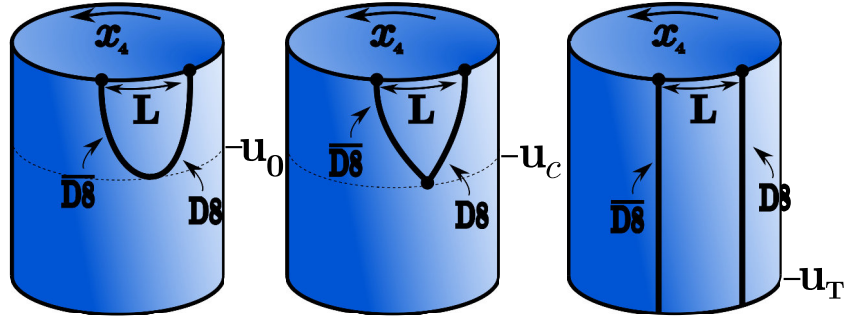


Figure 6.1: The three possible D8-brane configurations in the black hole background geometry from the left to the right: chirally broken without baryons, chirally broken with baryons and chirally restored. The first two configurations also exist in the confined background, i.e. the cylinder is replaced by the cigar.

where the lower bound of the integration has to be chosen according to the phase under consideration:

- $u_i = u_0$  in the phase with broken chiral symmetry without baryons;  $u_0$  is the junction point of the two D8-branes and we assume that  $a_0(u)$  and  $a_3(u)$  are continuous at  $u_0$
- $u_i = u_c$  in the phase with broken chiral symmetry with baryons;  $u_c$  is the junction point of the two D8-branes as well as the location of the baryons and we assume that  $a_0(u)$  and  $a_3(u)$  are continuous at  $u_c$
- $u_i = u_T$  in the phase with restored chiral symmetry;  $u_T$  denotes the location of the black hole horizon; we will see that  $x_4(u) \equiv 0$  is a solution to the equations of motion; due to regularity conditions  $a_0(u_T) = 0$  [104]; no restrictions imposed on  $a_3(u)$

These three configurations are summarized in Fig. 6.1. The constant  $\mathcal{N}$  is defined by the equation

$$\mathcal{N} \equiv 2 \frac{T_8 R^5 \Omega_4}{g_s} = \frac{N_c R^2}{6\pi^2 (2\pi\alpha')^3}. \quad (6.4)$$

The sign in front of the CS term accounts for its P-odd behavior, D8- and anti-D8-branes are oppositely charged with respect to the RR-flux. In (6.3) we have followed [23] and modified the original action  $S$  and denoted the new action by  $S'$ . The

reason is that proceeding with  $S$  results in an inconsistency: the conserved currents sourced by the boundary values of the gauge field turn out to be different from those currents calculated using the thermodynamic relations. In [23] this issue was related to the gauge variance of the CS action. The solution to this problem is to supplement the CS action with boundary terms residing at the holographic as well as at the spatial boundaries. After integration by parts this modification amounts to simply multiplying the CS contribution with a factor  $3/2$ . This procedure restores the thermodynamical consistency albeit at the cost of a correct implementation of the axial anomaly [152].

Note that since we identify the dimensionless baryon chemical potential with the asymptotic value of the zeroth component of the gauge field on both the D8-brane and the anti-D8-brane,  $a_0(u)$  must be P-even.

Since for  $N_f = 1$  there exist no non-singular solutions for the instanton, we approximate the instanton of typical size  $\lambda^{-1/2}$  by a point like configuration residing at the junction point of the D8-branes denoted by  $u_c$  in a phase with broken chiral symmetry and baryons and assume a homogeneous distribution of these point like baryons

$$\frac{1}{8\pi^2} \text{Tr} F^2 = \mp \frac{N_4}{V} \delta(u - u_c) du d^3x. \quad (6.5)$$

Similar to the rescaling of the gauge fields above we introduce the quantity

$$n_4 = \frac{N_4 N_c}{V} \frac{R}{\mathcal{N} 2\pi\alpha'}. \quad (6.6)$$

which we call dimensionless *baryon* density because  $\mathcal{N}$  scales with  $N_c$ . Plugging this into Eq. (4.7) yields

$$S_{\text{CS}}^{\text{baryon}} = -\frac{\mathcal{N}V}{2T} n_4 a_0(u_c), \quad (6.7)$$

where we have set

$$\int_{u_c}^{\infty} \delta(u - u_c) du = \frac{1}{2}.$$

As mentioned in chapter 4 we also have to take into account the energy density of  $|N_4|$  many D4-branes. According to the picture developed there, one of the D8-branes, i.e. one half of the full D8-brane configuration, has to counteract half of the gravitational pull affecting the D4-brane, therefore we compute

$$\frac{|N_4|}{2} S_{\text{D4}} = \frac{V}{2T} \frac{|N_4| N_c}{V} M_q = \frac{\mathcal{N}V}{2T} |n_4| \frac{u_c}{3} \sqrt{h_d(u_c)}. \quad (6.8)$$

Here we introduced the constituent quark mass in a baryon

$$M_q = \frac{R}{2\pi\alpha'} \frac{u_c}{3} \sqrt{h_d(u_c)}, \quad (6.9)$$

hence the baryon mass is given by  $m_B = N_c M_q$ .

## 6.2 Equations of motion, conserved currents and force balancing

In order to find the equations of motion for  $a_0$ ,  $a_3$  and  $x_4$  we vary the action with respect to these fields. The respective variations of the DBI action read

$$-\frac{\mathcal{N}V}{2T} \left[ \int_{u_i}^{\infty} du \frac{\partial}{\partial u} \left( -\frac{\sqrt{u^5 + b^2 u^2 a'_0}}{\sqrt{u^3 (x'_4)^2 f + \frac{h_d}{f} - (a'_0)^2 + (a'_3)^2 h_d}} \right) \delta a_0 \right. \\ \left. + \frac{\sqrt{u^5 + b^2 u^2 a'_0}}{\sqrt{u^3 (x'_4)^2 f + \frac{h_d}{f} - (a'_0)^2 + (a'_3)^2 h_d}} \delta a_0 \Big|_{u_i}^{\infty} \right], \quad (6.10)$$

$$\frac{\mathcal{N}V}{2T} \left[ \int_{u_i}^{\infty} du \frac{\partial}{\partial u} \left( -\frac{\sqrt{u^5 + b^2 u^2 a'_3 h_d}}{\sqrt{u^3 (x'_4)^2 f + \frac{h_d}{f} - (a'_0)^2 + (a'_3)^2 h_d}} \right) \delta a_3 \right. \\ \left. + \frac{\sqrt{u^5 + b^2 u^2 a'_3 h_d}}{\sqrt{u^3 (x'_4)^2 f + \frac{h_d}{f} - (a'_0)^2 + (a'_3)^2 h_d}} \delta a_3 \Big|_{u_i}^{\infty} \right], \quad (6.11)$$

$$\frac{\mathcal{N}V}{2T} \left[ \int_{u_i}^{\infty} du \frac{\partial}{\partial u} \left( -\frac{\sqrt{u^5 + b^2 u^2 u^3 x'_4 f}}{\sqrt{u^3 (x'_4)^2 f + \frac{h_d}{f} - (a'_0)^2 + (a'_3)^2 h_d}} \right) \delta a_3 \right. \\ \left. + \frac{\sqrt{u^5 + b^2 u^2 u^3 x'_4 f}}{\sqrt{u^3 (x'_4)^2 f + \frac{h_d}{f} - (a'_0)^2 + (a'_3)^2 h_d}} \delta x_4 \Big|_{u_i}^{\infty} \right]. \quad (6.12)$$

The term in parenthesis of the first line is also called electric displacement field  $\mathcal{E}(u)$  in analogy to electrodynamics. If there were no source terms coming from the CS terms which we will derive below, the equation of motion for  $a_0$  would tell us that the divergence of  $\mathcal{E}(u)$  vanishes. For the variation of the abelian CS action with respect

to  $a_0$  and  $a_3$  we find

$$\pm \frac{\mathcal{N}V}{2T} \frac{3b}{2} \left[ \int_{u_i}^{\infty} du - 2a'_3 \delta a_0 + a_3 \delta a_0 \Big|_{u_i}^{\infty} \right], \quad (6.13)$$

$$\pm \frac{\mathcal{N}V}{2T} \frac{3b}{2} \left[ \int_{u_i}^{\infty} du 2a'_0 \delta a_3 - a_0 \delta a_3 \Big|_{u_i}^{\infty} \right]. \quad (6.14)$$

Finally, for the variation of the non-abelian CS action only the one with respect to  $a_0$  contributes

$$\frac{\mathcal{N}V}{2T} n_4 \delta a_0 \Big|_{u_c}. \quad (6.15)$$

From the DBI action and the abelian CS action we obtain the integrated equations of motion valid in the region  $(u_i, \infty)$

$$\frac{\sqrt{u^5 + b^2 u^2 a'_0}}{\sqrt{u^3 f x_4'^2 + \frac{h_d}{f} - a_0'^2 + a_3'^2 h_d}} = \pm 3b a_3 + c^\pm, \quad (6.16)$$

$$\frac{\sqrt{u^5 + b^2 u^2 h_d a'_3}}{\sqrt{u^3 f x_4'^2 + \frac{h_d}{f} - a_0'^2 + a_3'^2 h_d}} = \pm 3b a_0 + d^\pm, \quad (6.17)$$

$$\frac{\sqrt{u^5 + b^2 u^2 f u^3 x_4'}}{\sqrt{u^3 f x_4'^2 + \frac{h_d}{f} - a_0'^2 + a_3'^2 h_d}} = k^\pm, \quad (6.18)$$

where  $c^\pm$ ,  $d^\pm$  and  $k^\pm$  denote integration constants. Since  $a_0$  is P-even we can immediately conclude from the first equation that  $c^+ = c^- \equiv c$  and  $a_3$  must be P-odd. Furthermore,

- If the D8-branes join, we also have  $a_3(u_i) = 0$  by the continuity assumption. Likewise we infer from the second equation  $d^+ = -d^- \equiv d$  and from the third  $k^+ = -k^- \equiv k$ .
- In the case where the D8-branes reach the horizon with  $x_4'(u_T) < \infty$ , we conclude that  $k = 0$  because  $f(u_T) = 0$ , hence  $x_4'(u) \equiv 0$ , i.e. the branes do not curve. Furthermore, due to the regularity constraint  $a_0(u_T) = 0$  and due to  $h_d(u_T) = f(u_T) = 0$  we infer from the second equation for regular  $a_3'(u_T)$  that  $d = 0$  in the restored phase.

Let us next focus on the boundary terms of the variations. If the D8-branes join, they yield further junction conditions, since we might think of the joined brane configuration as one single D8-brane, hence the sum of the terms at the lower boundary



$u_i$  must vanish, e.g.

$$-2\mathcal{E}(u_c) + 2n_4 = -2c + 2n_4 = 0.$$

Therefore, if baryons are present, we can identify  $c$  with  $n_4$ , while without baryons we find  $c = 0$ .

The electric displacement field  $\mathcal{E}$  is the component of a vector field pointing towards larger values of  $u$  on both D8-branes. When we move past the point  $u_i$  in the joined D-brane configuration, the direction of the electric field is flipped, since we assume that  $a_0$  is P-even. Therefore, since  $a_3(u_0) = 0$ , the integration constant  $c$  corresponds to a point-like charge at  $u_0$ . In the restored phase, on the other hand, in general  $c \neq 0$ , hence the horizon provides a charge that will be translated into the quark density at the boundary.

In addition to these point-like charges, if the magnetic field is nonzero, there is a contribution to the quark density from the gradient of  $a_3$ , which in general is distributed over the whole D8-brane world volume.

From the boundary terms evaluated at  $u \rightarrow \infty$  we find the conserved currents of the global symmetry of the dual field theory. According to the holographic dictionary they represent the response sourced by the fluctuations of the bulk gauge fields at the boundary. The non vanishing components of the current densities are given by

$$\mathcal{J}_V^0 = \mathcal{J}_R^0 + \mathcal{J}_L^0 = \frac{2\pi\alpha'\mathcal{N}}{R} \left( \frac{3b}{2}j + c \right), \quad (6.19)$$

$$\mathcal{J}_A^3 = \mathcal{J}_R^3 - \mathcal{J}_L^3 = \frac{2\pi\alpha'\mathcal{N}}{R} \left( \frac{3b}{2}\mu + d \right), \quad (6.20)$$

where we have used the equations of motion. The first line relates the baryon density with the *magnetic* chiral spiral and the point-like charges in the bulk. The second line is the axial current which we have already encountered in section 5.3.

The only parameters we are free to control are  $T$ ,  $\mu$  and  $\ell$ . So in the broken phase we still have to determine  $j$ ,  $d$ ,  $u_i$  and  $k$  as well as  $n_4$  if baryons are involved. We have to find their values that minimize the free energy, i.e. the on-shell action. Because we have to extremize the thermodynamic potential with respect to  $j$ , i.e., with respect to  $a_3(\infty)$ , we can immediately conclude that in the broken phase the axial current has to vanish, hence  $d = -3/2 b\mu$ . By using partial integration and the equations of

motion, the extremization with respect to  $n_4$  is

$$0 = \frac{\partial S_{\text{on-shell}}}{\partial n_4} = \left( \sum_{i=0,3} \frac{\partial \mathcal{L}_0}{\partial a'_i} \frac{\partial a_i}{\partial n_4} + \frac{\partial \mathcal{L}_0}{\partial x'_4} \frac{\partial x_4}{\partial n_4} \right)_{u=u_c}^{u=\infty} \pm \frac{u_c}{3} \sqrt{h_d(u_c)} - a_0(u_c) - n_4 \frac{\partial a_0(u_c)}{\partial n_4}, \quad (6.21)$$

where the upper (lower) sign holds for  $n_4 > 0$  ( $n_4 < 0$ ). The only non-vanishing contribution from the term in parenthesis – coming from the derivative of  $a_0(u_c)$  with respect to  $n_4$  – cancels the last term, since all other values of the fields at the boundary are fixed. This determines the value of  $a_0$  at the source location

$$a_0(u_c) = \pm \frac{1}{3} u_c \sqrt{h_d(u_c)}. \quad (6.22)$$

Therefore the baryon contributions from the CS-D8-brane action and from the D4-brane action cancel on shell.

Before proceeding with seeking the minimum of the free energy with respect to the junction point  $u_i$ , we algebraically rearrange equations (6.16)–(6.18)

$$a'_0 = \frac{\sqrt{h_d} u^{3/2} (3ba_3 + c)}{g(u)}, \quad (6.23)$$

$$a'_3 = \frac{u^{3/2} (3ba_0 + d)}{\sqrt{h_d} g(u)}, \quad (6.24)$$

$$x'_4 = \frac{\sqrt{h_d} k}{f u^{3/2} g(u)}, \quad (6.25)$$

$$g(u) := \left( f(u^8 + b^2 u^5) - k^2 + f u^3 (3ba_3 + c)^2 + \frac{f}{h_d} u^3 (3ba_0 + d)^2 \right)^{1/2}. \quad (6.26)$$

For the minimization with respect to  $u_i$  we find

$$0 = \frac{\partial S_{\text{on-shell}}}{\partial u_c} = \left( \sum_{i=0,3} \frac{\partial \mathcal{L}_0}{\partial a'_i} \frac{\partial a_i}{\partial u_c} + \frac{\partial \mathcal{L}_0}{\partial x'_4} \frac{\partial x_4}{\partial u_c} \right)_{u=u_c}^{u=\infty} - \mathcal{L}_0(u = u_c). \quad (6.27)$$

After some algebraic rearrangement and using the equations of motion this yields an equation for  $k$

$$\begin{aligned}
g(u)|_{u_i} &= \\
&\sqrt{f(u_i)(u_i^8 + b^2 u_i^5) - k^2 + f(u_i)u_i^3 c^2 - \frac{f(u_i)}{h_d(u_i)} u_i^3 (3ba_0(u_i) - 3/2 b\mu)^2} \\
&= \frac{n_4}{3} u_c^{3/2} \frac{f(u_c)[3 - h_d(u_c)]}{2h_d(u_c)}, \tag{6.28} \\
\Rightarrow k^2 &= f(u_i)(u_i^8 + b^2 u_i^5) + f(u_i)u_i^3 c^2 - \frac{f(u_i)}{h_d(u_i)} u_i^3 (3ba_0(u_i) - 3/2 b\mu)^2 \\
&\quad - \left( \frac{n_4}{3} u_c^{3/2} \frac{f(u_c)[3 - h_d(u_c)]}{2h_d(u_c)} \right)^2.
\end{aligned}$$

This together with Eq. (6.25) shows that in the case without baryons the D8-branes join smoothly, i.e.  $x'_4(u_0) = \infty$ , as might have been expected because  $g(u_0) = 0$ . On the other hand, in the baryonic phase the D8-branes are connected with a cusp at  $u_c$ . Eq. 6.28 is also referred to as force balance equation and can alternatively be derived from equating the gravitational force acting on the D4-brane mass and the proper tensions of the D8- and anti-D8-branes at  $u_c$ . The remaining parameters  $n_4$ ,  $u_c$  and  $j$  are then found by solving the boundary value problem.

In the chirally symmetric phase we have to set  $d = 0$  from the start, so the minimization with respect to  $j$  cannot be satisfied, hence we also set  $j = 0$  in the restored phase. This makes perfectly sense, since we interpret  $j$  as the phase of the chiral condensate. The axial current at *any temperature* – reinstating dimensionful quantities – reads

$$\mathcal{J}_A^3 = \frac{N_c}{4\pi^2} B\mu q. \tag{6.29}$$

This result differs from the corresponding expression (5.8) obtained in the NJL model by a factor 2, which is related to the modification of the CS term in the action in order to obtain a consistent thermodynamic description of the currents. For a thorough discussion of the effect of this modification on the chiral anomaly see Ref. [152]. The only parameters that are so far not determined in the restored phase are thus  $c$  and  $a_3(u_T)$ . The two equations of motion for  $a_0$  and  $a_3$  together with the boundary conditions  $a_0(\infty) = \mu$ ,  $a_0(0) = 0$  and  $a_3(\infty) = 0$  suffice to do so.

The differential equations (6.23)–(6.25) have to be solved numerically. However, as we will discuss now, there exist specific cases that reduce the necessary numerical effort tremendously.

### 6.3 Semianalytic solution to the equations of motion

Let us define the function  $y(u)$  by the differential equation

$$y' = \frac{3bu^{3/2}}{\sqrt{g(u)}}. \quad (6.30)$$

for which we have the freedom to choose  $y(u_i) = 0$ . Its value at the holographic boundary will be denoted by  $y_\infty$  in the following. Furthermore  $y'(u)$  is positive, hence we may regard  $y$  as a new coordinate, replacing  $u$ . Then the equations of motion (6.23)–(6.25) become

$$\partial_y a_0 = \sqrt{h_d} \left( a_3 + \frac{c}{3b} \right), \quad (6.31)$$

$$\partial_y a_3 = \frac{1}{\sqrt{h_d}} \left( a_0 + \frac{d}{3b} \right), \quad (6.32)$$

$$x'_4 = \frac{h_d}{f} \frac{k}{3bu^3} y'(u). \quad (6.33)$$

Note that the metric factor  $\sqrt{h_d}$  prevents us from solving the equations of motion for the gauge fields analytically in terms of the coordinate  $y$ . But there exist situations in which  $h_d \equiv 1$  is the case or we might approximate  $h_d \simeq 1$ :

- In the confined background  $h_d$  is simply equal to 1.
- In the deconfined background at  $T = 0$  we may set  $h_d(u_T = 0) = 0$  and  $h_d(u) = 1$  for  $u > 0$ ; this particular choice guarantees that one also finds the condition  $d \equiv 0$  in the chirally restored phase.
- As will be justified a posteriori, in the chirally broken phase for  $L \ll M_{\text{KK}}^{-1}$  we have  $u_i \gg u_T$  in the deconfined background as well as  $u_i \gg u_{\text{KK}}$ . Hence, as long as we are only interested in the physics of the broken phase, we might set  $u_{\text{KK}} = 0$  as well as  $u_T = 0$ , which amounts to solving equivalent equations, and no distinction between deconfined and confined background can be made regarding the chiral dynamics of the model. Henceforth we shall therefore simply

refer to this description of the chirally broken phase as zero temperature limit. We will utilize this approximation below. Of course, in case of the restored phase no such approximation is allowed, since the D8-branes probe the IR region of the gravitational background. This is of course not negligible and will be the only source for the nontrivial temperature dependence of the chiral phase transition presented here.

- In the special cases  $\mu = 0$  and/or  $b = 0$  at least one of the gauge fields is trivial and  $h_d$  can be absorbed in the definition of  $y'(u)$ .

In the zero temperature limit the equations of motion for  $a_0$  and  $a_3$  simplify considerably:

$$\partial_y a_0 = a_3 + \frac{c}{3b}, \quad \partial_y a_3 = a_0 + \frac{d}{3b}, \quad (6.34)$$

for which we can easily find the solutions

$$\begin{aligned} a_0 &= c_1 \cosh y + c_2 \sinh y - \frac{d}{3b}, \\ a_3 &= c_1 \sinh y + c_2 \cosh y - \frac{c}{3b}. \end{aligned} \quad (6.35)$$

Therefore, the expression for  $y'$  simplifies to

$$y' = \frac{3bu^{3/2}}{\sqrt{u^8 + u^5b^2 - k^2 + (3b)^2u^3(c_2^2 - c_1^2)}}, \quad (6.36)$$

with

$$k^2 = u_i^8 + b^2u_i^5 + u_i^3 \left( \frac{8n_4^2}{9} - 9b^2c_1^2 \right) \quad (6.37)$$

if the symmetry is broken and  $k = 0$  otherwise. This allows us to write the grand canonical potential, i.e., the on-shell action, as

$$\begin{aligned} \Omega = \mathcal{N} \left[ \int_{u_i}^{\infty} \frac{3b}{y'} du + \frac{k\ell}{2} - \frac{3b}{2} y_{\infty} (c_2^2 - c_1^2) \right. \\ \left. - \frac{c}{2} (\mu - c_1) + \frac{d}{2} (j - c_2) \right]. \end{aligned} \quad (6.38)$$

This expression is divergent. In order to obtain finite expressions we renormalize the grand canonical potential by the chirally symmetric vacuum contribution

$$\Omega(\mu = T = 0) = \mathcal{N} \int_0^{\Lambda} du \sqrt{u^5 + b^2u^2}. \quad (6.39)$$

	$\chi\text{Sb}$	baryonic $\chi\text{Sb}$	restored
$d$	$-\frac{3b}{2}\mu$	$-\frac{3b}{2}\mu$	0
$c_1$	$\frac{\mu}{\sinh y_\infty}$	$-\frac{\mu}{2} \pm \frac{u_c}{3}$	0
$c_2$	0	$\frac{c}{3b}$	$\frac{\mu}{\sinh y_\infty}$
$c$	0	$\frac{3b}{2}\mu \frac{\cosh y_\infty + 1}{\sinh y_\infty} \mp bu_c \coth y_\infty$	$3b\mu \coth y_\infty$
$j$	$\frac{\mu}{2} \tanh y_\infty$	$\pm \frac{u_c}{3} \frac{\cosh y_\infty - 1}{\sinh y_\infty}$	0

Table 6.1: The integration constants  $d$ ,  $c_1$ ,  $c_2$ ,  $c$  and the supercurrent  $j$  for the chirally broken phases with and without baryons and the restored phase.

Now we may calculate the remaining so far unspecified parameters by imposing the boundary conditions discussed below Eq. (6.1). The results are summarized in table 6.1.

We proceed with considering the three phases separately in the zero temperature limit.

## 6.4 Broken chiral symmetry without baryons

Inserting the supercurrent  $j$  and the constant  $c$  from table 6.1 into Eq. (6.19) yields the quark number density

$$n_q \equiv \mathcal{J}_V^0 = \frac{N_c}{8\pi^2} B \mu_q \tanh y_\infty. \quad (6.40)$$

The only equations that remain and in general have to be solved numerically for the variables  $u_0$  and  $y_\infty$  are

$$\frac{\ell}{2} = \sqrt{u_0^8 + b^2 u_0^5 - \left(\frac{3b\mu}{2 \cosh y_\infty}\right)^2} \int_{u_0}^{\infty} \frac{du}{u^{3/2} g(u)}, \quad (6.41)$$

$$y_\infty = 3b \int_{u_0}^{\infty} \frac{u^{3/2} du}{g(u)}, \quad (6.42)$$

where we have abbreviated

$$g(u) = \sqrt{u^8 + b^2 u^5 - \left(\frac{3b\mu}{2 \cosh y_\infty}\right)^2 u^3 - u_0^8 - b^2 u_0^5 - \left(\frac{3b\mu}{2 \cosh y_\infty}\right)^2 u_0^3}.$$

Note that the explicit dependence on the asymptotic separation  $\ell$  can be eliminated by the rescaling  $u \rightarrow \ell^2 u$ ,  $\mu \rightarrow \ell^2 \mu$ ,  $b \rightarrow \ell^3 b$  and  $\Omega \rightarrow \ell^7 \Omega$ . Therefore, in all plots shown below, the axes are measured in appropriate units of the D8-brane separation.

Let us first discuss the two limits of small and large magnetic fields  $b$ . For small magnetic fields<sup>2</sup>,  $y_\infty$  and thus the supercurrent  $j$  rise linearly with  $b$ , and therefore the lowest order contribution to the quark number density induced by the chiral spiral is quadratic in  $b$ . The location of the tip of the connected flavor branes is  $u_0 = u_0^{(0)} + \eta_1(\mu)b^2 + \mathcal{O}(b^3)$  with the value of  $u_0$  at  $b = 0$  and  $y_\infty = 3y_\infty^{(0)}b + \mathcal{O}(b^3)$ . These ansätze<sup>3</sup> are plugged into Eqs. (6.41) and (6.42), which can be solved algebraically and yield the solutions

$$u_0^{(0)} = \left[ \frac{4\sqrt{\pi}\Gamma\left(\frac{9}{16}\right)}{\ell\Gamma\left(\frac{1}{16}\right)} \right]^2 \simeq 0.5249 \ell^{-2}, \quad (6.43)$$

$$y_\infty^{(0)} = \frac{1}{(u_0^{(0)})^{3/2}} \frac{\sqrt{\pi}\Gamma\left(\frac{3}{16}\right)}{8\Gamma\left(\frac{11}{16}\right)}, \quad (6.44)$$

$$\eta_1(\mu) = \frac{\cot \frac{\pi}{16} - 1 - \left(\frac{3\mu}{2u_0^{(0)}}\right)^2 \left[ 1 - \frac{3\Gamma\left(\frac{1}{16}\right)\Gamma\left(\frac{3}{16}\right)}{16\Gamma\left(\frac{9}{16}\right)\Gamma\left(\frac{11}{16}\right)} \right]}{8(u_0^{(0)})^2}. \quad (6.45)$$

<sup>2</sup>As explained in [145], there exists a second solution in the region of small  $b$ , where  $u_0$  is small and  $y_\infty$  is large, which is separated from the solution discussed here by a first order phase transition. However, this first-order phase transition occurs in a region of large  $\mu$  where the chirally restored phase is preferred. Therefore we will not discuss this second solution here.

<sup>3</sup>It can easily be shown that possible terms linear in  $b$  in the power expansion of  $u_0$  as well as terms quadratic in  $b$  in the power expansion of  $y_\infty$  have to vanish.

Interestingly, the  $\mu$ -dependent coefficient  $\eta_1$  possesses a zero at  $\mu \simeq 0.2905/\ell^2$ , above which it becomes negative. This shows that the constituent quark mass (which is given by  $u_0$ ) can *decrease* with the magnetic field for sufficiently large chemical potentials. This behavior can be traced back to the incorporation of the chiral spiral.

The grand canonical potential (renormalized by the vacuum contribution (6.39)) is approximated for small  $b$  by

$$\Omega_{\text{ren}} \simeq -\mathcal{N} \left[ \frac{2}{7} (u_0^{(0)})^{7/2} \frac{\sqrt{\pi} \Gamma(\frac{9}{16})}{\Gamma(\frac{1}{16})} + \eta_2(\mu) b^2 \right], \quad (6.46)$$

where

$$\eta_2(\mu) \equiv \frac{\sqrt{\pi} \Gamma(\frac{9}{16})}{\Gamma(\frac{1}{16})} \sqrt{u_0^{(0)}} \left[ \cot \frac{\pi}{16} + \left( \frac{3\mu}{2u_0^{(0)}} \right)^2 \frac{\Gamma(\frac{3}{16}) \Gamma(\frac{17}{16})}{\Gamma(\frac{9}{16}) \Gamma(\frac{11}{16})} \right]. \quad (6.47)$$

At asymptotically large magnetic field,  $y_\infty$  diverges faster than linearly, thus  $j \simeq \mu/2$ , while  $u_0$  saturates at the value

$$u_0^{(\infty)} = \left[ \frac{4\sqrt{\pi} \Gamma(\frac{3}{5})}{\ell \Gamma(\frac{1}{10})} \right]^2 \simeq 1.2317 \ell^{-2}. \quad (6.48)$$

We see that  $u_0^{(\infty)} > u_0^{(0)}$ , i.e., for any  $\mu$  the constituent quark mass at asymptotically large  $b$  is larger than that at  $b = 0$ . This can be interpreted as magnetic catalysis and is similar to the NJL model. However, as we have shown in the left panel of Fig. 5.1, in the NJL model the constituent quark mass does not saturate for asymptotically large magnetic fields.

Plugging these results into  $\Omega$  and  $n_q$  yields

$$\Omega_{\text{ren}} \simeq -\mathcal{N} b \left[ \frac{\sqrt{\pi} \Gamma(\frac{3}{5})}{2\Gamma(\frac{1}{10})} (u_0^{(\infty)})^2 + \frac{3\mu^2}{8} \right], \quad n_q \simeq \frac{N_c}{8\pi^2} B \mu_q. \quad (6.49)$$

Remarkably, all model parameters have dropped out of the quark number density, which thus is solely expressed in terms of the dimensionful quantities  $B$  and  $\mu_q$ .



## 6.5 Broken chiral symmetry with baryons

The only equations that remain and in general have to be solved numerically for the variables  $u_c$  and  $y_\infty$  are

$$\frac{\ell}{2} = k \int_{u_c}^{\infty} \frac{du}{u^{3/2}g(u)}, \quad (6.50)$$

$$y_\infty = 3b \int_{u_c}^{\infty} \frac{u^{3/2}du}{g(u)}, \quad (6.51)$$

$$k^2 = u_c^8 + b^2 u_c^5 + (3b)^2 u_c^3 (c_1^2 - c_2^2) + b^2 u_c^3 c^2, \quad (6.52)$$

and we want to compare the (unrenormalized) thermodynamic potential with baryons given by

$$\begin{aligned} \Omega = & \frac{\mathcal{N}V}{T} \int_{u_c}^{\infty} \frac{3b}{\partial_u y} du + k \frac{\ell}{2} + \frac{3b}{2} \left[ \mu \left( -\frac{\mu}{2} + \frac{u_c}{3} \right) \frac{1 + \cosh y_\infty}{\sinh^2 y_\infty} (y_\infty + \sinh y_\infty) \right. \\ & \left. - \left( \frac{u_c}{3} \right)^2 \frac{1}{\sinh^2 y_\infty} (y_\infty + \sinh y_\infty \cosh y_\infty) \right] \end{aligned} \quad (6.53)$$

with the one from the other phases. Note that although each of the thermodynamical potentials is divergent the difference is always finite, no matter which phases are compared.

Inserting the values for the integration constants in table 6.1 gives us the total quark number density constituted by both the magnetic chiral spiral and the homogeneous distribution of the point like baryons<sup>4</sup>

$$j = \frac{u_c \cosh y_\infty - 1}{3 \sinh y_\infty}, \quad (6.54)$$

$$n_4 = c = \frac{3b}{2} \mu \frac{\cosh y_\infty + 1}{\sinh y_\infty} - b u_c \coth y_\infty, \quad (6.55)$$

which yields

$$n_q \equiv \mathcal{J}_V^0 = \frac{N_c}{4\pi^2} B (\mu_q - M_q) \frac{\cosh y_\infty + 1}{\sinh y_\infty}. \quad (6.56)$$

<sup>4</sup>We will restrict ourselves to positive  $n_4$  without loss of generality. Note, that for the lower sign in the constants found in table 6.1  $n_4 = c < 0$ , which can only be satisfied if  $\mu < 0$ . Our restriction means we restrict ourselves to positive chemical potential and only populate the system with baryons rather than anti-baryons.

The critical chemical potential at which the system can be populated with baryons is found from setting  $n_4 = 0$

$$\mu_{q,\text{onset}} = M_q \frac{2 \cosh y_\infty}{\cosh y_\infty + 1}, \quad (6.57)$$

and thus  $M_q(B) < \mu_{q,\text{onset}} < 2M_q(B)$ . The numerical comparison of the chirally broken phases shows that starting from this point towards larger chemical potentials the phase with baryons is always the preferred one. Since at  $n_4 = 0$  the two thermodynamic potentials are equal, it is a second order phase transition – with some abuse of terminology since no symmetry is broken (but in accordance with the classification by Ehrenfest). Henceforth we will refer to that transition as baryon onset. Before discussing the numerical solution further, let us again analyse the onset in the two limits  $b \rightarrow 0$  and  $b \rightarrow \infty$ .

At small  $b$  the explicit linear dependence of  $y_\infty$  coming from the numerator of  $y'(u)$  dominates. For the onset chemical potential we immediately find from (6.57)

$$\mu_{q,\text{onset}}^{(0)} = M_q^{(0)}. \quad (6.58)$$

At the onset  $n_4 = 0$  the solutions of the broken phase without baryons Eqs. (6.43) and (6.44) may be taken over to the case at hand; thus in terms of dimensionless quantities

$$\mu_{\text{onset}}^{(0)} = m_q^{(0)} := \frac{u_c^{(0)}}{3} \simeq \frac{0.175}{\ell^2}. \quad (6.59)$$

This result is in agreement with ref. [21], see for instance fig. 10 in this reference.

In the vicinity of the onset we may compute the density analytically. We start with the case  $b = 0$ . For chemical potentials larger than but close to  $\mu_{\text{onset}}^{(0)}$ , the dimensionless density behaves as (see appendix A.5 for the derivation)

$$n_4(b = 0) = \frac{2\ell(m_q^{(0)})^2}{\xi} (\mu - m_q^{(0)}) + \mathcal{O}[(\mu - m_q^{(0)})^2], \quad (6.60)$$

where

$$\xi \equiv \frac{1}{9} \left[ \pi \frac{\Gamma(\frac{1}{16}) \Gamma(\frac{3}{16})}{\Gamma(\frac{9}{16}) \Gamma(\frac{11}{16})} - \frac{2}{9} \right] \simeq 0.11. \quad (6.61)$$

We plot the linear approximation (6.60) in comparison to the full result in the left panel of fig. 6.2.

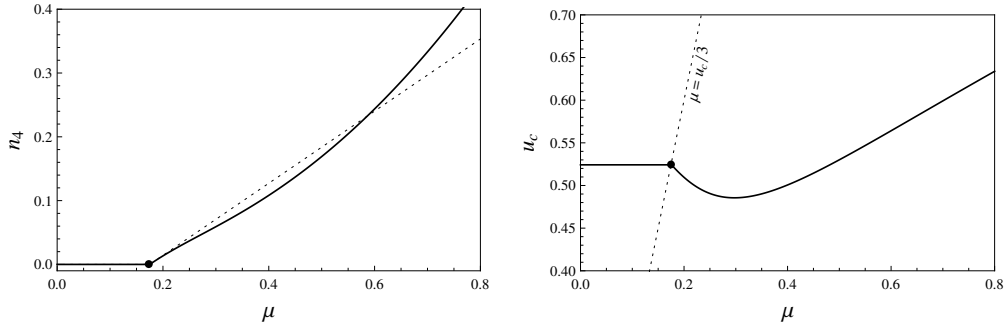


Figure 6.2: Solid lines: baryon density  $n_4$  (left) and location of the tip of the connected flavor branes  $u_c$  (right) at vanishing magnetic field. The baryonic phase becomes favored for  $\mu > u_c/3$ , indicated by the dotted line in the right panel. For chemical potentials smaller than that value, the mesonic phase is the ground state, in which – at vanishing magnetic field – the baryon density vanishes and  $u_c$  is constant. The dotted line in the left panel is the linear approximation (6.60). Here and in all other plots we have set  $\ell = 1$  for notational convenience. The dependence on  $\ell$  is always simple and corresponds to a rescaling of the axes, in this plot  $\mu \rightarrow \ell^2 \mu$ ,  $u_c \rightarrow \ell^2 u_c$ ,  $n_4 \rightarrow \ell^5 n_4$ .

This linear behavior might seem unexpected, because for fermions in 3+1 dimensions, at least in the non-interacting case, one would have  $n_4 \sim (\mu - m)^{3/2}$  just above the onset. It is therefore interesting to compare  $n_4$  from eq. (6.60) with the density of a Bose condensate instead. To this end, consider a  $\phi^4$  model with chemical potential at zero temperature,  $\Omega = \frac{m^2 - \mu^2}{2} \phi^2 + \frac{\lambda}{4} \phi^4$ . Minimizing  $\Omega$  with respect to the condensate  $\phi$  and inserting the result into the density  $n = -\frac{\partial \Omega}{\partial \mu}$  yields  $n = \mu \frac{\mu^2 - m^2}{\lambda} = \frac{2m^2}{\lambda} (\mu - m) + \mathcal{O}[(\mu - m)^2]$ . The linear term looks exactly like the one in eq. (6.60) (in the  $\phi^4$  model, the quadratic term is positive; this is in contrast to our holographic result, as fig. 6.2 shows). The similarity of the baryon density with the density of a Bose condensate is not too surprising, because we work in the large- $N_c$  limit. In this limit, changing the number of constituent quarks from even to odd, i.e., from  $N_c$  to  $N_c + 1$  does not make a difference. Therefore, in our context one may very well talk about a condensate of baryons. This terminology is for instance used in ref. [154]. It is instructive to express eq. (6.60) in terms of dimensionful quantities, see first row of table 6.2, where we show the dimensionful quark density  $\mathcal{J}^0$ . In the case  $B = 0$  this density only receives a contribution from "normal" baryons,  $\mathcal{J}^0(B = 0) = N_c N_4 / V$ . Comparing this expression with the  $\phi^4$  model, we may iden-

	quark density $N_c N_4/V$
$B = 0$	$N_c \frac{2(M_q^0)^2}{\frac{3\xi}{2}\lambda \frac{\pi/M_{KK}}{L}} (\mu_q - M_q^0)$
$B \rightarrow \infty$	$N_c \frac{B}{2\pi^2 \tilde{\xi}} (\mu_q - 2M_q^\infty)$

Table 6.2: Quark density  $N_c N_4/V$  induced by wrapped D4-branes close to the baryon onset at vanishing and at asymptotically large magnetic field  $B$ . Both expressions depend linearly on the difference between the quark chemical potential and the (effective) constituent quark mass, indicating a bosonic nature of the holographic large- $N_c$  baryons discussed here. Since, at nonzero magnetic field, the effective constituent quark mass in a baryon is modified by the meson supercurrent, the baryon onset for  $B \rightarrow \infty$  is at  $2M_q^\infty$ , not at  $M_q^\infty$ . For the values of the numerical constants  $\xi, \tilde{\xi}$  see eqs. (6.61) and (6.65).

tify  $\frac{3\xi}{2}\lambda \frac{\pi/M_{KK}}{L}$  with a coupling constant for an effective repulsive interaction between the baryons near the onset. We see that this coupling is proportional to the 't Hooft coupling  $\lambda$ . Interestingly, it gets strong for small asymptotic separations  $L$  of the flavor branes, measured relative to the maximal separation  $\pi/M_{KK}$ .

Let us now consider the opposite limit  $b \rightarrow \infty$ . As before in the case without baryons, in this limit  $y_\infty$  diverges faster than linearly and we might replace  $y_\infty^{(\infty)} := 3by_\infty$  and set  $y_\infty^{(\infty)} \rightarrow \infty$  in all equations. The onset is then given by

$$\mu_{q,\text{onset}}^{(\infty)} = 2M_q^{(\infty)}. \quad (6.62)$$

At the onset, again the solution for  $u_0^{(\infty)} = u_c^{(\infty)}$  from (6.48) holds. Hence in terms of dimensionless quantities

$$\mu_{\text{onset}}^{(\infty)} = 2m_q^{(\infty)} := \frac{2u_c^{(\infty)}}{3} \simeq \frac{0.8211}{\ell^2}. \quad (6.63)$$

Closely above that value the behavior of the asymptotic density of "normal" baryons  $n_4$  is given by (again for a derivation see appendix A.5)

$$n_4(b = \infty) = \frac{3b}{2} \frac{\mu - 2m_q^\infty}{\tilde{\xi}} + \mathcal{O}[(\mu - 2m_q^\infty)^2], \quad (6.64)$$

with

$$\tilde{\xi} \equiv 1 - \frac{2}{15\sqrt{\pi}} \frac{\Gamma(\frac{1}{10})}{\Gamma(\frac{3}{5})} \simeq 0.5194. \quad (6.65)$$

The corresponding dimensionful quark density is shown in the second row of table 6.2. (Remember that the total baryon density  $n$  also receives a contribution from the supercurrent,  $n = \frac{3}{2}bj + n_4$  with  $j(b = \infty)_{\text{baryon}} \equiv u_c/3$ .) Interestingly, at asymptotically large magnetic fields the explicit dependence on the model specific constants  $L$ ,  $\lambda$  and  $M_{\text{KK}}$  drops out. This kind of "universality" has already been observed in the phases without baryons.

One might have thought that the baryon onset always happens at  $\mu = \frac{u_c}{3}$  since  $N_c \frac{u_c}{3}$  is the baryon mass given by the action of the D4-branes. To understand why the result deviates from this expectation, it is instructive to consider the (unphysical) case of an isotropic meson condensate where the meson supercurrent vanishes,  $j = 0$ . In this "cleaner" case, the true vacuum with zero pressure  $P = 0$  and zero baryon density  $n = 0$  is the ground state below the baryon onset. Now,  $n_q = 0$  determines the onset which indeed occurs at  $\mu_{q,\text{onset}} = M_q(B)$  for arbitrary values of the magnetic field. As a consequence, the chemical potential equals the energy per baryon  $\epsilon/n$  at the onset (this follows from the thermodynamic relation  $P = -\epsilon + \mu n$  and  $P = 0$  at the onset). The situation with a nonzero supercurrent  $j$  is different. Here the pressure and the baryon density become nonzero as soon as we switch on  $\mu$ , and  $\mu$  is always larger than  $\epsilon/n$ . Then, at some point,  $\mu$  is large enough to support the baryon number induced by  $j$  and by "normal" baryons. This costs more energy than having only "normal" baryons and thus the onset happens later than for  $j = 0$ . We compare both onset lines, the unphysical one from  $j = 0$  (dashed) and the physical one with  $j \neq 0$  minimizing the free energy (solid), in fig. 6.3.

The difference between the two lines can also be thought of as follows. Between the dashed and solid lines the system might "think about" adding baryons because there is enough energy available from the chemical potential. If the system decided to do so, it would at the same time have to decrease the supercurrent discontinuously to have enough energy available for the baryons. (The dashed line is the extreme case where it would have to force the supercurrent to zero.) This, however, would lead to a decrease in the total baryon density upon increasing the chemical potential, which is a thermodynamically unstable situation. (At the dashed line, the baryon density would jump to zero because the energy is just enough to start adding baryons<sup>5</sup>.) For any given  $b$  the solid line marks the "earliest" possible point where

<sup>5</sup> This unphysical onset is considered in ref. [43]: the  $T = 0$  onset in fig. 9 of this reference corresponds to the dashed line in our fig. 6.3. It seems that this discrepancy originates from incorrectly

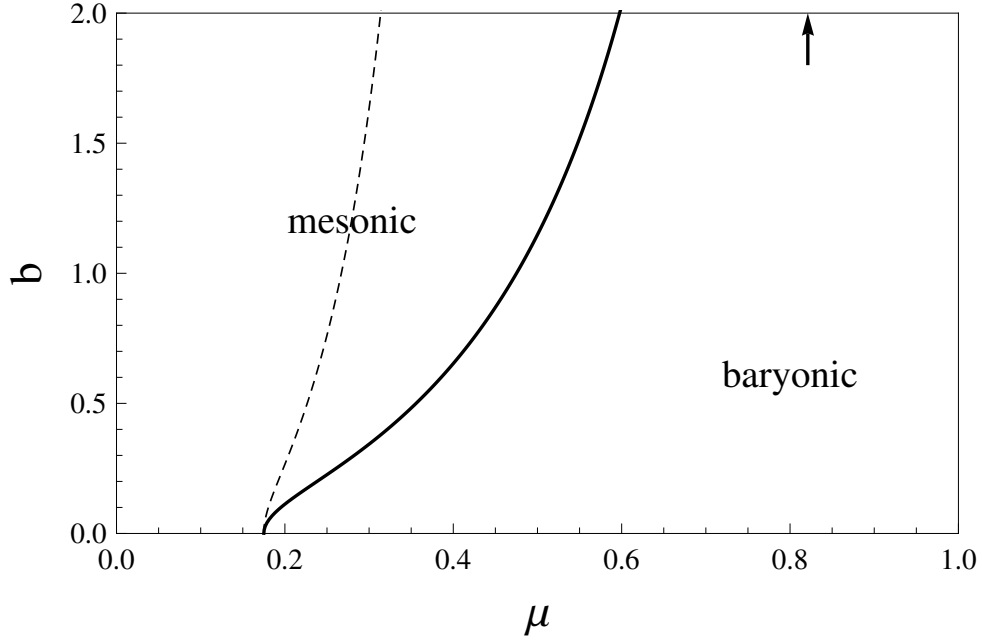


Figure 6.3: Onset of baryonic matter (solid line) in the plane of quark chemical potential  $\mu$  and magnetic field  $b$ . For comparison, the dashed line indicates the baryon onset in the unphysical case of a vanishing meson supercurrent. In this case, the onset occurs at  $\frac{\mu_c}{3}$  for all  $b$ . Due to the meson supercurrent, the effective baryon mass is more complicated and the onset is somewhere between  $\frac{\mu_c}{3}$  ( $b = 0$ ) and  $\frac{2\mu_c}{3}$  ( $b = \infty$ ). The arrow indicates the asymptotic value of the onset line given in eq. (6.63). In the present model, the baryon onset is always a second-order phase transition, in contrast to real nuclear matter. For now, we have ignored the chirally restored phase. We shall see in sec. 6.8 that for sufficiently large magnetic field,  $b \gtrsim 0.25$ , the transition to baryonic matter is replaced by a transition to chirally symmetric quark matter.

baryons can be put into the system without such a thermodynamic instability.

What can we learn about real-world baryonic matter from these results? We already know that the nature of the onset is different due to the lack of binding energy. But why do our holographic baryons effectively become heavier in a magnetic field? Can we draw any conclusions from this observation? Within our model, the increasing critical chemical potential has two reasons. First, as just discussed, it is

---

scaling  $S_{D4}$  with the total density  $n$ , not  $n_4$ , see eq. (2.4) in ref. [42] which apparently is used in ref. [43] (and in [41]). This difference is very important for the topology of the resulting phase diagram: as we shall see in sec. 6.8, the physical onset line intersects the chiral phase transition line, see fig. 6.9; this is not the case for the dashed line.

the meson gradient which is responsible for increasing the baryon onset from  $\frac{u_c}{3}$  to  $\frac{2u_c}{3}$ . Second,  $u_c$  itself increases with the magnetic field. In the mesonic phase  $u_c$  can be interpreted as a constituent quark mass [4, 110]. In the chiral limit of vanishing bare quark masses, it is the chiral condensate which induces such a mass. Therefore, the increase of  $u_c$  in a magnetic field suggests an increase of the chiral condensate and thus is a manifestation of magnetic catalysis (MC). The constituent quark mass in a baryon is different from the constituent mass in the mesonic phase,  $\frac{u_c}{3}$  vs.  $u_c$ , but both are proportional to  $u_c$ . Consequently, MC seems to be responsible for the heaviness of magnetized baryons.

## 6.6 Symmetric phase

The following analytical expressions are all valid in the zero-temperature limit. Only in the plots at the end of this section we include numerical finite-temperature results. Now only one equation remains to be solved numerically for  $y_\infty$ ,

$$y_\infty = \int_0^\infty \frac{3bu^{3/2}}{\sqrt{u^8 + b^2u^5 + \left(\frac{3b\mu}{\sinh y_\infty}\right)^2 u^3}} du. \quad (6.66)$$

For  $b > 0$ , this equation has in general three solutions:  $y_\infty = \infty$ , which is always a solution, and two finite solutions, the larger of which turns out to be unstable. At sufficiently large values of  $b$  for a given  $\mu$  only the divergent solution survives.

For the quark density we find

$$n_q = \frac{N_c}{2\pi^2} B\mu_q \coth y_\infty. \quad (6.67)$$

Let us first take the limit where  $b$  is small. In this case,  $y_\infty$  is linear in  $b$ , and we obtain for the (dimensionful) quark number density

$$n_q = \frac{\sqrt{N_c M_{\text{KK}}}}{3g_{\text{YM}}\pi^{3/2}} \mu_q^{5/2} \left[ \frac{\sqrt{\pi}}{\Gamma\left(\frac{3}{10}\right)\Gamma\left(\frac{6}{5}\right)} \right]^{5/2} + \mathcal{O}(B^2). \quad (6.68)$$

The unusual exponent  $5/2$  of  $\mu_q$  can only occur due to the presence of the dimensionful model parameter  $M_{\text{KK}}$  (due to the extra dimension in the model), which provides the missing mass dimensions.

The grand canonical potential becomes for small  $b$

$$\Omega_{\text{ren}} \simeq -\mathcal{N} \left\{ \frac{2}{7} \mu^{7/2} \left[ \frac{\sqrt{\pi}}{\Gamma(\frac{3}{10}) \Gamma(\frac{6}{5})} \right]^{5/2} + \eta_3 b^2 \sqrt{\mu} \right\}, \quad (6.69)$$

with

$$\eta_3 \equiv \frac{3}{2} \left[ \frac{\Gamma(\frac{3}{10}) \Gamma(\frac{6}{5})}{\sqrt{\pi}} \right]^{5/2} + \frac{\Gamma(\frac{9}{10}) \Gamma(\frac{3}{5})}{\pi^{1/4} \sqrt{\Gamma(\frac{3}{10}) \Gamma(\frac{6}{5})}}. \quad (6.70)$$

Taking the limit  $b \rightarrow \infty$  allows only the solution  $y_\infty = \infty$ , as mentioned before. However, note that this is also a valid solution at finite  $b$ , hence the following results carry over to any value of  $b$  as long as this particular phase is considered. Interestingly, the density in this case is

$$n_q = \frac{N_c}{2\pi^2} B \mu_q, \quad (6.71)$$

which takes precisely the form of the density of gapless free fermions in the lowest Landau level. Therefore, we may speak of an LLL-like phase in the Sakai-Sugimoto model, although there are, because of the strong-coupling nature, no quasiparticles and thus no Landau levels in the actual sense. The grand canonical potential is

$$\Omega_{\text{ren}} = -\mathcal{N} \frac{3b\mu^2}{2}. \quad (6.72)$$

Using (6.69) together with (6.72) we can derive the critical magnetic field of the first-order transition within the chirally restored phase to the LLL-like phase as a function of the chemical potential,

$$b_c \simeq 0.095 \mu^{3/2}. \quad (6.73)$$

In the left panel of Fig. 6.4 we plot the quark number density for different temperatures. As a comparison, we also plot the corresponding density for (massless) free fermions in a magnetic field, obtained by taking the derivative with respect to the chemical potential of the thermodynamic potential (5.10).

In the case of free fermions, the higher Landau levels cause oscillations in the density at small magnetic field. These oscillations are absent in the "higher Landau level phase" in the Sakai-Sugimoto model, given by the solution  $y_\infty < \infty$ . This might be a consequence of the strong coupling, in which case we do not expect a sharp



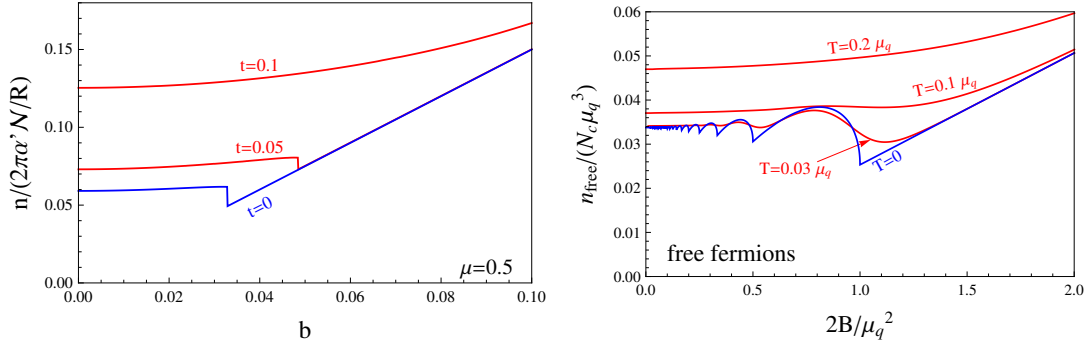


Figure 6.4: Quark number density as a function of the background magnetic field for a given chemical potential at various (dimensionless) temperatures  $t \equiv TR$  in the Sakai-Sugimoto model (left) and the NJL model (right).

Fermi surface, even at  $T = 0$ . Furthermore, in the NJL model, the transitions between the phases with differently filled Landau levels, in particular also the transition to the LLL phase, is second order, while in the Sakai-Sugimoto model it is first order. At finite temperature, the transitions become immediately smooth in the NJL model, while for given  $\mu$  it remains first order in the Sakai-Sugimoto model until a critical temperature is reached, which increases with increasing  $\mu$ . Above this temperature only one minimizing solution for  $y_\infty$  exists for all  $b$  and given  $\mu$ . As a result, the transition line in the  $b$ - $\mu$  plane has a critical endpoint for a given temperature, resulting in a critical line in the three-dimensional phase diagram, see Fig. 6.5. Another important difference is the location of the LLL-transition in the  $\mu$ - $b$  diagram: the critical magnetic field at zero temperature is proportional to  $\mu^{3/2}$ , compared to  $\mu^2/2$  for free fermions. Again this is due to the occurrence of  $\sqrt{M_{\text{KK}}}$ .

## 6.7 Chiral phase transition without baryons

First we discuss the critical temperature for chiral symmetry restoration at vanishing chemical potential. In this case, in the restored phase the only temperature dependence enters via the lower bound of the integrals over the holographic coordinate,  $u_T = (4\pi t/3)^2$ , with  $t = RT$ . Therefore, one easily determines the renormalized grand canonical potential of the restored phase for the cases  $b = 0$ ,  $\Omega_{\text{ren}} = -2/7\mathcal{N}u_T^{7/2}$ , and  $b \rightarrow \infty$ ,  $\Omega_{\text{ren}} = -\mathcal{N}bu_T^2/2$ . Then, together with the corresponding expressions for the broken phase from Eqs. (6.46) and (6.49) we compute the critical

temperatures

$$t_c(\mu = b = 0) = 0.1355/\ell, \quad (6.74)$$

$$t_c(\mu = 0, b \rightarrow \infty) = 0.1923/\ell. \quad (6.75)$$

(Remember that we have used the  $f(u) \simeq 1$  approximation for the broken phase which, strictly speaking, is only valid for very small temperatures.) We see that the Sakai–Sugimoto model reproduces the usual magnetic catalysis effect at zero chemical potential because the critical temperature at asymptotically large  $b$  is larger than that at vanishing  $b$ . This is supported by the numerical solution which shows that the critical temperature increases monotonically with the magnetic field. In contrast to the NJL model, the critical temperature saturates at the value given in equation (6.75), because the value for  $u_0$ , i.e., the holographic constituent quark mass, saturates.

At zero temperature, we use Eqs. (6.46) and (6.49) for the broken phase and Eqs. (6.69) and (6.72) for the restored phase to compute the critical chemical potentials

$$\mu_c(t = b = 0) = 0.4405/\ell^2, \quad (6.76)$$

$$\mu_c(t = 0, b \rightarrow \infty) = 0.4325/\ell^2. \quad (6.77)$$

This result already shows that inverse magnetic catalysis in the sense explained in Sec. 5.4 must be present in the Sakai–Sugimoto model. The full numerical solution of the surface of the chiral phase transition in the three dimensional  $T$ - $\mu$ - $B$  space is shown in Fig. 6.5; cuts through the surface at fixed  $t$ ,  $\mu$ , and  $b$ , are shown in Fig. 6.6. In order to discuss the inverse magnetic catalysis, we have plotted the zero-temperature phase diagram separately in Fig. 6.7. This phase diagram shows intriguing similarities with the corresponding NJL phase diagram in Fig. 5.3: inverse magnetic catalysis is present at small magnetic fields and is most pronounced when the restored phase has a LLL-like behavior. Even the manifestation of inverse magnetic catalysis in the analytical approximations is qualitatively the same as in the field-theoretical model as we now show. For large magnetic fields, Eqs. (6.49) and (6.69) can be used to write the free energy difference between restored and broken phases as

$$\Delta\Omega = \frac{N_c B}{4\pi^2} \left[ \mu_q^2 - M^2 \frac{\sqrt{\pi} \Gamma(\frac{3}{5})}{3\Gamma(\frac{1}{10})} \right] - \frac{N_c B}{16\pi^2} \mu_q^2, \quad (6.78)$$

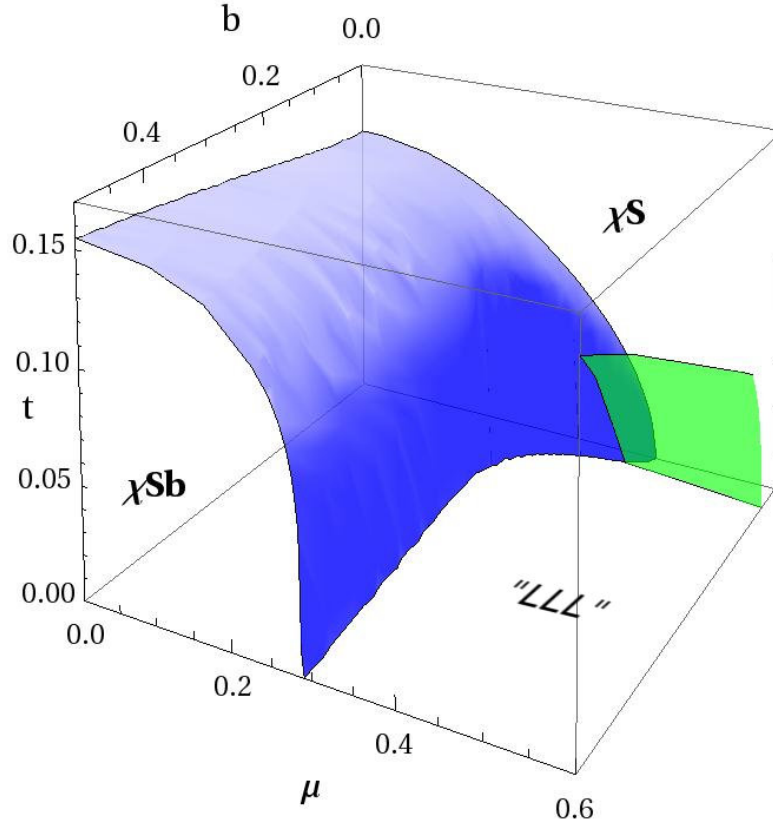


Figure 6.5: The surface of the chiral phase transition (blue) in the deconfined phase of the Sakai–Sugimoto model in the  $T$ - $\mu$ - $B$  space. The small (green) surface shows the transition from the "higher LL" phase to the "LLL" phase, explained in Sec. 6.6.

where we have identified  $Ru_0/(2\pi\alpha')$  with the constituent quark mass  $M$  [4, 110]. This large- $B$  expression for  $\Delta\Omega$  is remarkably similar to the weak-coupling expression (5.18) in the NJL model. We can thus conclude, for the reasons explained below Eq. (5.18), that in the large- $B$  regime the critical chemical potential must increase with  $B$ . This is confirmed by the chiral phase transition line of Fig. 6.7. Note the difference between the terms  $\propto \theta(\mu - M)$  in the NJL expression and the last term in Eq. (6.78). Both terms come from a nonzero quark density, which in our NJL calculation is only present if  $\mu > M$ , while in our Sakai-Sugimoto calculation there is a topological quark density at nonzero  $B$  for all  $\mu$  due to the chiral spiral.

For small magnetic fields we may apply an approximation in the spirit of Eq.

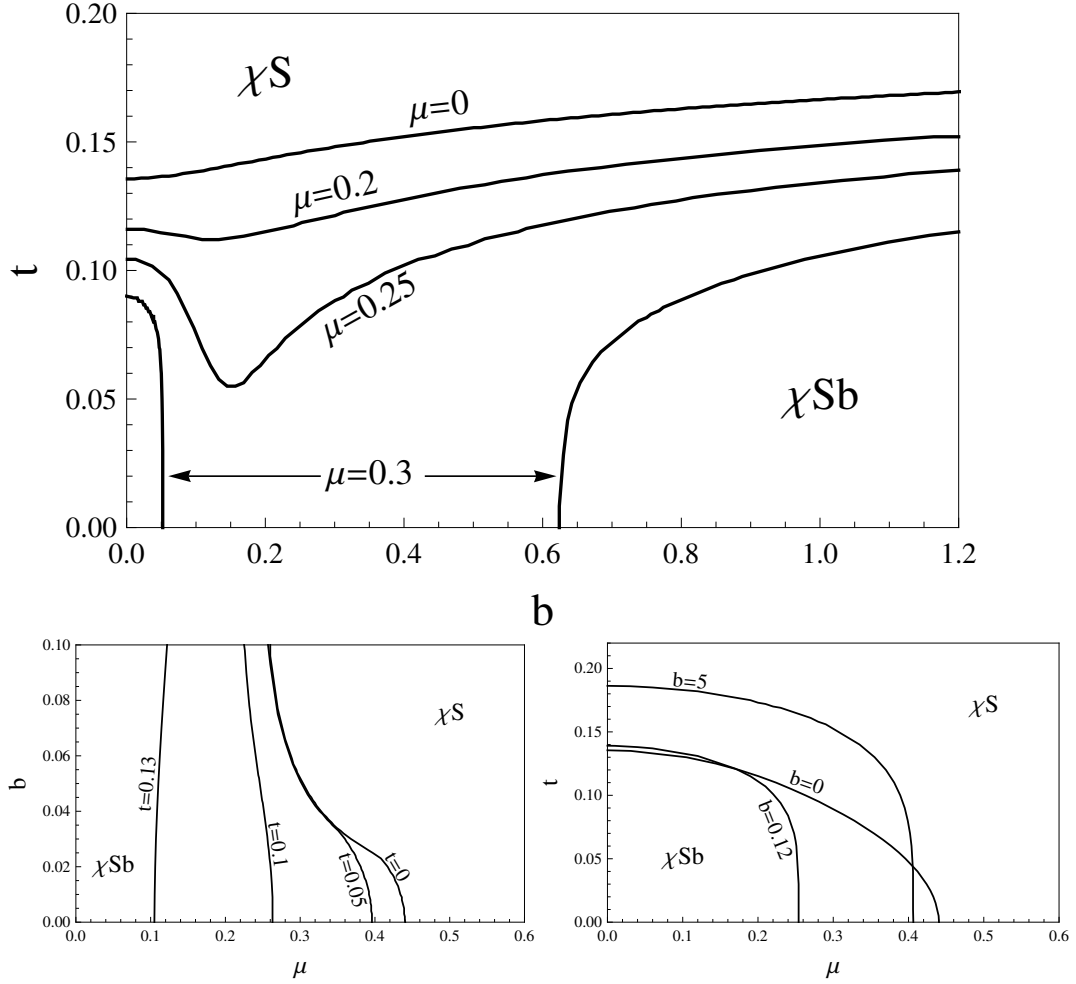


Figure 6.6: Two-dimensional cuts at various fixed temperatures, chemical potentials and magnetic fields, respectively, through the three-dimensional phase diagram. In the first plot, for instance, we see that the monotonically increasing critical temperature at  $\mu = 0$  becomes a non-monotonic curve at finite  $\mu$  and may even turn into two disconnected pieces, separating two chirally broken phases at small and large magnetic fields. The line  $b = 0$  in the lower right panel recovers the result in Ref. [104] and resembles the  $\mu - T$  phase diagram shown in Fig. 3.3 found in the NJL model.

(5.20). We compare the free energy of the broken phase for small magnetic fields (6.46) with the free energy of the LLL phase (6.72). The result can be written as

$$\Delta\Omega \simeq -\frac{2N_c^{1/2}\Gamma(\frac{9}{16})}{21\pi g_{\text{YM}}\Gamma(\frac{1}{16})} M_{\text{KK}}^{1/2} M_0^{7/2} + \frac{N_c}{4\pi^2} B\mu_q^2 - \frac{N_c^2 g_{\text{YM}}^2 \eta_2(\mu)}{24\pi^3 M_{\text{KK}} R} B^2, \quad (6.79)$$

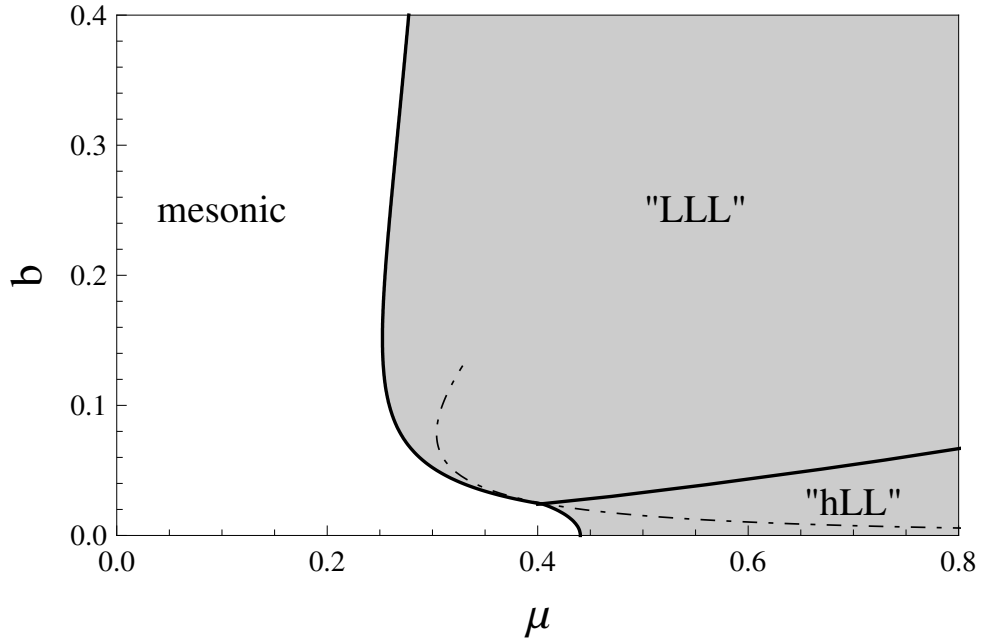


Figure 6.7: The chiral phase transition at zero temperature from the Sakai-Sugimoto model (ignoring baryonic matter). The chirally broken phase (white) is separated by a first-order phase transition (solid line) from the chirally restored phase (gray). The dashed-dotted line is the approximation from Eq. (6.79). Translating the dimensionless quantities  $b$  and  $\mu$  into physical units [145], one concludes that the magnetic field decreases the critical chemical potential from  $\mu_q \simeq 400$  MeV at  $|qB| = 0$  down to  $\mu_q \simeq 230$  MeV at  $|qB| \simeq 1.0 \times 10^{19}$  G where the critical line turns around and the critical chemical potential starts to increase with  $|qB|$ .

where  $M_0 \propto u_0^{(0)}$  is the constituent quark mass at  $B = 0$ . Again we recover the form of the NJL result (5.20). The main conclusion is that the energy cost for condensation is linear in  $B$ , whereas the energy gain from condensation, i.e., the magnetic catalysis is only quadratic in  $B$  for small  $B$ . This allows for inverse magnetic catalysis. The dashed-dotted line in Fig. 6.7 is the approximate phase transition from Eq. (6.79). Comparison with the full numerical result shows that the approximation captures the physics of inverse magnetic catalysis where it is most pronounced and that the "hLL" phase counteracts inverse magnetic catalysis.

Finally let us try to make a prediction for the quantitative behavior of the chiral phase transition in a background magnetic field. To this end we fit the parameters of the holographic model with the help of the critical temperature at  $\mu = B = 0$

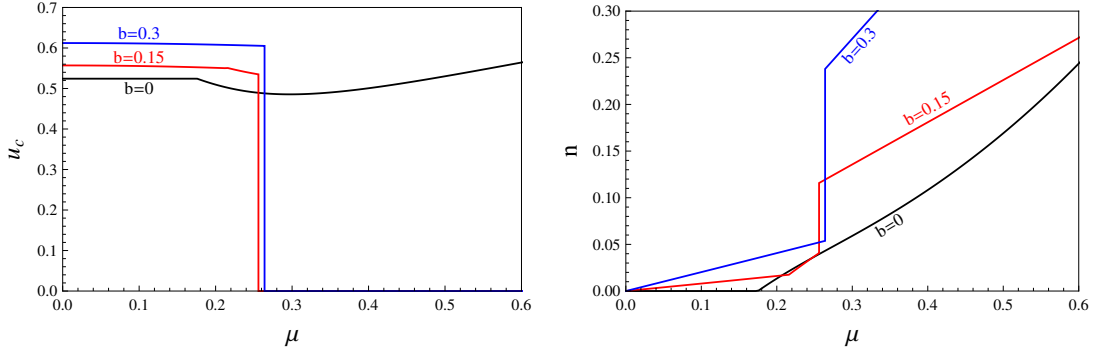


Figure 6.8: Left panel: location of the tip of the connected branes  $u_c$  (denoted  $u_0$  in the mesonic phase) as a function of  $\mu$  for three values of the magnetic field, i.e., along three horizontal cuts through the phase diagram in the right panel of fig. 6.9. One representative for each of the three qualitatively different cases is shown: baryon onset (small magnetic fields); baryon onset followed by chiral phase transition (intermediate magnetic fields); chiral phase transition (large magnetic fields). As fig. 6.9 shows, for chemical potentials beyond the scale of the plot the system reenters the chirally broken phase, resulting in an additional first-order phase transition in all three cases. Right panel: baryon number density  $n$  along the same cuts through the phase diagram. Through the axial anomaly the meson supercurrent produces a nonzero  $n$  also in the mesonic phase for  $b, \mu > 0$ .

from QCD lattice calculations [13, 12] and the (not very well known) critical chemical potential at  $T = B = 0$  from model calculations [150, 117]. We find that inverse magnetic catalysis persists up to  $B \simeq 1.0 \times 10^{19}$  G, where the critical chemical potential has decreased from 400 MeV to about 230 MeV. It is not clear whether the magnetic field inside compact stars is large enough to have any effect on the chiral phase transition. Our results indicate, however, that if it is large enough then only *inverse* magnetic catalysis will play a role, i.e., the transition from hadronic to quark matter occurs at smaller densities than naively expected from the  $B = 0$  case.

## 6.8 Chiral symmetry breaking with baryons

In fig. 6.8 we present the location  $u_c$  of the tip of the connected branes and the baryon density along lines of constant magnetic field. The interpretation of the former deserves a comment. In the mesonic phase,  $u_c$  is usually identified with the constituent quark mass since it is the distance between the color and flavor branes.

This is still true in the baryonic phase, but there it has a second meaning because  $\frac{N_c \mu_c}{3}$  is the baryon mass. (Note that the factor  $\frac{1}{3}$  originates from the geometry of the model and has nothing to do with the number of colors.)

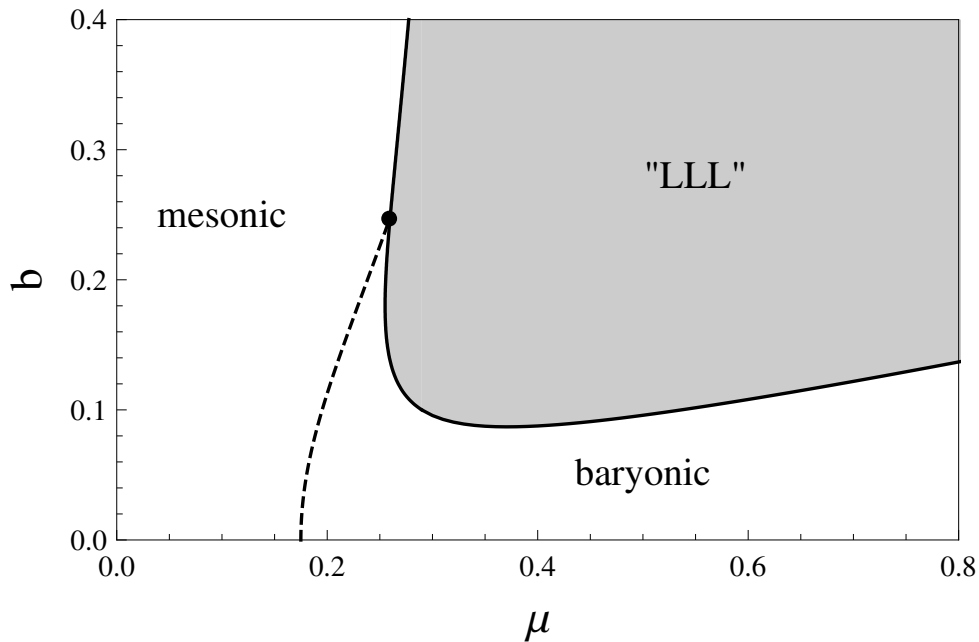


Figure 6.9: As Fig. 6.7, but including baryonic matter (from Ref. [146]). The dashed line is the (second-order) onset of baryonic matter. The transition within the chirally restored phase between the "LLL" and "hLL" phases has disappeared because baryonic matter is preferred in this region of the phase diagram.

The full phase diagram is shown in Fig. 6.9. The main observations can be summarized as follows.

- The effect of baryonic matter at small magnetic fields is dramatic: it prevents the system from restoring chiral symmetry for any chemical potential. In doing so, it completely expels the "hLL" phase from the phase diagram, such that the only surviving chirally restored phase is the "LLL" phase.
- From the phase diagram without baryons and the line describing the onset of baryons depicted in Fig. 6.3 one can already see that the onset line crosses the chiral phase transition line, therefore we conclude that for larger values of the magnetic field the chirally broken phase without baryons is directly superseded

by the restored phase. More precisely the baryon onset line terminates at a critical endpoint  $(\mu, b) \simeq (0.26, 0.25)$ .

- In the presence of baryonic matter, IMC plays an even more prominent role in the phase diagram: at *any* given chemical potential  $\mu \gtrsim 0.26$  a sufficiently large magnetic field induces chiral symmetry restoration.

Let us briefly comment on the first of these observations whose  $b = 0$  version was already made in ref. [21]. The fact that chiral symmetry remains broken along the entire  $\mu$  axis is an apparently puzzling result: in view of the similarity of the present non-antipodal version of the Sakai-Sugimoto model and the NJL model, one might have expected chiral symmetry to be intact for sufficiently large chemical potentials. This was true *before* including baryonic matter, in which case the entire phase structure with magnetic field was in amazing agreement with NJL calculations [145]. However, in the presence of baryonic matter it is questionable to expect this agreement to persist for the following reason. In related NJL studies [71, 106, 58, 34] baryon number is a rather simple concept: the only degrees of freedom are quarks whose masses acquire a contribution from the chiral condensate. When the chemical potential is larger than this constituent quark mass, a nonzero quark number is generated. Then, baryon number is simply this quark number divided by  $N_c$ . This is not true in our present approach. Holographic baryons *are* different from a mere collection of  $N_c$  quarks. This is clear from their construction and can easily be seen from the difference between the constituent quark mass in the mesonic phase  $u_c$  and the baryon mass  $\frac{N_c u_c}{3}$ . Whether we should therefore call our quarks confined is debatable, but it is certainly a qualitative difference to the NJL model.

To interpret the lack of chiral symmetry restoration, the following intriguing property of our baryonic matter at asymptotically large chemical potentials may be helpful. For simplicity, let us restrict ourselves to  $b = 0$ . In this case the free energy of the baryonic phase approaches the one of the chirally restored phase,

$$\frac{\Omega_{\text{bar.}}(b=0)}{\mathcal{N}} = -\frac{2}{7} \frac{\mu^{7/2}}{p^{5/2}} + \mathcal{O}(\mu^{5/2}), \quad \frac{\Omega_{\text{sym.}}(b=0)}{\mathcal{N}} = -\frac{2}{7} \frac{\mu^{7/2}}{p^{5/2}}, \quad (6.80)$$

where  $p = \Gamma\left(\frac{3}{10}\right) \Gamma\left(\frac{6}{5}\right) / \sqrt{\pi}$ . Therefore, at asymptotically large  $\mu$ , baryonic matter and quark matter become thermodynamically indistinguishable. One may speculate that this is a consequence of the point like nature of our baryons: due to this property, our baryons can only overlap at infinite density. This suggests that the expected



---

transition to quark matter at finite  $\mu$  is shifted to  $\mu = \infty$  (which, curiously, is undone by a sufficiently large magnetic field). It would be interesting to see whether this is different for  $N_f > 1$ , where baryons *can* be described by non-singular instantons.



# Walecka model with magnetic field

In this section we employ the Walecka model [175] at zero temperature in a background magnetic field. The Walecka model is a relativistic model for dense nuclear matter, where nucleons (or, in extensions of the model, hyperons) interact via Yukawa exchange of mesons. In the simplest, isospin-symmetric, version considered here, nucleons interact through the scalar sigma meson and the vector omega meson. This is sufficient to model the realistic nucleon-nucleon interaction which is known to have a repulsive short-range (omega) and an attractive intermediate and long-range (sigma) part. Nuclear matter being stable at zero pressure, having a finite binding energy  $E_0 \simeq -16.3$  MeV, a saturation density  $n_0 \simeq 0.153$  fm<sup>-3</sup>, and showing a first-order liquid-gas phase transition are all manifestations of this simple but crucial property of the interaction. Beyond the saturation density, the properties of nuclear matter are poorly known, and the Walecka model is only one of many competing models. However, for our comparison to holographic baryonic matter, we are primarily interested in the baryon onset, and we know that for this purpose – at least for vanishing magnetic field – the Walecka model describes, by construction, real-world nuclear matter.

## 7.1 Lagrangian

The following setup is essentially taken from works where dense nuclear matter in a magnetic field has been considered in the astrophysical context, see refs. [36, 37, 148] and references therein. In neutron stars, the simplest version of baryonic matter consists of neutrons, protons, and electrons. Their various chemical potentials are related through the conditions of beta equilibrium and (global) electric charge neutrality. For our purpose, these complications are irrelevant since for a comparison to our holographic results we are interested in the behavior of a single baryon species with a given electric charge and a single baryon chemical potential in a background magnetic field. Therefore, our results will be simpler and more transparent, albeit less realistic, compared to the results for astrophysical nuclear matter.

We start from the Lagrangian

$$\mathcal{L} = \mathcal{L}_B + \mathcal{L}_I + \mathcal{L}_M, \quad (7.1)$$

containing a baryonic part  $\mathcal{L}_B$ , an interaction part  $\mathcal{L}_I$ , and a mesonic part  $\mathcal{L}_M$ . The baryonic part is

$$\mathcal{L}_B = \bar{\psi} \left( i\gamma^\mu D_\mu - m_B + \mu_B \gamma^0 - \frac{1}{2} \kappa \sigma_{\mu\nu} F^{\mu\nu} \right) \psi, \quad (7.2)$$

with the baryon mass  $m_B$  and the baryon chemical potential  $\mu_B$ . The baryons feel the magnetic field through the covariant derivative  $D_\mu = \partial_\mu + iqA_\mu$  with the baryon electric charge  $q$  and the electromagnetic gauge field  $A_\mu$ , which encodes the background magnetic field in the  $x_3$ -direction,  $A_\mu = (0, x_2 B, 0, 0)$ . In addition, baryons have an anomalous magnetic moment  $\kappa$  whose effect is included by a magnetic dipole term with  $\sigma_{\mu\nu} = \frac{i}{2} [\gamma_\mu, \gamma_\nu]$  and the field strength tensor  $F^{\mu\nu} = \partial^\mu A^\nu - \partial^\nu A^\mu$ . It is important to keep in mind that this term is obviously an effective, not a fundamental, way to take into account the anomalous magnetic moment. In particular, the present approach can not be trusted for arbitrarily large magnetic fields, as we shall see more explicitly below.

The interaction term consists of two Yukawa contributions for the  $\sigma$  and the  $\omega$ ,

$$\mathcal{L}_I = g_\sigma \bar{\psi} \sigma \psi - g_\omega \bar{\psi} \gamma^\mu \omega_\mu \psi, \quad (7.3)$$

with coupling constants  $g_\sigma, g_\omega > 0$ . The mesonic part includes cubic and quartic scalar self-interactions,

$$\mathcal{L}_M = \frac{1}{2}(\partial_\mu \sigma \partial^\mu \sigma - m_\sigma^2 \sigma^2) - \frac{1}{4} \Omega^{\mu\nu} \Omega_{\mu\nu} + \frac{1}{2} m_\omega^2 \omega^\mu \omega_\mu - \frac{b}{3} m_B (g_\sigma \sigma)^3 - \frac{c}{4} (g_\sigma \sigma)^4, \quad (7.4)$$

with  $\Omega^{\mu\nu} = \partial^\mu \omega^\nu - \partial^\nu \omega^\mu$  and the sigma and omega masses  $m_\sigma$  and  $m_\omega$ . With the given values  $m_B = 939$  MeV,  $m_\omega = 783$  MeV,  $m_\sigma \sim 550$  MeV, the model has four free parameters which are fitted to reproduce the saturation density, the binding energy, the compressibility, and the Landau mass at saturation (all for  $B = 0$ ), which gives  $\frac{g_\sigma^2}{4\pi} = 6.003$ ,  $\frac{g_\omega^2}{4\pi} = 5.948$ ,  $b = 7.950 \times 10^{-3}$ , and  $c = 6.952 \times 10^{-4}$ . We shall employ the mean-field approximation where the meson fluctuations are neglected, and the meson condensates  $\bar{\sigma}$  and  $\bar{\omega}_0$  have to be determined from minimization of the free energy. The basic equations of the model in this approximation are as follows (see for instance ref. [158] for a pedagogical derivation). The pressure is

$$P = -\frac{1}{2} m_\sigma^2 \bar{\sigma}^2 - \frac{b}{3} m_B (g_\sigma \bar{\sigma})^3 - \frac{c}{4} (g_\sigma \bar{\sigma})^4 + \frac{1}{2} m_\omega^2 \bar{\omega}_0^2 + P_B, \quad (7.5)$$

where, at zero magnetic field, the renormalized baryonic pressure is given by

$$P_B = 2T \int \frac{d^3 \vec{k}}{(2\pi)^3} \ln \left[ 1 + e^{-(\epsilon_k - \mu_*)/T} \right]. \quad (7.6)$$

Here,  $\mu_* \equiv \mu_B - g_\omega \bar{\omega}_0$  plays the role of the Fermi energy at zero temperature (the chemical potential in the thermodynamic sense it still  $\mu_B$ , not  $\mu_*$ ). The baryon dispersion is  $\epsilon_k = \sqrt{k^2 + m_*^2}$  with an effective baryon mass  $m_* \equiv m_B - g_\sigma \bar{\sigma}$ . The stationarity equations for the meson condensates are

$$m_* = m_B - \frac{g_\sigma^2}{m_\sigma^2} n_s + \frac{g_\sigma^2}{m_\sigma^2} \left[ b m_B (m_B - m_*)^2 + c (m_B - m_*)^3 \right], \quad (7.7a)$$

$$\bar{\omega}_0 = \frac{g_\omega}{m_\omega^2} n_B, \quad (7.7b)$$

where  $n_B = \frac{\partial P_B}{\partial \mu_B}$  and  $n_s = -\frac{\partial P_B}{\partial m_B}$  are the baryon and scalar densities, respectively.

Next we include the magnetic field, wherefore we need to distinguish between charged and neutral baryons. For our purpose the only relevant effect of the magnetic field concerns the single-baryon dispersion relations, which can be found in ref. [148].

## 7.2 Charged baryons

Our reference example of charged baryonic matter is pure proton matter with charge  $q = +e$  and an anomalous magnetic moment  $\kappa = 1.79 \mu_N$  where  $\mu_N = \frac{e}{2m_p} \simeq 3.15 \times 10^{-18} \text{ MeV G}^{-1}$  is the nuclear magneton. We shall, however, vary the anomalous magnetic moment below to study its effect on the baryon onset. Remember that we ignore any neutrality constraint and Coulomb effects. For charged baryons the dispersion  $\epsilon_k$  has to be replaced by

$$\epsilon_{k_{\parallel}, \ell, s} = \sqrt{k_{\parallel}^2 + M_{\ell, s}^2}, \quad M_{\ell, s} \equiv \sqrt{m_*^2 + 2\ell|q|B - s\kappa B}, \quad (7.8)$$

with  $k_{\parallel}$  being the momentum in the direction of the magnetic field,  $s = \pm 1$ , and  $\ell = n + (1 - s \text{sgn } q)/2$  with  $n = 0, 1, 2, \dots$ , such that for positive charge we have  $\ell = 0, 1, 2, \dots$  for  $s = +1$  and  $\ell = 1, 2, 3, \dots$  for  $s = -1$ , and vice versa for negative charge. This means that the lowest Landau level (LLL)  $\ell = 0$  is only populated by  $s = +1$  fermions for  $q > 0$  and  $s = -1$  fermions for  $q < 0$ , while both  $s = +1$  and  $s = -1$  contribute to all higher Landau levels. The three-dimensional momentum integral has to be replaced by a one-dimensional integral over  $k_{\parallel}$  and a sum over Landau levels and spin degrees of freedom,

$$2 \int \frac{d^3 \vec{k}}{(2\pi)^3} \rightarrow \frac{|q|B}{2\pi^2} \sum_{s=\pm} \sum_{\ell} \int_0^{\infty} dk_{\parallel}. \quad (7.9)$$

With these replacements in the baryonic pressure (7.6) we obtain at zero temperature

$$P_B = \frac{|q|B}{4\pi^2} \sum_{s=\pm} \sum_{\ell}^{\ell_{\max}} \left( \mu_* k_{F, \ell, s} - M_{\ell, s}^2 \ln \frac{k_{F, \ell, s} + \mu_*}{M_{\ell, s}} \right), \quad (7.10)$$

and

$$n_B = \frac{|q|B}{2\pi^2} \sum_{s=\pm} \sum_{\ell}^{\ell_{\max}} k_{F, \ell, s}, \quad (7.11a)$$

$$n_s = \frac{|q|B m_*}{2\pi^2} \sum_{s=\pm} \sum_{\ell}^{\ell_{\max}} \frac{M_{\ell, s}}{\sqrt{m_*^2 + 2\ell|q|B}} \ln \frac{k_{F, \ell, s} + \mu_*}{M_{\ell, s}}, \quad (7.11b)$$

where  $k_{F, \ell, s} = \sqrt{\mu_*^2 - M_{\ell, s}^2}$  is the longitudinal Fermi momentum, and where the Landau levels are occupied up to  $\ell_{\max} = \left\lfloor \frac{(\mu_* + s\kappa B)^2 - m_*^2}{2|q|B} \right\rfloor$ . By inserting eqs. (7.11) into

eqs. (7.7) and solving the resulting equations for  $m_{*}, \bar{\omega}_0$ , one can compute the thermodynamic properties for arbitrary  $\mu_B$  and  $B$ . Since we are only interested in the baryon onset, we have the additional condition  $P = 0$ , where  $P$  is obtained by inserting eq. (7.10) into eq. (7.5). Hence, we have a system of three equations to be solved for  $m_{*}, \bar{\omega}_0$ , and  $\mu_B$  at any given  $B$ .

The result for pure proton matter and three more (unphysical) types of charged baryonic matter with  $q = +e$ , distinguished by different values for  $\kappa$ , is shown in fig. 7.1 where we plot the onset lines and, for proton matter, the baryon density along the onset. (In order to reproduce the nuclear ground state density  $n_0$  at  $B = 0$  we have multiplied the pressure by a factor of 2. In other words, we have started from the isospin-symmetric,  $B = 0$  Walecka model for protons and neutrons and have added the effect of the magnetic field as if both nuclear species had the same charge and anomalous magnetic moment.)

The  $B = 0$  onset occurs at  $\mu_B = m_B + E_0 \simeq 922.7$  MeV where  $E_0 \simeq -16.3$  MeV is the nuclear binding energy. Magnetic fields of the order of  $10^{18}$  G and larger change this significantly, in accordance with the simple estimate in chapter 0. We observe oscillations due to the Landau level structure in the onset line as well as in the onset density. At sufficiently large magnetic fields only the LLL is occupied. (If there was no binding energy, the density at the onset would be infinitesimally small, and all along the onset line the LLL would be the only relevant state. In other words, only due to the presence of a finite binding energy the onset line shows a behavior reminiscent of de Haas-van Alphen oscillations at small magnetic fields.<sup>1</sup>) Since we have, without loss of generality, fixed the electric charge to be positive, the LLL is occupied by  $s = +1$  baryons in all four cases considered here. Note that in one of the four cases shown in the figure, the anomalous magnetic moment  $\kappa$  is negative. Since  $\kappa < 0$  favors  $s = -1$  baryons, it can in principle be less costly to put baryons in the  $\ell = 1, s = -1$  state than in the  $\ell = 0, s = +1$  state such that for sufficiently large magnetic fields all baryons sit in the first, not in the lowest, Landau level. This

<sup>1</sup>The higher Landau levels in fact induce cusps in some of the onset lines, see for instance the case  $\kappa = 0$  where  $\mu_B^{\text{cusp}} \simeq 920$  MeV. In a small vicinity around this cusp there are, for a given  $B$ , two solutions for the onset: one where only the LLL becomes occupied, and one where the lowest and the first Landau level become occupied simultaneously. The resulting two onset lines intersect, and for any given  $B$  the line where the onset occurs at a lower  $\mu_B$  is the physical one. The reason is that the "later" onset would keep the system in the vacuum state  $P = 0$ , in a region where the "earlier" onset already leads to  $P > 0$ . (For  $\mu_B < \mu_B^{\text{cusp}}$ , the LLL onset is "earlier", for  $\mu_B > \mu_B^{\text{cusp}}$  it is "later", hence the cusp.)

does not occur for the cases shown here, but a simple estimate shows that it occurs if the anomalous moment and the charge have opposite sign and  $|\kappa|$  becomes of the order of or larger than the modulus of the normal magnetic moment  $\frac{|q|}{2m_B}$ .

One can check that for large magnetic fields the onset lines are well approximated by the curves  $\mu_* = m_* - \kappa B$ , which turn out to become straight lines for large  $B$ . However, we need to remember that we have used an effective approach for the anomalous magnetic moment. As a consequence, we should not trust our results for  $\kappa B$  becoming of the order of or larger than  $m_*$ . In that case, as we see for instance from eq. (7.8),  $M_{\ell=0, S=+1}$  would become negative (for  $\kappa > 0$ ). In the case of proton matter we find  $\kappa B \simeq 0.4 m_*$  at  $B = 5 \times 10^{19} \text{G}$ , which suggests that our approach is still reliable in the plotted range. We expect that in a full treatment the onset lines saturate for asymptotic values of  $B$ . This is the case for  $\kappa = 0$ , where our approach can be used for arbitrarily large  $B$ .



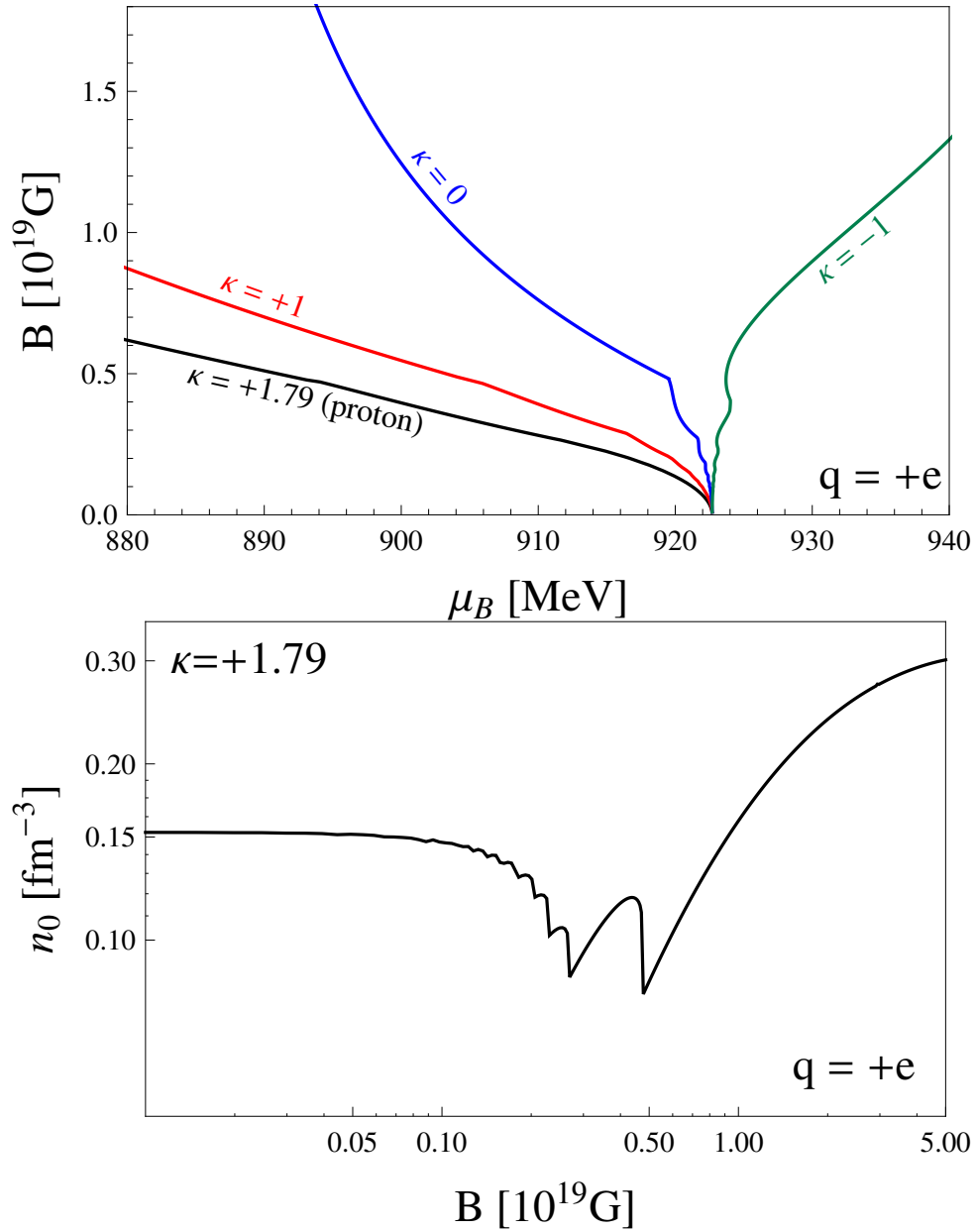


Figure 7.1: Upper panel: zero-temperature transition in the plane of baryon chemical potential  $\mu_B$  and magnetic field  $B$  from the vacuum (to the left of each line) to baryonic matter (to the right of each line) for charged baryons with  $q = +e$  and various values of the anomalous magnetic moment  $\kappa$  (in units of the nuclear magneton  $\mu_N$ ). Each line represents a first-order phase transition since the baryon density jumps from zero to a finite value  $n_0$ . Lower panel: corresponding baryon density  $n_0$  along the onset line on a doubly logarithmic plot for the case of pure proton matter,  $\kappa = +1.79$  (the other three cases from the left plot would lead to similar curves). The oscillations are due to successive occupation of Landau levels. For  $B \gtrsim 0.5 \times 10^{19}$  G only the LLL is occupied.

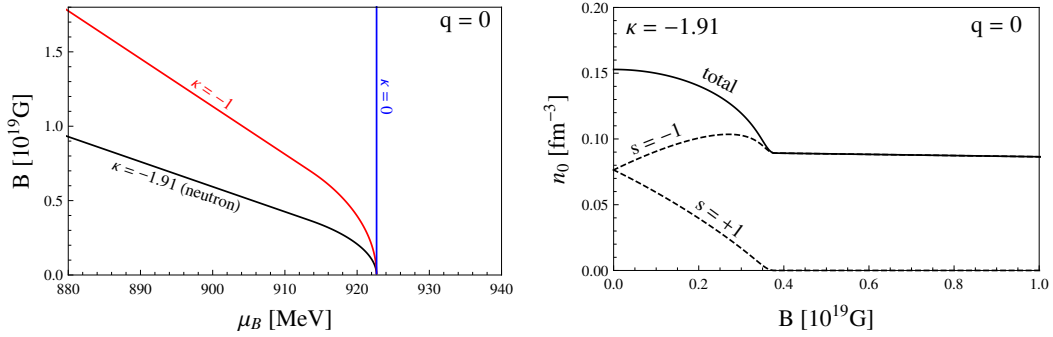


Figure 7.2: Same as fig. 7.1, but for neutral baryons,  $q = 0$ . Due to the symmetry under  $\kappa \rightarrow -\kappa$ , we can restrict ourselves to negative  $\kappa$ . The density along the onset in the right panel is shown for pure neutron matter. We have plotted the total baryon density (solid) and the contributions from the  $s = +1$  and  $s = -1$  states (dashed). We see that at  $B \gtrsim 0.4 \times 10^{19}$  G the system is fully polarized in the  $s = -1$  state.

### 7.3 Neutral baryons

For the case of neutral baryons we may think of pure neutron matter with  $q = 0$  and  $\kappa = -1.91 \mu_N$ . In this case there is no Landau quantization and the single-baryon excitations become

$$\epsilon_{\vec{k},s} = \sqrt{k_{\parallel}^2 + \left[ \sqrt{m_*^2 + k_{\perp}^2} - s\kappa B \right]^2}, \quad (7.12)$$

where  $\vec{k}_{\perp}$  is the momentum perpendicular to the magnetic field. Replacing the momentum integral in the nucleonic pressure (7.6),

$$2 \int \frac{d^3 \vec{k}}{(2\pi)^3} \rightarrow \frac{1}{2\pi^2} \sum_{s=\pm} \int_0^{\infty} dk_{\perp} k_{\perp} \int_0^{\infty} dk_{\parallel}, \quad (7.13)$$

and performing the integrals at zero temperature yields

$$P_B = \sum_{s=\pm} \frac{\Theta(\mu_* + s\kappa B - m_*)}{2\pi^2} \left[ \mu_* k_{F,s} \left( \frac{k_{F,s}^2}{12} - \frac{M_s^2}{8} - \frac{s\kappa B M_s}{3} \right) + \frac{s\kappa B \mu_*^3}{6} \arccos \frac{M_s}{\mu_*} + M_s^3 \left( \frac{M_s}{8} + \frac{s\kappa B}{6} \right) \ln \frac{\mu_* + k_{F,s}}{M_s} \right], \quad (7.14)$$

with  $M_s \equiv m_* - s\kappa B$  and the longitudinal Fermi momentum  $k_{F,s} = \sqrt{\mu_*^2 - M_s^2}$ . The baryon and scalar densities become

$$n_B = \sum_{s=\pm} \frac{\Theta(\mu_* + s\kappa B - m_*)}{2\pi^2} \times \left[ \frac{k_{F,s}^3}{3} + \frac{s\kappa B}{2} \left( \mu_*^2 \arccos \frac{M_s}{\mu_*} - k_{F,s} M_s \right) \right], \quad (7.15a)$$

$$n_s = m_* \sum_{s=\pm} \frac{\Theta(\mu_* + s\kappa B - m_*)}{4\pi^2} \left( \mu_* k_{F,s} - M_s^2 \ln \frac{\mu_* + k_{F,s}}{M_s} \right). \quad (7.15b)$$

We observe that the system is symmetric under  $\kappa \rightarrow -\kappa$  because after a sign change of  $\kappa$  the contributions from  $s = +1$  and  $s = -1$  have simply exchanged their roles. Analogously to the charged case we can now compute the baryon onset. The results are shown in fig. 7.2. For large magnetic fields, the onset curves can be approximated by the simple straight lines  $\mu_B = m_B - |\kappa|B$ . In this regime the system is fully polarized, i.e., the baryons are all in the  $s = -1$  ( $s = +1$ ) state if  $\kappa < 0$  ( $\kappa > 0$ ), as can be seen in the right panel of the figure. Having in mind the symmetry under  $\kappa \rightarrow -\kappa$  it is instructive to go back to the results for charged baryons. In the upper panel of fig. 7.1, the onset lines for  $\kappa = +\mu_N$  and  $\kappa = -\mu_N$  are obviously far from identical. This is a LLL effect: in the LLL the baryons with  $q > 0$  become heavier for  $\kappa < 0$  and lighter for  $\kappa > 0$ . If we let  $q \rightarrow 0$  the higher Landau levels become more and more important, and the two curves indeed approach each other and become identical for  $q = 0$ , see onset line for  $\kappa = -\mu_N$  in fig. 7.2. Now the baryons in the lowest energy state become lighter for either sign of  $\kappa$ .

## 7.4 Binding energy

Let us now compare the baryon onset in the holographic model, fig. 6.3, with the ones in the Walecka model for charged and neutral baryons, figs. 7.1 and 7.2. The first simple observation is that in the holographic case the larger the magnetic field, the larger the energy needed to create baryons. This seems to be in contrast to the results from the previous two sections which suggest that a magnetic field tends to make nuclear matter energetically less costly. In order to compare the holographic

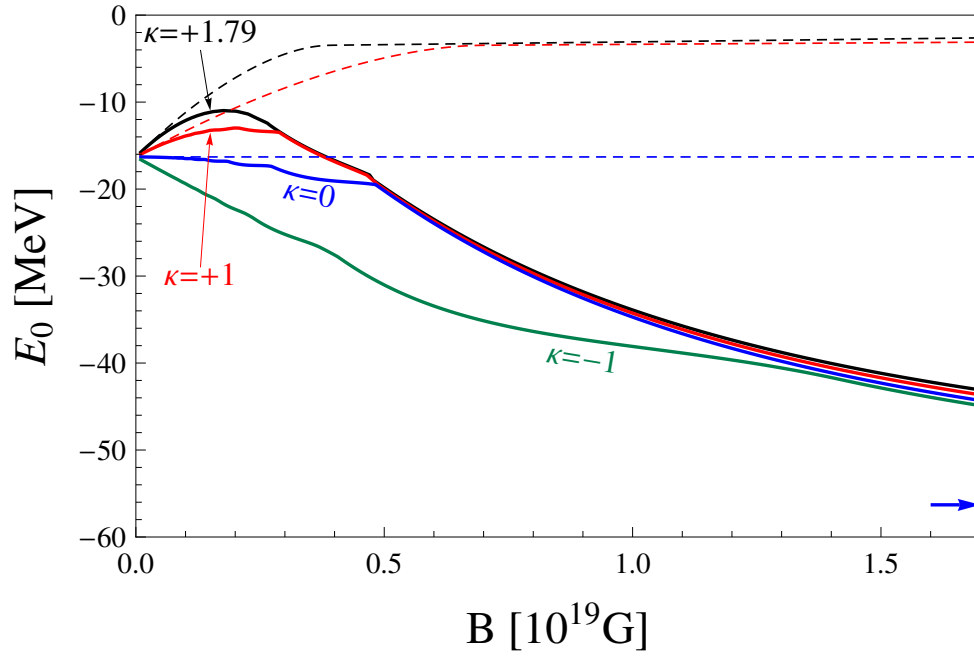


Figure 7.3: Solid lines: binding energy  $E_0$  along the baryon onset for charged baryons with charge  $q = +e$  and various anomalous magnetic moments  $\kappa$ , corresponding to the four cases shown in fig. 7.1. Dashed lines: binding energies for baryons with the same values for  $\kappa$ , but  $q = 0$ . They approximate the curves for the charged baryons at small  $B$  where many Landau levels are occupied. The arrow at  $E_0 = -56.3$  MeV indicates the asymptotic value of the binding energy for  $\kappa = 0$ , see Eq. (7.17) (for  $\kappa \neq 0$  our approach does not allow for arbitrarily large magnetic fields).

with the Walecka result in a sensible way, we need to isolate the effect of the binding energy  $E_0$ .

In the absence of a magnetic field the binding energy is given by  $E_0 = \frac{E}{A} - m_B$ , i.e., by the energy per baryon  $\frac{E}{A} = \frac{\epsilon}{n_B}$  relative to its mass  $m_B$ . To be precise, by mass we mean the energy that is needed to put a single, non-interacting baryon into the lowest single-particle state of the system. To generalize this concept to finite magnetic fields, let us first consider charged baryons. In this case, the single-particle ground state energy without nucleon-nucleon interaction is  $m_B - \kappa B \text{sgn } q$  according to eq. (7.8). Thus we define

$$E_0 = \frac{\epsilon}{n_B} - (m_B - \kappa B \text{sgn } q), \quad (7.16)$$

where, at the onset,  $\frac{c}{n_B} = \mu_B$ . We plot  $E_0$  as a function of the magnetic field in fig. 7.3. The plot shows that in the regime where higher Landau levels are occupied, the binding energy depends strongly on the anomalous magnetic moment, while it varies very little with  $\kappa$  in the LLL regime. For  $\kappa = 0$  we can take the limit of asymptotically large magnetic fields and find that the onset approaches the line  $\mu_* = m_*$ , hence with the definitions of  $\mu_*$  and  $m_*$  below eq. (7.6) we have

$$E_0(\kappa = 0, B \rightarrow \infty) = g_\omega \bar{\omega}_0 - g_\sigma \bar{\sigma} \simeq -56.3 \text{ MeV}. \quad (7.17)$$

Here,  $\bar{\omega}_0$  and  $\bar{\sigma}$  are complicated functions of the parameters of the model. Nevertheless, this expression is very instructive since it shows the effect of the meson condensates in a very transparent way:  $E_0$  is negative because the scalar meson condensate, responsible for the attractive interaction, becomes sufficiently large compared to the vector meson condensate, which is responsible for the repulsive interaction. There is no such simple expression for  $B = 0$ . Interestingly,  $E_0(B \rightarrow \infty)$  is non-vanishing only in the presence of scalar self-interactions. For asymptotically large  $B$ , one can show analytically that after setting  $b = c = 0$  in eq. (7.5) and (7.7a) we would obtain  $\mu_B = m_B$  and thus  $E_0 = 0$ .

As a result of this discussion we conclude that the magnetic field has two effects: it changes the mass and the binding energy. For charged baryons whose charge and anomalous magnetic moment have the same sign, both effects work in favor of creating baryonic matter, at least for sufficiently large magnetic fields: first, they decrease the mass  $m_B - \kappa B \text{sgn } q$ , and second, they lead to a larger binding energy  $|E_0|$ . At smaller magnetic field and/or different signs of  $q$  and  $\kappa$ , things are more complicated and can be read off from figs. 7.1 and 7.3. For neutral baryons, a magnetic field always decreases the mass,  $m_B - |\kappa|B$ , and baryonic matter is always favored by a nonzero magnetic field. If we compare charged with neutral baryons at the same anomalous magnetic moment, for instance the curves for  $\kappa = +\mu_N$  in figs. 7.1 and 7.2, we see that neutral baryonic matter is favored a bit less than charged one. The reason is that for neutral baryons  $|E_0|$  becomes smaller for large magnetic fields, as fig. 7.3 demonstrates.

## 7.5 Large $N_c$

How does this picture change when we go to the large- $N_c$  limit? One way to answer this question is to simply rescale the parameters of the model with the appropriate powers of  $N_c$ , as suggested from large- $N_c$  arguments [180, 125]. This has been done without magnetic field in Ref. [33]. While the rescaling of most parameters is unambiguous, one has to make a decision about the generalization of the scalar meson to large values of  $N_c$ . In the traditional quark-anti-quark picture, its mass would scale like  $N_c^0$ . However, we may take the heaviness of the lightest scalar meson in the Sakai-Sugimoto model as a hint that this picture is incorrect, see also refs. [141, 140, 139]. The alternative that we shall consider here is that the lightest scalar meson is a tetraquark state [109]. Let us denote the generalization to arbitrary values of  $N_c$  of this tetraquark state by  $\chi$ . This state is composed of  $N_c - 1$  quarks and  $N_c - 1$  anti-quarks such that its mass scales like  $m_\chi \sim 2(N_c - 1) \sim N_c$  [122]. There are other possibilities for the nature of the scalar meson which we do not consider here. The results of ref. [33], however, suggest that the main conclusions of our following discussion do not depend on the detailed nature of this controversial meson state. Consequently, we rescale [33, 180, 125]

$$m_B, m_\chi, \kappa, q \sim N_c, \quad m_\omega, g_\chi \sim N_c^0, \quad g_\omega \sim N_c^{1/2}. \quad (7.18)$$

(The  $N_c$ -dependence of  $\kappa$  has been computed in ref. [100]; note that we also assume the charge  $q$  to scale with  $N_c$ ). The  $N_c$ -dependence of the self-interactions of  $\chi$  is given by  $b \sim e^{-N_c}$ ,  $c \sim N_c$ ; this is suggested by the arguments explained in ref. [33].

Let us first briefly discuss the scenario without magnetic field. In this case the stationarity equations of the Walecka model (7.7) imply that the Fermi momentum  $k_F = \sqrt{\mu_*^2 - m_*^2}$  scales like  $N_c^0$ , although both  $\mu_*$  and  $m_*$  are proportional to  $N_c$ . Therefore, in the large- $N_c$  limit, one can expand the pressure for small  $k_F \ll m_*, \mu_*$  (which, as an aside, yields  $P \sim N_c$ ). The resulting equation  $P = 0$  for the baryon onset then becomes very simple and yields, together with the stationarity equations the trivial solution  $m_* = m_B$ ,  $\mu_* = \mu_B$  and  $E_0 = 0$ , i.e., the baryon onset becomes a second-order transition. This result is in fact obtained for all  $N_c \geq 4$  [33].

Now we switch on the magnetic field. Our numerical results show that, not surprisingly, the binding energy remains zero, and as a consequence the baryon onset curves are simply straight lines in the  $B$ - $\mu_B$  plane for all  $N_c \geq 4$ : for charged baryons

they are given by  $B = \frac{m_B - \mu_B}{\kappa}$ , while for neutral baryons  $B = \frac{m_B - \mu_B}{|\kappa|}$ . Note the slight subtlety related to the order of limits  $q \rightarrow 0$  and  $N_c \rightarrow \infty$ : consider the onset lines of charged baryons at  $N_c = 3$  for  $\kappa = \pm\mu_N$ , see fig. 7.1. These are two very different lines. As discussed above, these lines merge for  $q \rightarrow 0$ . They remain on top of each other if now we let  $N_c \rightarrow \infty$ . On the other hand, if we first take the limit  $N_c \rightarrow \infty$  they remain separated and become linear with opposite slopes. Now letting  $q \rightarrow 0$  does not change the result. Hence the symmetry of the onset magnetic field under  $\kappa \rightarrow -\kappa$ , if we take the large- $N_c$  limit of our neutral baryons and the *anti*-symmetry for the charged baryons.

With these preparations, what can we learn from our holographic result? We know that there is no binding energy in this case, and the onset line simply indicates the  $B$ -dependent baryon mass (at least without meson supercurrent, otherwise the situation is more complicated, as discussed in sec. 6.5). This mass gets larger with increasing magnetic field. In the Walecka model, the only case with increasing mass is the case of charged baryons with  $q$  and  $\kappa$  having opposite sign. Since in the present context a nonzero electric charge is equivalent to the existence of Landau levels, it is interesting to ask whether there is any Landau level structure for our holographic baryons. We know that in the chirally restored phase of the Sakai-Sugimoto model there is indeed a phase transition which has similar properties as a transition into the LLL [145, 121]. In terms of the solution to the equations of motion, the "LLL" phase corresponds to a trivial solution,  $y_\infty = \infty$ . This solution always exists, but in some regions of the parameter space is disfavored compared to a nontrivial solution, interpreted as a phase of higher Landau levels. In the baryonic phase, there is also a trivial solution, namely  $y_\infty = 0$ , see Eqs. (6.50) and (6.51). However, this solution is unphysical because it leads to an infinite baryon density and thus infinite free energy. Although we find several nontrivial solutions in certain parameter regions, the solution which is continuously connected to the solution at the onset is always the energetically preferred one. Hence there is no phase transition within the baryonic phase. This is consistent with the apparent bosonic nature of the holographic large- $N_c$  baryons (see sec. 6.5) because for a Bose condensate at zero temperature we do not expect de Haas-van Alphen oscillations.

Besides the overall tendency of the  $B$ -dependent mass, how about its linear behavior seen in the large- $N_c$  limit of the Walecka model? The holographic results show an approximately linear behavior only for intermediate magnetic fields. For large

fields, a comparison to the Walecka results would only be sensible if the latter included a more elaborate treatment of the anomalous magnetic moment. But also at small magnetic fields our holographic onset line differs from the linear behavior, in fact we find  $\mu_{\text{onset}} = m_q^0 + \text{const} \times b^2 + \dots$ . It would be interesting to compute the onset in other field-theoretical approaches. After all, the Walecka model does not know about dynamical chiral symmetry breaking and thus cannot be expected to show effects from MC and the meson supercurrent, which, as mentioned above, seem to be the driving forces for the  $B$ -dependence of our effective holographic baryon mass. On the other hand, also our holographic approach should be refined for a more meaningful comparison. In particular, a generalization to two flavors is necessary to describe realistic nuclear matter.



# Conclusion

In the main part of this thesis we have investigated equilibrium phases at finite temperature, chemical potential, and magnetic field for one massless flavor in the Nambu–Jona-Lasinio model and the Sakai–Sugimoto model. For small flavor brane separations, the Sakai–Sugimoto model is conjectured to be dual to a (non-local) NJL model. Indeed, we have found intriguing qualitative similarities between both models.

There is an exact equality of the number density at zero temperature of the lowest Landau level in the restored phase of the NJL model and the large magnetic field phase with restored chiral symmetry in the Sakai–Sugimoto model. The higher Landau level phase in the NJL model, however, differs from the small magnetic field phase with restored chiral symmetry in the Sakai–Sugimoto model. For example, there occur no de Haas–van Alphen oscillations in the holographic model. One possible interpretation is that in the holographic model – dual to a strongly coupled gauge theory – there are no quasiparticles and no sharp Fermi surface. Furthermore, the axial current found on the field theory side is also reproduced in the holographic model. In the version of the model discussed here [23], the holographic current reproduces the field-theoretical current only up to a factor of 2. This discrepancy can be resolved by properly implementing the axial anomaly [152], however at the price of losing a consistent thermodynamic description.

Also the phase diagrams in both models share the same qualitative features. The main differences are the order of the phase transitions (first and second order in NJL vs. first order in Sakai-Sugimoto), the saturation of the critical temperature as well as the critical chemical potential at asymptotically large magnetic fields (which only occurs in Sakai-Sugimoto), and the absence of de Haas–van Alphen oscillations of the phase transition line in the Sakai–Sugimoto model.

The main physical effect, first discussed in detail in the holographic context [145], is the nontrivial behavior of the chiral phase transition in a magnetic field at finite quark chemical potential. Somewhat unexpectedly, at sufficiently large chemical potentials and small temperatures and not too large magnetic fields, the effect of inverse magnetic catalysis dominates. We have explained inverse magnetic catalysis in both models by a free energy argument. This argument shows that, even when the magnetic field increases the constituent quark mass (due to the usual magnetic catalysis) and thus increases the condensation energy, it also increases the energy cost for forming a chiral condensate. In particular, in the LLL, where the effect is most pronounced, the cost for overcoming the separation of fermions and anti-fermions due to the chemical potential increases linearly in  $B$ , while the constituent quark mass rises quadratically at small magnetic fields (and  $g > 1$  in the NJL model). It is interesting that at asymptotically large magnetic fields the free energy difference in the Sakai-Sugimoto model resembles the corresponding expression in the weak-coupling limit of the NJL model. In this regime magnetic catalysis is dominant in both models, and the situation is analogous to weak-coupling superconductivity with mismatched Fermi surfaces [51].

This correspondence allowed us to analyze the term describing the costs for forming quark–anti-quark pairs further. Instead of having two fermion species with different Fermi surfaces, say at  $\mu_1$  and  $\mu_2$ , the chemical potential itself separates fermions from anti-fermions, making pairing more costly. The picture that one has in mind is that in order to form the pairs one first has to reshuffle the fermions in the Fermi-seas of both particle species in such a way that both Fermi surfaces agree on a fictitious common energy level. In the case at hand this is the vacuum. For simplicity we restrict to the LLL again. In our case this reshuffling amounts to removing all fermions with  $\varepsilon \in (0, \mu)$  – for each particle we need the energy amount  $\mu/2$  (on average  $\mu$  cost due the chemical potential and  $\mu/2$  gain from the kinetic energy). The density of states is given by the the degeneracy factor per energy level, i.e. for fermions in

a box of volume  $V$  we have to reshuffle

$$V \frac{B}{2\pi^2} \mu \quad (8.1)$$

many times in total, which multiplied by the cost  $\mu/2$  yields exactly the free energy cost for the LLL found in the NJL model as well as in the Sakai–Sugimoto model.

Note, that the degeneracy of states in the LLL can be related to the Euclidean anomaly in two dimensions, which is a topological, and therefore robust result. The magnetic field entering in the LLL only via this degeneracy is the agent for both the catalysis of chiral symmetry breaking as well as the inverse catalysis. On the one hand it increases the number of available partners for particle–anti-particle pairing at the fictitious common energy surface  $\varepsilon = 0$ , on the other hand it increases the separation of particles from anti-particles at finite chemical potential. How strong the magnetic field catalyses chiral symmetry breaking of course depends on the choice of the model and the choice of a specific set of model parameters, e.g. the coupling.

We have included an anisotropic chiral condensate in the Sakai–Sugimoto model, but not in the NJL model. For comparison, it is easy to show that in the holographic calculation the assumption of an isotropic chiral condensate does not change the qualitative features of the phase diagram. One finds that the effects of inverse magnetic catalysis are rather enhanced. On the other hand, including an anisotropic chiral condensate in the NJL model changes the phase diagram drastically [71]. Most notably, there exists a phase with anisotropic chiral condensate even at  $B = 0$ ; in the Sakai–Sugimoto model,  $B \neq 0$  is necessary for having such a phase. Moreover, this phase inevitably has a finite quark density. In order to realize this in the holographic model at  $B = 0$  one needs solitonic baryon sources which are related to Skyrmions and thus rather different from "baryons" in the NJL model which consist of dislocated quarks.

We have discussed baryonic matter in a magnetic field, using the deconfined geometry of the Sakai–Sugimoto model where baryons are introduced by D4-branes wrapped on the internal  $S^4$ . Our main focus has been the onset of baryonic matter and its effect on the chiral phase transition at zero temperature and finite chemical potential.

The critical chemical potential for the onset of holographic baryonic matter increases monotonically with the magnetic field, saturating at a finite value for asymptotically large magnetic fields. For subcritical chemical potentials the system is in

the mesonic phase with a meson supercurrent in the direction of the magnetic field. Because of the axial anomaly, the system has non-vanishing baryon number for all nonzero magnetic fields and chemical potentials. Due to the presence of the supercurrent the baryon onset is significantly "delayed" to larger chemical potentials. In contrast to real-world baryonic matter, the onset is a second-order phase transition, because of the absence of binding energy. Besides the holographic study, we have computed the onset also in the Walecka model, a field-theoretical model for dense nuclear matter where the onset is a first-order transition. Within this model, we have demonstrated that the onset depends strongly on the electric charge and the anomalous magnetic moment of the baryons. In most cases, however, the magnetic field favors baryonic matter because it decreases the baryon mass, although for neutral baryons it also decreases the (modulus of the) binding energy. In the holographic calculation there is no binding energy and the baryon mass is increased by the magnetic field. Our results indicate that this increase is closely related to the effect of magnetic catalysis.

With baryonic matter, chiral symmetry is only restored for sufficiently large magnetic fields, where we have found that baryons play no role. For small magnetic fields there is a transition from mesonic to baryonic matter but no subsequent transition to quark matter. This enforces the unusual effect of inverse magnetic catalysis: the magnetic field now *restores* chiral symmetry for any given chemical potential larger than, roughly speaking, the one where the baryon onset line and the chiral phase transition line meet in a critical endpoint, see fig. 6.9.

As our comparison with the Walecka model has shown, one has to be very careful with drawing conclusions from the holographic results for the QCD phase structure and the interior of neutron stars, where the extreme conditions studied here might be realized. Most importantly, our holographic calculation has been restricted to the  $N_c \rightarrow \infty$  limit, and there are indications that large- $N_c$  nuclear matter is very different from real nuclear matter. Therefore, generalizations to finite  $N_c$  would be very interesting, as it has been done for instance in related D3/D7 models [28]. On the other hand, in certain aspects our approach seems to be more realistic than widely used models of dense matter. This is understandable since in the NJL model there are no baryons; baryon number is only generated by deconfined quarks. In the Sakai-Sugimoto model, however, baryons are clearly distinct from a set of  $N_c$  deconfined quarks. Furthermore, the Walecka does not incorporate chiral symmetry breaking

---

dynamically and therefore exhibits no magnetic catalysis.

It would be interesting to extend our study to more than one flavor in order to describe more realistic baryonic matter. Moreover, one might include superfluidity of nuclear matter, as suggested for the present model in ref. [149]. In the Sakai-Sugimoto model as well as in bottom-up AdS/QCD approaches, it has also been suggested that – even for vanishing magnetic field – the ground state breaks rotational and/or translational invariance at sufficiently large baryon densities [55, 50, 138, 19]. It would be interesting to study the effect of such phases on our phase diagram. We should also keep in mind that the quark matter phase considered here is not in a state expected from QCD – cold and sufficiently dense quark matter is a color superconductor in the CFL phase. This phase also breaks chiral symmetry at asymptotically large  $\mu$ , like our holographic baryons, but the mechanism is very different and heavily relies on the fact that  $N_c = 3$ .

Another phenomenon that was not included in our discussion is the so-called chiral shift [90, 91], a chiral asymmetry in the Fermi surfaces of right- and left-handed charged fermions induced by a magnetic field. It would be interesting to discuss its effect on the chiral phase transition and thus on inverse magnetic catalysis. However, the chiral shift is related to the Fock exchange terms, which are suppressed at large  $N_c$ . Therefore, this effect is difficult to study in a holographic model where  $N_c \rightarrow \infty$  is necessary for the validity of the supergravity approximation.



## A.1 Chiral Symmetry of the NJL Lagrangian

From the transformation properties of the fermions

$$\psi \rightarrow e^{i\alpha} \psi, \quad (\text{A.1})$$

$$\psi \rightarrow e^{-i\alpha^j \beta^j} \psi, \quad (\text{A.2})$$

$$\psi \rightarrow e^{-i\gamma^5 \alpha^j \beta^j} \psi, \quad (\text{A.3})$$

one first concludes

$$\bar{\psi} \rightarrow \bar{\psi} e^{-i\alpha} \psi, \quad (\text{A.4})$$

$$\bar{\psi} \rightarrow \bar{\psi} e^{i\alpha^j \beta^j} \psi, \quad (\text{A.5})$$

$$\bar{\psi} \rightarrow \bar{\psi} e^{-i\gamma^5 \alpha^j \beta^j} \psi, \quad (\text{A.6})$$

where we used  $\bar{\psi} = \psi^\dagger \gamma^0$  and  $\{\gamma^\mu, \gamma^5\} = 0$ . The symmetry of the Lagrangian with respect to  $U(1)_V$  is trivial.

In case of  $SU(2)_V$  it is also obvious for all the isoscalar spinor-bilinears. For isovector bilinear terms we have for any  $g \in SU(2)_V$  and any element  $\Gamma$  of the Dirac algebra

$$\bar{\psi} \Gamma g^{-1} \sigma^j g \psi = \bar{\psi} \Gamma R^i_j (g^{-1}) \sigma^j \psi, \quad (\text{A.7})$$

where the matrix  $R(g)$  belongs to the adjoint representation of  $SU(2)$ , hence  $R$  is an  $SO(3)$ -matrix. Since the isovector terms only appear in interior products, which are invariant under  $SO(3)$  the assertion is proven.

The case of the axial transformations is more difficult to show. For isoscalar vector as well as pseudo-vector bilinears invariance is obvious, since there is, apart from the  $\gamma^0$  in  $\bar{\psi}$ , a further factor proportional to  $\gamma^\mu$ , which flips the overall sign in the exponent in equation (A.6). By a similar argument scalar, pseudo-scalar, as well as tensor bilinears are not invariant under axial transformations irrespective of the isospin representation. That is precisely the reason why chiral symmetry forbids fermion mass terms. However, in the interaction Lagrangian we find scalar and pseudo-scalar terms squared. We use the abbreviations  $\sigma := \bar{\psi}\psi$  and  $\pi^i = \bar{\psi}i\gamma^5\sigma^i\psi$  as in the main text, which transform as

$$\sigma \rightarrow \sigma \cos \alpha - \hat{\alpha} \cdot \pi \sin \alpha, \quad (\text{A.8})$$

$$\pi^i \rightarrow \pi^i - \hat{\alpha}^i \hat{\alpha} \cdot \pi + \hat{\alpha}^i (\hat{\alpha} \cdot \pi) \cos \alpha + \hat{\alpha}^i \sigma \sin \alpha, \quad (\text{A.9})$$

where  $\alpha = \sqrt{\alpha^i \alpha^i}$  and  $\hat{\alpha}^i = \alpha^i / \alpha$  denotes a unit vector. Therefore, the interaction terms transform as

$$\sigma^2 \rightarrow \sigma^2 \cos \alpha + (\hat{\alpha} \cdot \pi)^2 \sin^2 \alpha - \sigma \hat{\alpha} \cdot \pi \sin 2\alpha, \quad (\text{A.10})$$

$$\pi^2 \rightarrow \pi^2 + \sigma^2 \sin^2 \alpha - (\hat{\alpha} \cdot \pi)^2 \sin^2 \alpha + \sigma \hat{\alpha} \cdot \pi \sin 2\alpha, \quad (\text{A.11})$$

and in the sum all unwanted terms cancel. As a general rule, in order to ensure chiral invariance, for each isoscalar Dirac-bilinear squared there has to be a squared isovector term which has the dual Dirac algebra structure. Likewise, in order to additionally make the theory invariant with respect to  $U(1)_A$ , for each Dirac-bilinear squared one would need a dual Dirac-bilinear squared in the same isospin representation.

## A.2 Noether's theorem

We ask the question, how the action varies with respect to (infinitesimal) transformations of the field content together with rigid coordinate transformations. In terms of fibre bundle theory, the total variation of the field can be split into an internal transformation, i.e. a change within the fibre over some point, and a change of this point in the base manifold:  $\delta\phi = \alpha\Delta\phi + \delta_x$

$$\delta\phi = \Delta\phi + \delta x^\mu \partial_\mu \phi. \quad (\text{A.12})$$



For the total variation of the action we find

$$\delta I = \int d^4x \left( \frac{\partial \mathcal{L}}{\partial \phi} - \partial_\mu \frac{\partial \mathcal{L}}{\partial \partial_\mu \phi} \right) \Delta \phi + \partial_\mu \left( \frac{\partial \mathcal{L}}{\partial \partial_\mu \phi} \Delta \phi \right) + \partial_\mu \mathcal{L} \delta x^\mu = \quad (\text{A.13})$$

$$= \int d^4x \partial_\mu \left( \frac{\partial \mathcal{L}}{\partial \partial_\mu \phi} \delta \phi \right) - \partial_\mu \left[ \left( \frac{\partial \mathcal{L}}{\partial \partial_\mu \phi} \partial_\nu \phi - \delta_\nu^\mu \mathcal{L} \right) \delta x^\nu \right], \quad (\text{A.14})$$

where we used the Euler–Lagrange equation to get from the first to the second line. The term inside the parenthesis is called the canonical stress-energy tensor  $\Theta^\mu{}_\nu$ . The full expression has vanishing divergence and constitutes a conserved current. In physics applications one usually splits off the infinitesimal constant parametrizing the transformation appearing in  $\delta \phi$  and  $\delta x$ , e.g. the parameter  $\alpha$  in the preceding section. Due to the continuity equation  $\partial_\mu J^\mu = \partial_t J^0 + \nabla \cdot J = 0$  we can conclude that there exists a charge, which is constant in time

$$Q := \int_\Sigma d^3x J^0, \quad (\text{A.15})$$

$$\frac{d}{dt} Q = \int_\Sigma d^3x \partial_t J^0 = - \int_\Sigma d^3x \nabla \cdot J = - \int_{\partial \Sigma} d^a A \nabla \cdot J^a = 0, \quad (\text{A.16})$$

provided suitable fall-off conditions for  $J^a$ . The spatial integral is over the constant time hypersurface  $\Sigma$  and the surface integral over its boundary denoted by  $\partial \Sigma$ . In general this criterion is not satisfied and the charge is ill-defined. However, the commutator of charges, i.e. the so-called current algebra is well defined.

### A.3 Imaginary time formalism and thermal field theory

We follow the introduction to thermal field theory given in [159]. In the course of setting up the partition function for fermions one first concludes that the trace over some operator  $A$  in a system with one state that is either occupied  $|1\rangle$  or empty  $|0\rangle$  can be expressed using Berezin's integration theory of Grassmann variables (here denoted by  $\eta$ ) by

$$\text{tr} A = \int d\eta^* d\eta e^{-\eta^* \eta} \langle -\eta | A | \eta \rangle. \quad (\text{A.17})$$

Using fermionic ladder operators  $\{a, a^\dagger\} = 1$  a general fermionic state in the Hilbert space is described by

$$|\eta\rangle = e^{-\eta a^\dagger} |0\rangle = |0\rangle - \eta |1\rangle \quad (\text{A.18})$$

$$\Rightarrow \langle \eta | = \langle 0 | - \eta^* \langle 1 | = \langle 0 | e^{-a \eta^*}. \quad (\text{A.19})$$

For the norm of the general state we find

$$\langle \eta | \eta \rangle = 1 + \eta^* \eta = e^{\eta^* \eta}, \quad (\text{A.20})$$

where we used

$$\eta \eta^* = -\eta^* \eta, \quad \Rightarrow f(\eta, \eta^*) = \alpha + \beta \eta + \gamma \eta^*. \quad (\text{A.21})$$

Hence unity should be given by

$$\int d\eta^* d\eta e^{-\eta^* \eta} |\eta\rangle \langle \eta|, \quad (\text{A.22})$$

which can be checked explicitly by using the rules of integration of Grassmann variables. For these we demand that linearity and translational invariance, then we deduce

$$\int d\eta f(\eta + \zeta) = \int d\eta f(\eta) \quad (\text{A.23})$$

$$\int d\eta A f(\eta) + B g(\eta) = \int d\eta A f(\eta) + \int d\eta B g(\eta) \quad (\text{A.24})$$

$$\Rightarrow \int d\eta f(\eta + \zeta) \equiv \int d\eta [\alpha + \beta(\eta + \zeta)] \quad (\text{A.25})$$

$$= (\alpha + \beta\zeta) \int d\eta + \beta \int d\eta \eta = \quad (\text{A.26})$$

$$\stackrel{!}{=} \int d\eta f(\eta) = \alpha \int d\eta + \beta \int d\eta \eta \quad (\text{A.27})$$

$$\Rightarrow \int d\eta = 0, \quad (\text{A.28})$$

and we normalize

$$\int d\eta \eta = 1, \quad (\text{A.29})$$

hence this so called Berezin integration looks like differentiation. Finally we find equation (A.17) by inserting the Berezin representation of unity in  $\text{Tr}A = \langle 0|A|0\rangle + \langle 1|A|1\rangle$

$$\text{Tr}A = \langle 0|A|0\rangle + \langle 1|A|1\rangle = \int d\eta^* d\eta e^{-\eta^* \eta} (\langle \eta|A|0\rangle - \eta \langle \eta|A|1\rangle), \quad (\text{A.30})$$

from which equation (A.17) follows using  $\eta \langle \eta| = \langle -\eta|$  and switching integration variables  $\eta \rightarrow -\eta, \eta^* \rightarrow -\eta^*$  for the first term in parenthesis.

We are ultimately interested in  $Z = \text{Tr} \exp(-\beta H)$ . So we use  $A = \exp(-\beta H)$  and compute the transition function  $\langle -\eta | \exp(-i\Delta t H) | \eta \rangle$ , i.e. we identify inverse temperature  $\beta = 1/T$  with the imaginary time interval  $\Delta\tau = i\Delta t$ . Since we are interested in the transition from a state into its negative we can realize this situation by compactifying the imaginary time interval to an  $S^1$  with circumference  $1/T$  and imposing antiperiodic boundary conditions on the fermions. We start from

$$\text{tr} e^{-\beta H} = \int d\eta^* d\eta e^{-\eta^* \eta} \langle -\eta | e^{-\Delta\tau H} | \eta \rangle, \quad (\text{A.31})$$

and first do some relabeling

$$\text{tr} e^{-\beta H} = \int d\eta_N^* d\eta_0 e^{-\eta_N^* \eta_0} \langle \eta_N | e^{-\Delta\tau H} | \eta_0 \rangle \Big|_{\eta_N = -\eta_0}. \quad (\text{A.32})$$

This we do because we will now split the Euclidean time interval into  $N$  pieces  $\Delta\tau_i = \Delta\tau/N$

$$\text{tr} e^{-\beta H} = \int d\eta_N^* d\eta_0 e^{-\eta_N^* \eta_0} \langle \eta_N | e^{-\Delta\tau_N H} \dots e^{-\Delta\tau_1 H} | \eta_0 \rangle \Big|_{\eta_N = -\eta_0}, \quad (\text{A.33})$$

and insert unity from equation (A.22)  $N-1$  times in between the exponential factors which yields

$$\text{tr} e^{-\beta H} = \int d\eta_N^* d\eta_0 e^{-\eta_N^* \eta_0} \prod_{i=1}^{N-1} d\eta_i^* d\eta_i e^{-\Delta\tau_i H(\eta_i^*, \eta_{i-1}) - \eta_i^* (\eta_i - \eta_{i-1})} \Big|_{\eta_N = -\eta_0}. \quad (\text{A.34})$$

Next we again relabel a bit:  $\eta_i \rightarrow \eta_{i+1}$

$$\text{tr} e^{-\beta H} = \int \prod_{i=1}^N d\eta_i^* d\eta_i e^{-\Delta\tau_i H(\eta_i^*, \eta_i) - \eta_i^* (\eta_{i+1} - \eta_i)} \Big|_{\eta_{N+1} = -\eta_1} \quad (\text{A.35})$$

After performing the limit  $N \rightarrow \infty$  and using

$$\mathcal{D}\eta^* \mathcal{D}\eta := \lim_{N \rightarrow \infty} \prod_{i=1}^N d\eta_i^* d\eta_i, \quad (\text{A.36})$$

$$\lim_{N \rightarrow \infty} \eta_i^* \frac{\eta_{i+1} - \eta_i}{\Delta\tau} \Delta\tau_i = \eta^* \frac{\partial}{\partial\tau} \eta d\tau, \quad (\text{A.37})$$

$$\lim_{N \rightarrow \infty} \sum_{i=1}^N f_i \Delta\tau_i = \int d\tau f(\tau), \quad (\text{A.38})$$

we find for the partition function

$$Z = \int_{\eta(\beta)=-\eta(0)} \mathcal{D}\eta^* \mathcal{D}\eta e^{-\int_0^\beta d\tau (\eta^* \frac{\partial}{\partial \tau} \eta + H(\eta^*, \eta))}. \quad (\text{A.39})$$

This can be easily promoted to a field theory of fermions

$$Z = \int_{\psi(\beta)=-\psi(0)} \mathcal{D}\psi^\dagger \mathcal{D}\psi e^{-\int_0^\beta d\tau \int d^3x (\psi^\dagger \frac{\partial}{\partial \tau} \psi + \mathcal{H}(\psi^\dagger, \psi))}. \quad (\text{A.40})$$

Assuming that the only time derivatives acting on the fermions appear in the kinematic part of the Lagrangian

$$\mathcal{L} = \bar{\psi} i \gamma^0 \partial_0 \psi + \dots \rightarrow \mathcal{L}_E = -\psi^\dagger \partial_\tau \psi + \dots \quad (\text{A.41})$$

the Euclidean momentum conjugate to  $\psi$  is given by

$$\Pi_\psi^E = \frac{\partial \mathcal{L}_E}{\partial \partial_\tau \psi} = -\psi^\dagger. \quad (\text{A.42})$$

Since the Lagrangian can be written as

$$\mathcal{L}_E = \Pi_\psi^E \partial_\tau \psi - \mathcal{H}(\Pi_\psi^E, \psi) \Big|_{\Pi_\psi^E = -\psi^\dagger}, \quad (\text{A.43})$$

the partition function for fermions reads

$$Z(\beta) = \int_{\psi(\beta)=-\psi(0)} \mathcal{D}\psi^\dagger \mathcal{D}\psi e^{\int_0^\beta d\tau \int d^3x \mathcal{L}_E}, \quad (\text{A.44})$$

which is the Euclidean path integral with anti-periodic boundary conditions. The Euclidean Lagrangian is defined by  $\mathcal{L}_E := \mathcal{L}(t \rightarrow -i\tau)$ . We might think of  $\mathcal{L}$  as the negative of the sum of kinetic and potential energy  $-T - V$ . Whereas in the vacuum theory the path integral becomes increasingly oscillatory away from the classical path, the Euclidean path integral is damped for larger energy, as is the Boltzmann (weighting) factor  $\exp(-\beta E)$ .

Note that using the pairs of variables  $(\psi^\dagger, \psi)$  and  $(\bar{\psi}, \psi)$  is unitarily equivalent and we will deliberately switch between both cases.

### 1PI effective action

In analogy with zero temperature quantum field theory we define the functional

$$W_E[J] = \ln Z[\beta, J], \quad (\text{A.45})$$

$$Z[\beta, J] = \int_{\psi(\beta)=-\psi(0)} \mathcal{D}\psi^\dagger \mathcal{D}\psi e^{\int_0^\beta d\tau \int d^3x (\mathcal{L}_E + \psi^\dagger J + J^\dagger \psi)}, \quad (\text{A.46})$$

where we introduced Schwinger sources  $J$  for the fermions.  $W_E[J]$  is the generating functional for connected  $n$ -point correlation functions

$$\langle \psi_1 \cdots \psi_n^\dagger \rangle_{\text{connected } n\text{-point}} = \frac{\delta}{\delta J_1^\dagger} \cdots \frac{-\delta}{\delta J_n} W[J] \Big|_{J=0=J^\dagger}. \quad (\text{A.47})$$

From that one obtains the generating functional for one-particle irreducible (1PI)  $n$ -point functions a.k.a. the effective action by a Legendre transform

$$\Gamma_E[\psi_c^\dagger, \psi_c] = W_E[J] - \int d\tau \int d^3x \psi_c^\dagger J + J^\dagger \psi_c, \quad (\text{A.48})$$

$$\text{with } \psi_c^\dagger = -\frac{\delta W_E[J]}{\delta J}, \quad \psi_c = \frac{\delta W_E[J]}{\delta J^\dagger}, \quad (\text{A.49})$$

that is a functional of  $\psi_c^\dagger$  and  $\psi_c$ , which are the vacuum expectation values of the fields  $\psi^\dagger$  and  $\psi$  respectively in the presence of external Grassmann sources. Conversely, in the absence of external sources

$$\frac{\delta \Gamma_E}{\delta \psi_c} = 0 = \frac{\delta \Gamma_E}{\delta \psi_c^\dagger}, \quad (\text{A.50})$$

which are the field equation, determining the values of  $\psi_c$  and  $\psi_c^\dagger$ . The formulae developed so far allow us to take over the zero temperature results for the 1PI effective action obtained in [108] and promote it to the finite temperature case by using the following substitutions

$$\tau = it, \quad (\text{A.51})$$

$$\Gamma_E[\psi_c^\dagger, \psi_c] = i\Gamma[\bar{\psi}_c, \psi_c]. \quad (\text{A.52})$$

Furthermore in front of any term involving the logarithm of the functional determinant of the boson propagator in Eq. (2.14) of Ref. [108] replace the factor 1/2 by

–1 and finally replace  $iD^{-1}$  by the operator  $S^{-1} := \partial_\tau + h_D$ , where  $h_D$  denotes the single particle Hamilton–Dirac operator for free fermions

$$h_D = \alpha^i \frac{1}{i} \nabla_i + \gamma^0 M, \quad (\text{A.53})$$

with  $\alpha^i = \gamma^0 \gamma^i$  and where  $M$  is some mass operator<sup>1</sup>.

Since thermodynamics is dealing with stationary situations, we can immediately expand the fermion wavefunctions  $\psi$  into eigenfunctions of  $\partial_\tau$

$$\psi(\tau, x) = \sum_{n=-\infty}^{\infty} e^{i\omega_n \tau} \psi_n(x), \omega_n = (2n + 1)\pi T, \quad (\text{A.54})$$

where the discreteness and the form of the so called fermionic Matsubara frequencies  $\omega_n$  stems from the anti periodic boundary conditions on the finite imaginary time interval  $1/T$ . Assume, that we found a basis  $\psi_{n,\{m\}}$  that also diagonalizes the single particle Hamilton–Dirac operator with eigenvalues  $\varepsilon_{\{m\}}$ , then we can write the operator  $S^{-1}$  in this spectral decomposition as

$$S^{-1} = \frac{i\omega_n + \varepsilon_{\{m\}}}{T}, \quad (\text{A.55})$$

where we used

$$\int_0^\beta d\tau e^{i\omega_n \tau} = \frac{1}{T} \delta_{n,0}. \quad (\text{A.56})$$

## Chemical potential

Provided our theory has conserved charges, e.g. particle number  $\int d^3x \psi^\dagger \psi$ , we may introduce the conjugate chemical potential  $\mu$  by the substitution  $\mathcal{H} \rightarrow \mathcal{H} - \mu \mathcal{N}$ , where  $\mathcal{N}$  denotes the charge density, e.g.  $\psi^\dagger \psi$ . In our spectral decomposition above this amounts to the substitution  $\varepsilon_{\{m\}} \rightarrow \varepsilon_{\{m\}} - \mu$

## Matsubara sum

In our calculations we have to deal with the sum over the Matsubara frequencies at several places in the main text. Most notably for the effective potential (which we

<sup>1</sup>Here we might think of some vacuum expectation value of bosons coupled via Yukawa coupling or external gauge fields apart from the bare fermion mass term.

will also call grand canonical potential or thermodynamic potential) given by

$$\Omega = -\frac{T}{V}\Gamma_E \quad (\text{A.57})$$

we need to evaluate the so called "trace-log" term

$$\text{Tr} \ln \frac{i\omega_n + \varepsilon_{\{m\}} - \mu}{T}. \quad (\text{A.58})$$

First we rewrite the logarithm using an integral representation

$$\ln \frac{i\omega_n + \varepsilon_{\{m\}}}{T} = \int_0^{(\varepsilon_{\{m\}} - \mu)/T} dx \frac{1}{\frac{i\omega_n}{T} + x} + \text{const.} \quad (\text{A.59})$$

The constant terms are irrelevant for the system's dynamics and so will be omitted in the following. Now we deal with the Matsubara sum. First we simply state that it is the sum over the residue of some complex function  $f(z)$  and use Cauchy's integral formula

$$\sum_n \frac{1}{\frac{i\omega_n}{T} + x} = \sum_n \text{Res}(f, z = \frac{i\omega_n}{T}) = \frac{1}{2\pi i} \sum_n \oint_{C_n} f(z), \quad (\text{A.60})$$

where the  $C_n$  denote curves enclosing the points  $z = z_n := i(2n+1)\pi$ . Suppose that  $f$  has simple poles at  $z_n$  and that  $f$  can be written as  $f(z) = \phi(z)/\rho(z)$  with  $\rho(z_n) = 0$  and  $\rho'(z_n) \neq 0$  then the residue is given by  $\text{Res}(f, z_n) = \phi(z_n)/\rho'(z_n)$ . The simplest function available with zeros at  $z_n$  is  $\rho(z) = 2\cosh(z/2)$ , hence  $\rho'(z) = \sinh(z/2)$ . Since  $f(z) = 1/(z+x) = \phi(z)/\sinh(z/2)$ ,  $\phi(z) = \sinh(z/2)/(z+x)$ . Hence,

$$\sum_n \frac{1}{\frac{i\omega_n}{T} + x} = \frac{1}{2\pi i} \sum_n \oint_{C_n} f(z) = \quad (\text{A.61})$$

$$= -\frac{1}{2\pi i} \sum_n \oint_{C_{-x}} \frac{\tanh(z/2)}{2(z+x)} = \frac{1}{2} \tanh(x/2). \quad (\text{A.62})$$

Plugging this back into the integral formula for the logarithm yields

$$\sum_n \ln \frac{i\omega_n + \varepsilon_{\{m\}} - \mu}{T} = \ln \cosh \frac{\varepsilon_{\{m\}} - \mu}{2T}. \quad (\text{A.63})$$

In all situations relevant for this work we will deal with a spectrum of eigenvalues that is  $\mathbb{Z}_2$ -symmetric, i.e.  $\varepsilon_{\{m\}} = e\varepsilon_{\{\tilde{m}\}}$  with  $\varepsilon_{\{\tilde{m}\}} \geq 0$  and  $e = \pm 1$ . One usually refers to the wavefunctions with  $e = 1$  or  $e = -1$  as fermions or anti fermions respectively. We use that to rewrite the Matsubara sum as

$$\sum_n \ln \frac{i\omega_n + \varepsilon_{\{m\}} - \mu}{T} = \frac{\varepsilon_{\{\tilde{m}\}} - e\mu}{2T} + \ln \left( 1 + e^{-\frac{\varepsilon_{\{\tilde{m}\}} - e\mu}{T}} \right) \quad (\text{A.64})$$

## A.4 Chern–Simons 5-form

The  $U(N_f)$  Chern–Simons 5-form is decomposed with respect to the factorization of the gauge group  $U(N_f) \simeq SU(N_f) \times U(1)$  as

$$\begin{aligned} \mathcal{A} &= A + 1\hat{A}, \\ Q_5(\mathcal{A}, \mathcal{F}) &= \text{Tr} \left( \mathcal{A}\mathcal{F} - \frac{1}{2}\mathcal{A}^3\mathcal{F} + \frac{1}{10}\mathcal{A}^5 \right) = \\ &= Q_5(A, F) + \hat{A}\text{Tr}F^2 + N_f\hat{A}\hat{F}^2 + 2\hat{F}\text{Tr}AF - \frac{1}{2}\hat{A}\text{Tr}A^2F, \end{aligned} \quad (\text{A.65})$$

where we used

$$\begin{aligned} \text{tr}A^{2n} &= 0, \quad n \in \mathbb{N}, \\ \text{tr}F &= 0 = \text{tr}A, \\ \hat{A}^2 &= 0. \end{aligned}$$

Using  $F = dA + A^2$  we find

$$Q_5(\mathcal{A}, \mathcal{F}) = Q_5(A, F) + 3\hat{A}\text{Tr}F^2 + N_f\hat{A}\hat{F}^2 + d \left[ \hat{A} \left( 2AF - \frac{1}{2}A^3 \right) \right]. \quad (\text{A.66})$$

In the case of two flavors one can easily show that  $Q_5(A, F) = 0$  using  $\text{Tr}(i^i j^j k^k) = i/4\epsilon^{ijk}$ ,  $\text{Tr}(i^i j^j k^k l^l) = 1/8(\delta^{ij}\delta^{kl} - \delta^{ik}\delta^{jl} + \delta^{jk}\delta^{il})$  and  $\text{Tr}(i^i j^j k^k l^l m^m) \propto \epsilon^{ijklm} \pm \text{perm.}$

## A.5 Approximations close to the baryon onset

### Vanishing B

In this appendix we derive eq. (6.60), i.e., the behavior of the baryon density  $n_4$  close to the onset at vanishing magnetic field. For  $b = 0$  and with  $y_\infty = 3by_\infty^{(0)}$ , eqs. (6.50) and (6.51) can be written as

$$(u_c^{(0)})^{3/2} y_\infty^{(0)} = \int_1^\infty \frac{u^{3/2} du}{\sqrt{u^8 - 1 + \frac{n_4^2}{(u_c^{(0)})^5} (u^3 - \frac{8}{9})}}, \quad (\text{A.67})$$

$$\frac{(u_c^{(0)})^{1/2} \ell}{2} = \sqrt{1 + \frac{8}{9} \frac{n_4^2}{(u_c^{(0)})^5}} \int_1^\infty \frac{du}{u^{3/2} \sqrt{u^8 - 1 + \frac{n_4^2}{(u_c^{(0)})^5} (u^3 - \frac{8}{9})}}. \quad (\text{A.68})$$



Furthermore, from (6.55) we find

$$n_4(b=0) = \frac{\mu - m_q^{(0)}}{y_\infty^{(0)}}. \quad (\text{A.69})$$

For chemical potentials close to, but above, the onset chemical potential  $\mu_{\text{onset}}^{(0)} = m_q^{(0)}$ , the numerical results suggest the ansatz

$$u_c^{(0)} \simeq u_{c,\text{onset}}^{(0)} + \alpha\epsilon, \quad y_\infty^{(0)} \simeq y_{\infty,\text{onset}}^{(0)} + \beta\epsilon, \quad (\text{A.70})$$

with  $\alpha, \beta$  to be determined, and

$$\epsilon \equiv \mu - \mu_{\text{onset}}^{(0)}. \quad (\text{A.71})$$

Inserting this ansatz into eq. (A.69) yields

$$n_4 \simeq \frac{3 + \alpha}{3y_{\infty,\text{onset}}^{(0)}} \epsilon. \quad (\text{A.72})$$

To compute  $\alpha$  it is sufficient to consider eq. (A.68), where  $\beta$  does not appear. We are interested in the terms linear in  $\epsilon$ . The linear term on the left-hand side is easily obtained. On the right-hand side, we subtract the constant term and neglect the quadratic term in the square root in front of the integral. If our ansatz is correct, the integral then must yield a linear term but, as written, also yields terms of higher order in  $\epsilon$ ,

$$-\frac{\alpha\ell}{4(u_{c,\text{onset}}^{(0)})^{1/2}} \epsilon \simeq \int_1^\infty du \left[ \frac{1}{u^{3/2} \sqrt{u^8 - 1 + v^2 \epsilon^2 (u^3 - \frac{8}{9})}} - \frac{1}{u^{3/2} \sqrt{u^8 - 1}} \right]. \quad (\text{A.73})$$

Here we have abbreviated

$$v \equiv \frac{3 + \alpha}{3y_{\infty,\text{onset}}^{(0)} (u_{c,\text{onset}}^{(0)})^{5/2}}. \quad (\text{A.74})$$

Let us for the following arguments denote the integral in eq. (A.73) by  $\mathcal{I}$ . One can check numerically that  $\mathcal{I}$  is indeed linear in  $\epsilon$  for small  $\epsilon$ . Obviously, we cannot proceed by naively expanding the integrand in  $\epsilon$  since this procedure would miss the linear term. Instead, we employ the following trick. Neglecting higher order terms,  $\mathcal{I}$  divided by  $\epsilon$  should not depend on  $\epsilon$  anymore, i.e.,  $\frac{\partial \mathcal{I}}{\partial \epsilon} \simeq 0$ . We evaluate this

equation by first rewriting the derivative with respect to  $\epsilon$  as a derivative with respect to  $u$ ,

$$\frac{\partial}{\partial \epsilon} \frac{1}{\sqrt{u^8 - 1 + v^2 \epsilon^2} (u^3 - \frac{8}{9})} = \frac{2\epsilon v^2 (u^3 - \frac{8}{9})}{u^2 (8u^5 + 3v^2 \epsilon^2)} \frac{\partial}{\partial u} \frac{1}{\sqrt{u^8 - 1 + v^2 \epsilon^2} (u^3 - \frac{8}{9})}. \quad (\text{A.75})$$

Then, with partial integration we obtain

$$\frac{\mathcal{I}}{\epsilon} \simeq -\frac{v}{12} - 2\epsilon v^2 \int_1^\infty du \frac{1}{\sqrt{u^8 - 1 + v^2 \epsilon^2} (u^3 - \frac{8}{9})} \frac{\partial}{\partial u} \frac{u^3 - \frac{8}{9}}{u^{7/2} (8u^5 + 3v^2 \epsilon^2)}, \quad (\text{A.76})$$

where the first term on the right-hand side is the boundary term. Now the left-hand side and the boundary term are constant in  $\epsilon$  while the second term on the right-hand side is linear in  $\epsilon$  and can thus be dropped (the integral is finite and yields a term constant in  $\epsilon$ , but no  $\epsilon^{-1}$  term). Consequently, we have arrived at the very simple result  $\mathcal{I} = -\frac{v}{12}\epsilon$  which can be confirmed numerically and which we insert into eq. (A.73). The result is

$$\alpha = \frac{3}{9y_{\infty, \text{onset}}^{(0)} (u_{c, \text{onset}}^{(0)})^{2\ell - 1}}. \quad (\text{A.77})$$

With the same trick eq. (A.67) can be evaluated to obtain  $\beta$ . Here we are only interested in the baryon density for which we insert eq. (A.77) into eq. (A.72). With  $u_{c, \text{onset}}^{(0)}$  and  $y_{\infty, \text{onset}}^{(0)}$  from Eqs. (6.43) and (6.44) we obtain the final result given in eq. (6.60) in the main text.

## Asymptotically large B

Here we derive eq. (6.64), i.e. the behavior of the usual baryon density  $n_4$  close to the onset at asymptotically large magnetic fields. In this case, due to the supercurrent, the onset does not occur at the baryon mass but at twice the baryon mass,  $\mu_{\text{onset}}^{(\infty)} = 2m_q^{(\infty)}$ , where  $m_q^{(\infty)} = u_{c, \text{onset}}^{(\infty)}/3$  denotes the (dimensionless) constituent quark mass in a baryon at  $b \rightarrow \infty$ . As in the previous subsection, we first need to compute  $y_\infty$  and  $u_c$ . With  $y_\infty \rightarrow \infty$  for  $b \rightarrow \infty$  we conclude from eq. (6.55) that

$$n_4^{(\infty)} = \frac{3b}{2} \left( \mu - \frac{2u_c^{(\infty)}}{3} \right), \quad (\text{A.78})$$

and thus we can write Eq. (6.50) as

$$\frac{\ell(u_c^{(\infty)})^{1/2}}{2} = \sqrt{1 - \left(\frac{n_4^{(\infty)}}{3bu_c^{(\infty)}}\right)^2} \int_1^\infty \frac{du}{u^{3/2} \sqrt{u^5 - 1 + \left(\frac{n_4^{(\infty)}}{3bu_c^{(\infty)}}\right)^2}}. \quad (\text{A.79})$$

This single equation can now be used to determine the behavior of  $u_c^\infty$  at the onset. Again, as for  $b = 0$ , the numerical result suggests the ansatz

$$u_c^{(\infty)} \simeq u_{c,\text{onset}}^\infty + \tilde{\alpha}\tilde{\epsilon}, \quad \tilde{\epsilon} \equiv \mu - \mu_{\text{onset}}^{(\infty)} \quad (\text{A.80})$$

with  $\tilde{\alpha}$  to be determined. Inserting eq. (A.80) into eq. (A.78) yields

$$n_4^{(\infty)} \simeq \frac{3b}{2}\tilde{v}\tilde{\epsilon}, \quad \tilde{v} \equiv 1 - \frac{2\tilde{\alpha}}{3}. \quad (\text{A.81})$$

It is obvious that the left-hand side of eq. (A.79) has a linear term in  $\tilde{\epsilon}$ . For the right-hand side, however, we need to apply a similar trick as in the previous appendix to extract the linear term. We write the linear terms of eq. (A.79) as

$$\frac{\ell\tilde{\alpha}\tilde{\epsilon}}{4(u_{c,\text{onset}}^{(\infty)})^2} = \left[ \frac{\partial}{\partial\tilde{\epsilon}} \int_1^\infty \frac{du}{\sqrt{u^5 - 1 + \frac{\tilde{v}^2\tilde{\epsilon}^2}{4(u_{c,\text{onset}}^{(\infty)})^2}}} \right]_{\tilde{\epsilon}=0} \tilde{\epsilon}. \quad (\text{A.82})$$

Now, analogously to eq. (A.75) we rewrite the differentiation with respect to  $\tilde{\epsilon}$  by a differentiation with respect to  $u$  and compute the integral via partial integration. Then, for  $\tilde{\epsilon} = 0$  only the boundary term survives, and we can easily compute the result for  $\tilde{\alpha}$ ,

$$\tilde{\alpha} = \frac{12}{8 - 15(u_{c,\text{onset}}^{(\infty)})^{1/2}\ell} \quad (\text{A.83})$$

Inserting this into eq. (A.80) and the result into eq. (A.78) yields  $n_4^\infty$  as given in eq. (6.64) in the main text.



# Bibliography

- [1] S. L. Adler. Calculation of the axial vector coupling constant renormalization in beta decay. *Phys.Rev.Lett.*, 14:1051–1055, 1965.
- [2] S. L. Adler. Sum rules for the axial vector coupling constant renormalization in beta decay. *Phys.Rev.*, 140:B736, 1965.
- [3] S. L. Adler. Axial-Vector Vertex in Spinor Electrodynamics. *Physical Review*, 177:2426–2438, Jan. 1969.
- [4] O. Aharony, J. Sonnenschein, and S. Yankielowicz. A Holographic model of deconfinement and chiral symmetry restoration. *Annals Phys.*, 322:1420–1443, 2007.
- [5] M. G. Alford, K. Rajagopal, and F. Wilczek. Color flavor locking and chiral symmetry breaking in high density QCD. *Nucl.Phys.*, B537:443–458, 1999.
- [6] M. G. Alford, A. Schmitt, K. Rajagopal, and T. Schäfer. Color superconductivity in dense quark matter. *Rev.Mod.Phys.*, 80:1455–1515, 2008.
- [7] J. O. Andersen and A. Tranberg. The Chiral transition in a magnetic background: Finite density effects and the functional renormalization group. *JHEP*, 1208:002, 2012.
- [8] P. Anderson. Random-phase approximation in the theory of superconductivity. *Phys.Rev.*, 112:1900–1916, 1958.
- [9] P. W. Anderson. Coherent excited states in the theory of superconductivity: Gauge invariance and the meissner effect. *Phys.Rev.*, 110:827–835, 1958.

- 
- [10] P. W. Anderson. Plasmons, Gauge Invariance, and Mass. *Phys.Rev.*, 130:439–442, 1963.
- [11] E. Antonyan, J. Harvey, S. Jensen, and D. Kutasov. NJL and QCD from string theory. arXiv:hep-th/0604017, 2006.
- [12] Y. Aoki, G. Endrődi, Z. Fodor, S. Katz, and K. Szabó. The Order of the quantum chromodynamics transition predicted by the standard model of particle physics. *Nature*, 443:675–678, 2006.
- [13] Y. Aoki, Z. Fodor, S. Katz, and K. Szabó. The QCD transition temperature: Results with physical masses in the continuum limit. *Phys.Lett.*, B643:46–54, 2006.
- [14] S. S. Avancini, D. P. Menezes, M. B. Pinto, and C. Providencia. The QCD Critical End Point Under Strong Magnetic Fields. *Phys.Rev.*, D85:091901, 2012.
- [15] G. Bali, F. Bruckmann, G. Endrődi, Z. Fodor, S. Katz, et al. The QCD phase diagram for external magnetic fields. *JHEP*, 1202:044, 2012.
- [16] J. Bardeen, L. Cooper, and J. Schrieffer. Microscopic theory of superconductivity. *Phys.Rev.*, 106:162, 1957.
- [17] J. Bardeen, L. Cooper, and J. Schrieffer. Theory of superconductivity. *Phys.Rev.*, 108:1175–1204, 1957.
- [18] W. A. Bardeen, H. Fritzsch, and M. Gell-Mann. Light cone current algebra,  $\pi^0$  decay, and  $e^+ e^-$  annihilation. 1972. report no.: CERN-TH-1538, republished in arXiv:hep-ph/0211388.
- [19] C. B. Bayona, K. Peeters, and M. Zamaklar. A Non-homogeneous ground state of the low-temperature Sakai-Sugimoto model. *JHEP*, 1106:092, 2011.
- [20] J. S. Bell and R. Jackiw. A PCAC puzzle:  $\pi^0 \rightarrow \gamma\gamma$  in the  $\sigma$ -model. *Nuovo Cimento A Serie*, 60:47–61, Mar. 1969.
- [21] O. Bergman, G. Lifschytz, and M. Lippert. Holographic Nuclear Physics. *JHEP*, 0711:056, 2007.

- 
- [22] O. Bergman, G. Lifschytz, and M. Lippert. Response of Holographic QCD to Electric and Magnetic Fields. *JHEP*, 0805:007, 2008.
- [23] O. Bergman, G. Lifschytz, and M. Lippert. Magnetic properties of dense holographic QCD. *Phys.Rev.*, D79:105024, 2009.
- [24] J. Beringer et al. Review of Particle Physics (RPP). *Phys.Rev.*, D86:010001, 2012.
- [25] J. Bernstein, S. Fubini, M. Gell-Mann, and W. Thirring. On the decay rate of the charged pion. *Il Nuovo Cimento*, 17(5):757–766, 1960.
- [26] J. Bernstein, M. Gell-Mann, and L. Michel. On the renormalization of the axial vector coupling constant in  $\pi$ -decay. *Il Nuovo Cimento Series 10*, 16(3):560–568, 1960.
- [27] R. A. Bertlmann. *Anomalies in quantum field theory*. Internat. Ser. Mono. Phys. Clarendon Press, London, 1996.
- [28] F. Bigazzi, A. L. Cotrone, J. Mas, A. Paredes, A. V. Ramallo, et al. D3-D7 Quark-Gluon Plasmas. *JHEP*, 0911:117, 2009.
- [29] J. Bjorken. Asymptotic Sum Rules at Infinite Momentum. *Phys.Rev.*, 179:1547–1553, 1969.
- [30] R. Bjorklund, W. E. Crandall, B. J. Moyer, and H. F. York. High energy photons from proton-nucleon collisions. *Phys. Rev.*, 77:213–218, Jan 1950.
- [31] N. Bogoliubov. On the theory of superfluidity. *J. Phys. (USSR)*, 11:23, 1947.
- [32] S. Bolognesi and D. Tong. Magnetic Catalysis in AdS4. *Class.Quant.Grav.*, 29:194003, 2012.
- [33] L. Bonanno and F. Giacosa. Does nuclear matter bind at large  $N_c$ ? *Nucl.Phys.*, A859:49–62, 2011.
- [34] J. K. Boomsma and D. Boer. The Influence of strong magnetic fields and instantons on the phase structure of the two-flavor NJL model. *Phys.Rev.*, D81:074005, 2010.

- 
- [35] G. Breit, E. Condon, and R. Present. Theory of Scattering of Protons by Protons. *Phys.Rev.*, 50:825–845, 1936.
- [36] A. Broderick, M. Prakash, and J. Lattimer. The Equation of state of neutron star matter in strong magnetic fields. *Astrophys.J.*, 2000.
- [37] A. Broderick, M. Prakash, and J. Lattimer. Effects of strong magnetic fields in strange baryonic matter. *Phys.Lett.*, B531:167–174, 2002.
- [38] W. E. Brown, J. T. Liu, and H.-c. Ren. On the perturbative nature of color superconductivity. *Phys.Rev.*, D61:114012, 2000.
- [39] W. E. Brown, J. T. Liu, and H.-c. Ren. The Transition temperature to the superconducting phase of QCD at high baryon density. *Phys.Rev.*, D62:054016, 2000.
- [40] M. Buballa. NJL model analysis of quark matter at large density. *Phys.Rept.*, 407:205–376, 2005.
- [41] P. Burikham. Magnetic properties of holographic multiquarks in the quark-gluon plasma. *JHEP*, 1004:045, 2010.
- [42] P. Burikham. Magnetic Phase Diagram of Dense Holographic Multiquarks in the Quark-gluon Plasma. *JHEP*, 1105:121, 2011.
- [43] P. Burikham and T. Chullaphan. Magnetized Domain Walls in the Deconfined Sakai-Sugimoto Model at Finite Baryon Density. *JHEP*, 1108:026, 2011.
- [44] J. Callan, Curtis G., A. Guijosa, K. G. Savvidy, and O. Tafjord. Baryons and flux tubes in confining gauge theories from brane actions. *Nucl.Phys.*, B555:183–200, 1999.
- [45] N. Callebaut, D. Dudal, and H. Verschelde. Holographic rho mesons in an external magnetic field. *JHEP*, 1303:033, 2013.
- [46] B. Cassen and E. U. Condon. On nuclear forces. *Phys. Rev.*, 50:846–849, Nov 1936.
- [47] B. Chandrasekhar. A note on the maximum critical field of high-field superconductors. *Appl.Phys.Lett.*, 1:7, 1962.



- [48] B. Chatterjee, H. Mishra, and A. Mishra. Vacuum structure and chiral symmetry breaking in strong magnetic fields for hot and dense quark matter. *Phys.Rev.*, D84:014016, 2011.
- [49] W. Chinowsky and J. Steinberger. Absorption of Negative Pions in Deuterium: Parity of the Pion. *Phys.Rev.*, 95:1561–1564, 1954.
- [50] W.-y. Chuang, S.-H. Dai, S. Kawamoto, F.-L. Lin, and C.-P. Yeh. Dynamical Instability of Holographic QCD at Finite Density. *Phys.Rev.*, D83:106003, 2011.
- [51] A. Clogston. Upper Limit for the Critical Field in Hard Superconductors. *Phys.Rev.Lett.*, 9:266–267, 1962.
- [52] L. N. Cooper. Bound electron pairs in a degenerate Fermi gas. *Phys.Rev.*, 104:1189–1190, 1956.
- [53] M. D'Elia, S. Mukherjee, and F. Sanfilippo. QCD Phase Transition in a Strong Magnetic Background. *Phys.Rev.*, D82:051501, 2010.
- [54] P. Depommier, J. Heintze, A. Mukhin, C. Rubbia, V. Soergel, and K. Winter. Determination of the  $\pi^+ - \pi^0 + e^+ + \nu$  decay rate. *Physics Letters*, 2(1):23 – 26, 1962.
- [55] S. K. Domokos and J. A. Harvey. Baryon number-induced Chern-Simons couplings of vector and axial-vector mesons in holographic QCD. *Phys.Rev.Lett.*, 99:141602, 2007.
- [56] M. R. Douglas. Branes within branes. 1995. arXiv:hep-th/9512077.
- [57] R. C. Duncan and C. Thompson. Formation of very strongly magnetized neutron stars - implications for gamma-ray bursts. *Astrophys.J.*, 392:L9, 1992.
- [58] D. Ebert, K. Klimenko, M. Vdovichenko, and A. Vshivtsev. Magnetic oscillations in dense cold quark matter with four fermion interactions. *Phys.Rev.*, D61:025005, 2000.
- [59] J. Erdmenger, V. G. Filev, and D. Zoakos. Magnetic Catalysis with Massive Dynamical Flavours. *JHEP*, 1208:004, 2012.

- 
- [60] J. Erdmenger, R. Meyer, and J. P. Shock. AdS/CFT with flavour in electric and magnetic Kalb-Ramond fields. *JHEP*, 0712:091, 2007.
- [61] S. Fayazbakhsh, S. Sadeghian, and N. Sadooghi. Properties of neutral mesons in a hot and magnetized quark matter. *Phys.Rev.*, D86:085042, 2012.
- [62] S. Fayazbakhsh and N. Sadooghi. Phase diagram of hot magnetized two-flavor color superconducting quark matter. *Phys.Rev.*, D83:025026, 2011.
- [63] T. Fazzini, G. Fidecaro, A. W. Merrison, H. Paul, and A. V. Tollestrup. Electron decay of the pion. *Phys. Rev. Lett.*, 1:247–249, Oct 1958.
- [64] E. Fermi. An attempt of a theory of beta radiation. 1. *Z.Phys.*, 88:161–177, 1934.
- [65] G. N. Ferrari, A. F. Garcia, and M. B. Pinto. Chiral Transition Within Effective Quark Models Under Magnetic Fields. *Phys.Rev.*, D86:096005, 2012.
- [66] R. Feynman and M. Gell-Mann. Theory of Fermi interaction. *Phys.Rev.*, 109:193–198, Jan 1958.
- [67] V. G. Filev, C. V. Johnson, R. Rashkov, and K. Viswanathan. Flavoured large N gauge theory in an external magnetic field. *JHEP*, 0710:019, 2007.
- [68] V. G. Filev, C. V. Johnson, and J. P. Shock. Universal Holographic Chiral Dynamics in an External Magnetic Field. *JHEP*, 0908:013, 2009.
- [69] V. G. Filev and R. C. Rashkov. Magnetic Catalysis of Chiral Symmetry Breaking. A Holographic Prospective. *Adv.High Energy Phys.*, 2010:473206, 2010.
- [70] H. Fritzsch and M. Gell-Mann. Current algebra: Quarks and what else? *eConf*, C720906V2:135–165, 1972.
- [71] I. Frolov, V. C. Zhukovsky, and K. Klimenko. Chiral density waves in quark matter within the Nambu-Jona-Lasinio model in an external magnetic field. *Phys.Rev.*, D82:076002, 2010.
- [72] K. Fukushima and Y. Hidaka. Magnetic Catalysis vs Magnetic Inhibition. *Phys.Rev.Lett.*, 110:031601, 2013.

- 
- [73] K. Fukushima, D. E. Kharzeev, and H. J. Warringa. The Chiral Magnetic Effect. *Phys.Rev.*, D78:074033, 2008.
- [74] K. Fukushima and J. M. Pawłowski. Magnetic catalysis in hot and dense quark matter and quantum fluctuations. *Phys.Rev.*, D86:076013, 2012.
- [75] M. Gell-Mann. Isotopic Spin and New Unstable Particles. *Phys.Rev.*, 92:833–834, 1953.
- [76] M. Gell-Mann. The interpretation of the new particles as displaced charged multiplets. *Nuovo Cimento Suppl.*, 4:848–866, 1956.
- [77] M. Gell-Mann. The Eightfold Way: A Theory of strong interaction symmetry, 1961. report no.: TID-12608, California Inst. of Tech., Pasadena. Synchrotron Lab.
- [78] M. Gell-Mann. Symmetries of baryons and mesons. *Phys.Rev.*, 125:1067–1084, 1962.
- [79] M. Gell-Mann. A Schematic Model of Baryons and Mesons. *Phys.Lett.*, 8:214–215, 1964.
- [80] M. Gell-Mann and M. Levy. The axial vector current in beta decay. *Nuovo Cim.*, 16:705, 1960.
- [81] M. Gell-Mann and Y. Ne'eman. Current-generated algebras. *Annals Phys.*, 30:360–369, 1964.
- [82] M. Gell-Mann and A. Pais. Theoretical views on the new particles. In *Proceedings of the Glasgow International Conference on Nuclear Physics*, pages 342–350, 1954.
- [83] I. Giannakis, D.-f. Hou, H.-c. Ren, and D. H. Rischke. Gauge field fluctuations and first-order phase transition in color superconductivity. *Phys.Rev.Lett.*, 93:232301, 2004.
- [84] M. Goldberger and S. Treiman. Conserved Currents in the Theory of Fermi Interactions. *Phys.Rev.*, 110:1478–1479, 1958.

- 
- [85] M. Goldberger and S. Treiman. Decay of the pi meson. *Phys.Rev.*, 110:1178–1184, June 1958.
- [86] M. Goldberger and S. Treiman. Form-factors in Beta decay and muon capture. *Phys.Rev.*, 111:354–361, 1958.
- [87] J. Goldstone. Field Theories with Superconductor Solutions. *Nuovo Cim.*, 19:154–164, 1961.
- [88] J. Goldstone, A. Salam, and S. Weinberg. Broken Symmetries. *Phys.Rev.*, 127:965–970, 1962.
- [89] E. Gorbar, V. Gusynin, V. Miransky, and I. Shovkovy. Dynamics in the quantum Hall effect and the phase diagram of graphene. *Phys.Rev.*, B78:085437, 2008.
- [90] E. Gorbar, V. Miransky, and I. Shovkovy. Chiral asymmetry of the Fermi surface in dense relativistic matter in a magnetic field. *Phys.Rev.*, C80:032801, 2009.
- [91] E. Gorbar, V. Miransky, and I. Shovkovy. Normal ground state of dense relativistic matter in a magnetic field. *Phys.Rev.*, D83:085003, 2011.
- [92] O. Greenberg. The Parton model. 2008. arXiv:0805.2588 [hep-ph].
- [93] D. J. Gross and F. Wilczek. Ultraviolet Behavior of Nonabelian Gauge Theories. *Phys.Rev.Lett.*, 30:1343–1346, 1973.
- [94] V. Gusynin, V. Miransky, S. Sharapov, and I. Shovkovy. Excitonic gap, phase transition, and quantum Hall effect in graphene. *Phys.Rev.*, B74:195429, 2006.
- [95] V. Gusynin, V. Miransky, and I. Shovkovy. Catalysis of dynamical flavor symmetry breaking by a magnetic field in (2+1)-dimensions. *Phys.Rev.Lett.*, 73:3499–3502, 1994.
- [96] V. Gusynin, V. Miransky, and I. Shovkovy. Dimensional reduction and dynamical chiral symmetry breaking by a magnetic field in (3+1)-dimensions. *Phys.Lett.*, B349:477–483, 1995.
- [97] V. Gusynin, V. Miransky, and I. Shovkovy. Dynamical chiral symmetry breaking by a magnetic field in QED. *Phys.Rev.*, D52:4747–4751, 1995.

- [98] V. Gusynin, V. Miransky, and I. Shovkovy. Dynamical flavor symmetry breaking by a magnetic field in (2+1)-dimensions. *Phys.Rev.*, D52:4718–4735, 1995.
- [99] M. Han and Y. Nambu. Three Triplet Model with Double SU(3) Symmetry. *Phys.Rev.*, 139:B1006–B1010, 1965.
- [100] K. Hashimoto, T. Sakai, and S. Sugimoto. Holographic Baryons: Static Properties and Form Factors from Gauge/String Duality. *Prog. Theor. Phys.*, 120:1093–1137, 2008.
- [101] H. Hata, T. Sakai, S. Sugimoto, and S. Yamato. Baryons from instantons in holographic QCD. *Prog.Theor.Phys.*, 117:1157, 2007.
- [102] T. Hatsuda and T. Kunihiro. Possible critical phenomena associated with the chiral symmetry breaking. *Phys.Lett.*, B145:7–10, 1984.
- [103] W. Heisenberg. On the structure of atomic nuclei. *Z.Phys.*, 77:1–11, 1932.
- [104] N. Horigome and Y. Tanii. Holographic chiral phase transition with chemical potential. *JHEP*, 0701:072, 2007.
- [105] J. Hubbard. Calculation of partition functions. *Phys.Rev.Lett.*, 3:77–80, 1959.
- [106] T. Inagaki, D. Kimura, and T. Murata. Four fermion interaction model in a constant magnetic field at finite temperature and chemical potential. *Prog.Theor.Phys.*, 111:371–386, 2004.
- [107] D. Iwanenko. Interaction of neutrons and protons. *Nature*, 133:981–982, 1934.
- [108] R. Jackiw. Functional evaluation of the effective potential. *Phys.Rev.*, D9:1686, 1974.
- [109] R. L. Jaffe. Multi-Quark Hadrons. 1. The Phenomenology of  $Q^2\bar{Q}^2$  Mesons. *Phys.Rev.*, D15:267, 1977.
- [110] C. V. Johnson and A. Kundu. External Fields and Chiral Symmetry Breaking in the Sakai-Sugimoto Model. *JHEP*, 0812:053, 2008.

- 
- [111] N. Kemmer. The charge-dependence of nuclear forces. *Mathematical Proceedings of the Cambridge Philosophical Society*, 34:354–364, 7 1938.
- [112] D. E. Kharzeev, L. D. McLerran, and H. J. Warringa. The Effects of topological charge change in heavy ion collisions: 'Event by event P and CP violation'. *Nucl.Phys.*, A803:227–253, 2008.
- [113] D. E. Kharzeev and H. J. Warringa. Chiral Magnetic conductivity. *Phys.Rev.*, D80:034028, 2009.
- [114] S. Klevansky. The Nambu-Jona-Lasinio model of quantum chromodynamics. *Rev.Mod.Phys.*, 64:649–708, 1992.
- [115] K. Klimenko. Three-dimensional Gross-Neveu model at nonzero temperature and in an external magnetic field. *Theor.Math.Phys.*, 90:1–6, 1992.
- [116] K. Klimenko. Three-dimensional Gross-Neveu model in an external magnetic field. *Theor.Math.Phys.*, 89:1161–1168, 1992.
- [117] A. Kurkela, P. Romatschke, and A. Vuorinen. Cold Quark Matter. *Phys.Rev.*, D81:105021, 2010.
- [118] D. Lai and S. Shapiro. Cold equation of state in a strong magnetic field - Effects of inverse beta-decay. *Astrophys.J.*, 383:745–751, 1991.
- [119] C. Lattes, G. Occhialini, and C. Powell. Observations on the tracks of slow mesons in photographic emulsions. *Nature*, 160:453–456, Oct 1947.
- [120] T. Lee and C.-N. Yang. Question of Parity Conservation in Weak Interactions. *Phys.Rev.*, 104:254–258, 1956.
- [121] G. Lifschytz and M. Lippert. Holographic Magnetic Phase Transition. *Phys.Rev.*, D80:066007, 2009.
- [122] C. Liu. Baryonium, tetra-quark state and glue-ball in large  $N_c$  QCD. *Eur. Phys. J.*, C53:413–419, 2008.
- [123] J. M. Maldacena. The Large N limit of superconformal field theories and supergravity. *Adv.Theor.Math.Phys.*, 2:231–252, 1998.

- [124] T. Matsuura, K. Iida, T. Hatsuda, and G. Baym. Thermal fluctuations of gauge fields and first order phase transitions in color superconductivity. *Phys.Rev.*, D69:074012, 2004.
- [125] L. McLerran and R. D. Pisarski. Phases of cold, dense quarks at large  $N(c)$ . *Nucl.Phys.*, A796:83–100, 2007.
- [126] D. Menezes, M. Benghi Pinto, S. Avancini, A. Perez Martinez, and C. Providencia. Quark matter under strong magnetic fields in the Nambu-Jona-Lasinio Model. *Phys.Rev.*, C79:035807, 2009.
- [127] M. A. Metlitski and A. R. Zhitnitsky. Anomalous axion interactions and topological currents in dense matter. *Phys.Rev.*, D72:045011, 2005.
- [128] T. Nakano and K. Nishijima. Charge Independence for V-particles. *Prog.Theor.Phys.*, 10:581–582, 1953.
- [129] Y. Nambu. Axial vector current conservation in weak interactions. *Phys.Rev.Lett.*, 4:380–382, 1960.
- [130] Y. Nambu. Quasiparticles and Gauge Invariance in the Theory of Superconductivity. *Phys.Rev.*, 117:648–663, 1960.
- [131] Y. Nambu and G. Jona-Lasinio. Dynamical Model of Elementary Particles Based on an Analogy with Superconductivity. 1. *Phys.Rev.*, 122:345–358, 1961.
- [132] Y. Nambu and G. Jona-Lasinio. Dynamical model of elementary particles based on an analogy with superconductivity. II. *Phys.Rev.*, 124:246–254, 1961.
- [133] S. H. Neddermeyer and C. D. Anderson. Note on the nature of cosmic-ray particles. *Phys. Rev.*, 51:884–886, May 1937.
- [134] Y. Ne'eman. Derivation of strong interactions from a gauge invariance. *Nucl.Phys.*, 26:222–229, 1961.
- [135] K. Nishijima. Some Remarks on the Even-odd Rule. *Prog.Theor.Phys.*, 12:107–108, 1954.
- [136] K. Nishijima. Charge Independence Theory of V Particles. *Prog.Theor.Phys.*, 13:285–304, 1955.

- 
- [137] G. Occhialini and C. Powell. Nuclear disintegrations produced by slow charged particles of small mass. *Nature*, 159:186–190, Feb 1947.
- [138] H. Ooguri and C.-S. Park. Spatially Modulated Phase in Holographic Quark-Gluon Plasma. *Phys.Rev.Lett.*, 106:061601, 2011.
- [139] D. Parganlija, F. Giacosa, and D. H. Rischke. Vacuum Properties of Mesons in a Linear Sigma Model with Vector Mesons and Global Chiral Invariance. *Phys.Rev.*, D82:054024, 2010.
- [140] J. Pelaez. Light scalars as tetraquarks or two-meson states from large  $N(c)$  and unitarized chiral perturbation theory. *Mod.Phys.Lett.*, A19:2879–2894, 2004.
- [141] J. Pelaez. On the Nature of light scalar mesons from their large  $N(c)$  behavior. *Phys.Rev.Lett.*, 92:102001, 2004.
- [142] M. E. Peskin and D. V. Schroeder. *An Introduction to Quantum Field Theory; 1995 ed.* Westview, Boulder, CO, 1995. Includes exercises.
- [143] G. Policastro, D. Son, and A. Starinets. The Shear viscosity of strongly coupled  $N=4$  supersymmetric Yang-Mills plasma. *Phys.Rev.Lett.*, 87:081601, 2001.
- [144] H. D. Politzer. Reliable Perturbative Results for Strong Interactions? *Phys.Rev.Lett.*, 30:1346–1349, 1973.
- [145] F. Preis, A. Rebhan, and A. Schmitt. Inverse magnetic catalysis in dense holographic matter. *JHEP*, 1103:033, 2011.
- [146] F. Preis, A. Rebhan, and A. Schmitt. Holographic baryonic matter in a background magnetic field. *J.Phys.G*, G39:054006, 2012.
- [147] F. Preis, A. Rebhan, and A. Schmitt. Inverse magnetic catalysis in field theory and gauge-gravity duality. *Lect.Notes Phys.*, 871:51–86, 2013.
- [148] A. Rabhi, P. Panda, and C. Providencia. Warm and dense stellar matter under strong magnetic fields. *Phys.Rev.*, C84:035803, 2011.
- [149] S. Rama, S. Sarkar, B. Sathiapalan, and N. Sircar. Strong Coupling BCS Superconductivity and Holography. *Nucl.Phys.*, B852:634–680, 2011.



- [150] A. Rebhan and P. Romatschke. HTL quasiparticle models of deconfined QCD at finite chemical potential. *Phys.Rev.*, D68:025022, 2003.
- [151] A. Rebhan, A. Schmitt, and S. A. Stricker. Meson supercurrents and the Meissner effect in the Sakai-Sugimoto model. *JHEP*, 0905:084, 2009.
- [152] A. Rebhan, A. Schmitt, and S. A. Stricker. Anomalies and the chiral magnetic effect in the Sakai-Sugimoto model. *JHEP*, 1001:026, 2010.
- [153] G. Rochester and C. Butler. Evidence for the existence of new unstable elementary particles. *Nature*, 160:855–857, 1947.
- [154] M. Rozali, H.-H. Shieh, M. Van Raamsdonk, and J. Wu. Cold Nuclear Matter In Holographic QCD. *JHEP*, 01:053, 2008.
- [155] L. H. Ryder. *Quantum field theory*. Cambridge Univ. Press, Cambridge, 1985.
- [156] T. Sakai and S. Sugimoto. Low energy hadron physics in holographic QCD. *Prog.Theor.Phys.*, 113:843–882, 2005.
- [157] T. Sakai and S. Sugimoto. More on a holographic dual of QCD. *Prog.Theor.Phys.*, 114:1083–1118, 2005.
- [158] A. Schmitt. Dense matter in compact stars: A pedagogical introduction. *Lect.Notes Phys.*, 811:1–111, 2010.
- [159] A. Schmitt. Lecture notes on 'thermal field theory', 2013. <http://hep.itp.tuwien.ac.at/aschmitt/thermal13.pdf>.
- [160] A. Schmitt, Q. Wang, and D. H. Rischke. When the transition temperature in color superconductors is not like in BCS theory. *Phys.Rev.*, D66:114010, 2002.
- [161] V. Schön and M. Thies. Emergence of Skyrme crystal in Gross-Neveu and 't Hooft models at finite density. *Phys.Rev.*, D62:096002, 2000.
- [162] J. S. Schwinger. On gauge invariance and vacuum polarization. *Phys.Rev.*, 82:664–679, 1951.
- [163] S. Seki and J. Sonnenschein. Comments on Baryons in Holographic QCD. *JHEP*, 01:053, 2009.

- [164] V. Skokov, A. Y. Illarionov, and V. Toneev. Estimate of the magnetic field strength in heavy-ion collisions. *Int.J.Mod.Phys.*, A24:5925–5932, 2009.
- [165] T. Skyrme. A Nonlinear field theory. *Proc.Roy.Soc.Lond.*, A260:127–138, 1961.
- [166] R. L. Stratonovich. On a Method of Calculating Quantum Distribution Functions. *Soviet Physics Doklady*, 2:416, July 1957.
- [167] G. 't Hooft. A Planar Diagram Theory for Strong Interactions. *Nucl.Phys.*, B72:461, 1974.
- [168] G. 't Hooft. Computation of the Quantum Effects Due to a Four-Dimensional Pseudoparticle. *Phys.Rev.*, D14:3432–3450, 1976.
- [169] I. Tamm. Exchange forces between neutrons and protons and fermi's theory. *Nature*, 133:981, 1934.
- [170] J. Taylor. Beta Decay of the Pion. *Phys.Rev.*, 110:1216–1216, 1958.
- [171] E. G. Thompson and D. T. Son. Magnetized baryonic matter in holographic QCD. *Phys.Rev.*, D78:066007, 2008.
- [172] M. A. Tuve, N. P. Heydenburg, and L. R. Hafstad. The scattering of protons by protons. *Phys. Rev.*, 50:806–825, Nov 1936.
- [173] G. Veneziano. U(1) Without Instantons. *Nucl.Phys.*, B159:213–224, 1979.
- [174] M. Volkov. Meson Lagrangians in a Superconductor Quark Model. *Annals Phys.*, 157:282–303, 1984.
- [175] J. Walecka. A Theory of highly condensed matter. *Annals Phys.*, 83:491–529, 1974.
- [176] S. Weinberg. Phenomenological Lagrangians. *Physica*, A96:327, 1979.
- [177] W. I. Weisberger. Renormalization of the Weak Axial Vector Coupling Constant. *Phys.Rev.Lett.*, 14:1047–1051, 1965.
- [178] E. Wigner. On the Consequences of the Symmetry of the Nuclear Hamiltonian on the Spectroscopy of Nuclei. *Phys.Rev.*, 51:106–119, 1937.

- 
- [179] K. G. Wilson. Confinement of quarks. *Phys. Rev. D*, 10:2445–2459, Oct 1974.
- [180] E. Witten. Baryons in the  $1/N$  Expansion. *Nucl.Phys.*, B160:57, 1979.
- [181] E. Witten. Current Algebra Theorems for the U(1) Goldstone Boson. *Nucl.Phys.*, B156:269, 1979.
- [182] E. Witten. Current Algebra, Baryons, and Quark Confinement. *Nucl.Phys.*, B223:433–444, 1983.
- [183] E. Witten. Global Aspects of Current Algebra. *Nucl.Phys.*, B223:422–432, 1983.
- [184] E. Witten. Anti-de Sitter space, thermal phase transition, and confinement in gauge theories. *Adv.Theor.Math.Phys.*, 2:505–532, 1998.
- [185] E. Witten. Baryons and branes in anti-de Sitter space. *JHEP*, 9807:006, 1998.
- [186] C. Wu, E. Ambler, R. Hayward, D. Hoppes, and R. Hudson. Experimental Test of Parity Conservation in Beta Decay. *Phys.Rev.*, 105:1413–1414, 1957.
- [187] H. Yukawa. On the interaction of elementary particles. *Proc.Phys.Math.Soc.Jap.*, 17:48–57, 1935.

# Florian Preis - Curriculum Vitae

---

CONTACT INFORMATION	Vienna University of Technology Institute for Theoretical Physics (E136) Wiedner Hauptstraße 8-10 1040 Vienna, Austria <i>Mobile:</i> +43 664 1439161 <i>E-mail:</i> fpreis@hep.itp.tuwien.ac.at
PERSONAL INFORMATION	<i>Day of Birth:</i> 1st of January 1982 <i>Place of Birth:</i> Graz, Austria <i>Nationality:</i> Austrian
EDUCATION	<i>since 2010/01:</i> Ph.D. studies, Vienna University of Technology, Austria <ul style="list-style-type: none"><li>• Thesis Topic: <i>Chiral symmetry breaking in strong magnetic fields</i></li><li>• Thesis Advisor: Professor Anton Rebhan and Dr. Andreas Schmitt</li></ul> <i>2002/10-2009/10:</i> Studies of physics, Vienna University of Technology, Austria <ul style="list-style-type: none"><li>• Master's degree (Dipl.-Ing.) on 9th of October 2009</li><li>• Thesis Topic: <i>Spherically symmetric models in Loop Quantum Gravity</i></li><li>• Thesis Advisor: Dr. Herbert Balasin</li></ul> <i>2001/10-2002/10:</i> Community service (in lieu of military service) <i>2000/10-2001/09:</i> Studies of philosophy, University of Vienna, Austria  <i>1992/09-2000/06:</i> Bundes Real Gymnasium Perau in Villach, Austria <ul style="list-style-type: none"><li>• graduation on 15th of June 2000</li></ul>
SCIENTIFIC EMPLOYMENT	<i>since 2010/01:</i> Project assistant (FWF, project P22114-N16) at the Institute for Theoretical Physics, Vienna University of Technology, Austria <i>2012/10/15-2013/09/30:</i> paternity leave  <i>2008/03-2008/07:</i> Project assistant in collaboration with Dr. Daniel Grumiller and Dr. Herbert Balasin, project Ariadna ID 07/1301, AO/1-5582/07/NL/CB of the European Space Agency Advanced Concept Team

- REFEREED JOURNAL PUBLICATIONS
- F. Preis, A. Rebhan and A. Schmitt, *Inverse magnetic catalysis in dense holographic matter*, JHEP 1103 (2011) 033, [arXiv:1012.4785 \[hep-th\]](#)
- S. Carloni, D. Grumiller and F. Preis, *Solar system constraints on Rindler acceleration*, Phys.Rev. D83 (2011) 124024, [arXiv:1103.0274 \[astro-ph.EP\]](#)
- D. Grumiller and F. Preis, *Rindler force at large distances*, IJMP D20, No. 14, pp. 2761-2766 (2011), [arXiv:1107.2373 \[astro-ph.CO\]](#)
- F. Preis, A. Rebhan and A. Schmitt, *Holographic baryonic matter in a background magnetic field*, J.Phys. G39 (2012) 054006, [arXiv:1109.6904 \[hep-th\]](#)
- F. Preis, A. Rebhan and A. Schmitt, *Inverse magnetic catalysis in field theory and gauge-gravity duality*, Lect.Notes Phys. 871 (2013) 51-86, [arXiv:1208.0536 \[hep-ph\]](#)
- CONFERENCE PROCEEDINGS
- F. Preis, A. Rebhan and A. Schmitt, *Chiral transition in dense, magnetized matter*, AIP Conf.Proc. 1492 (2012) 264-268, [arXiv:1209.4468 \[hep-ph\]](#)
- CONFERENCES AND WORKSHOPS
- Spanish Relativity Meeting 2008*, Salamanca, Spain, 2008/09/15-2008/09/19
- Jürgen-Ehlers-Spring-School of the University Potsdam and the Max-Planck-Institute for Gravitational Physics*, Golm, Germany, 2009/03/16-2009/03/27
- Norwegian Winter Workshop on QCD in Extreme Conditions*, Trondheim, Norway, 2010/02/24-2010/02/26
- Chiral Symmetry and Confinement in Cold, Dense Quark Matter*, Trento, Italy, 2010/07/19-2010/07/23
- ESI Programme on AdS Holography and the Quark-Gluon Plasma*, Vienna, Austria, 2010/08/02-2010/10/29
- INT Summer School on Applications of String Theory*, Seattle, USA, 2011/07/18-2011/07/29
- 8th Vienna Central European Seminar on Particle Physics and Quan-*

*tum Field Theory*, Vienna, Austria,  
2011/11/25-2011/11/27

*Strong and Electroweak Matter 2012*, Swansea, United Kingdom,  
2012/07/10-2012/07/13

*Quark Confinement and the Hadron Spectrum X*, Munich, Germany,  
2012/10/08-2012/10/12

TALKS

F. Preis, *Inverse magnetic catalysis in dense holographic matter*, Vienna Theory Lunch Seminar, Vienna, Austria,  
2011/03/08

F. Preis, *Inverse magnetic catalysis in dense holographic matter*, INT Summer School on Applications of String Theory, Seattle, USA,  
2011/07/25

F. Preis, *Inverse magnetic catalysis in dense matter*, Quark Confinement and the Hadron Spectrum X, Munich, Germany,  
2012/10/08

POSTERS

F. Preis, A. Rebhan, A. Schmitt and S. Stricker, *Dense Matter in the Sakai–Sugimoto model*, Chiral Symmetry and Confinement in Cold, Dense Quark Matter, Trento, Italy,  
2010/07/19-2010/07/23

F. Preis, A. Rebhan and A. Schmitt, *Inverse magnetic catalysis in dense matter*, Strong and Electroweak Matter 2012, Swansea, UK,  
2012/07/10-2012/07/13

SCHOLARSHIPS

2009/10-2010/09: Scholarship of *Pro Scientia Austria*

JOURNAL  
REFEREE

Journal referee for *Physical Review D*

ORGANIZATION  
OF SEMINARS

2011/10-2012/09: Organizer of the *Vienna Theory Lunch Seminar*  
<http://www.univie.ac.at/lunch-seminar>

TEACHING  
EXPERIENCE

2008/03-2008/06: Tutorial for Electrodynamics 1

2010/03-2010/06: Tutorial for Electrodynamics 1

SKILLS AND  
INTERESTS

*Languages*: German (native), English (fluent), French (basics)

*Computer skills*: C, Mathematica, Maple, TeX

*Scientific interests:* Classical and quantum gravity, quantum field theory at finite temperature and density, gauge/gravity duality, the QCD phase diagram, physics of compact stars, cosmology